Bachelor of Science Thesis

Sediment-petrographical analysis of the Delft Sandstone

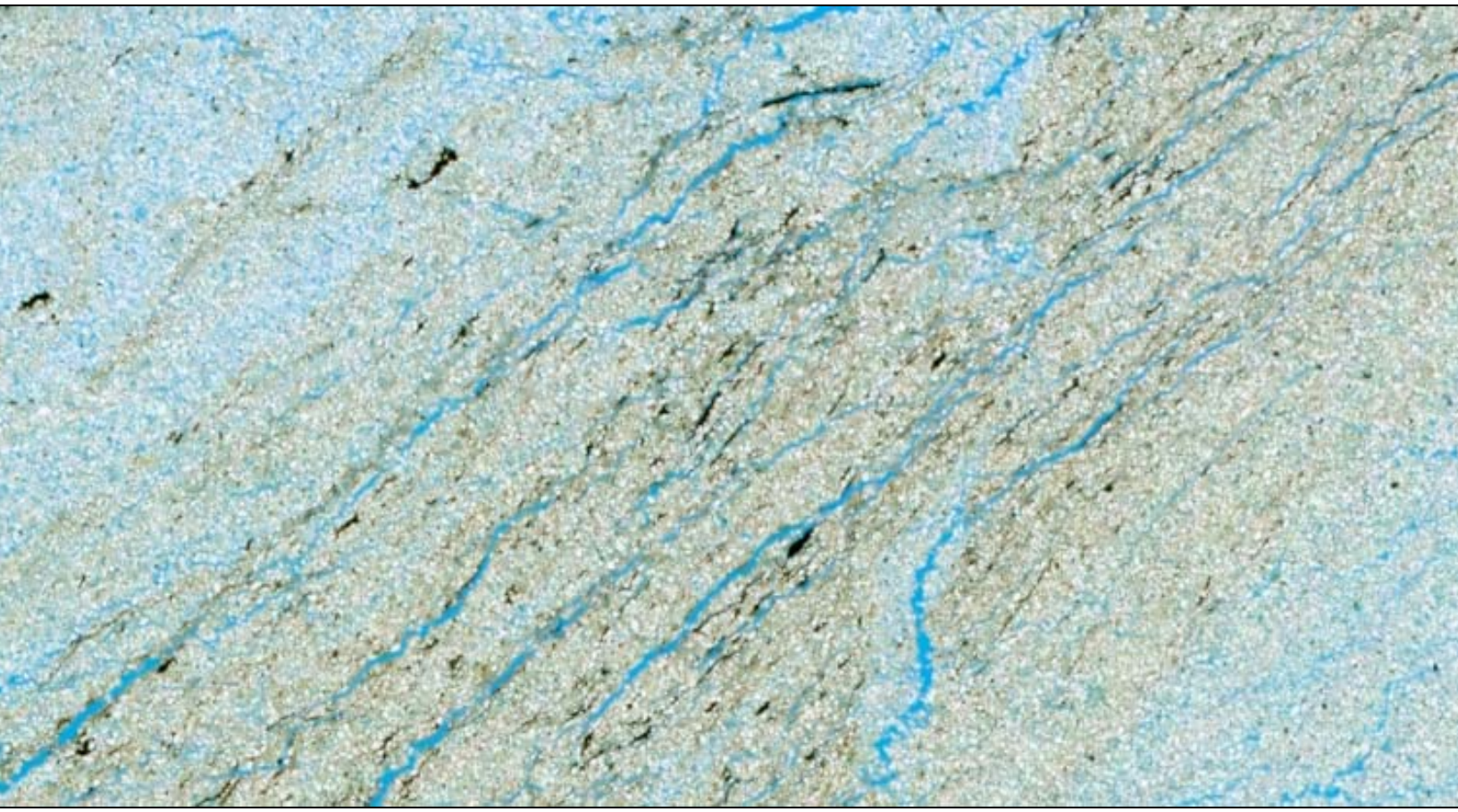

G.I.A. Drost
t1336592
M.H.A. Korenromp
t1310399

August 2009
Applied Earth Sciences
TU Delft
Supervised by dr. M.E. Donselaar

Table of contents

Abstract

The Delft Geothermal Project is an ongoing study in search for the best way to produce renewable energy from the Delft Sandstone Member. So far, a homogeneous reservoir model, a study of the regional geology and a study of the fluid flow and heat transfer have been made. For these studies, information is used from the Moerkapelle oil field located twelve kilometers to the east of Delft. Because of the oil production there, a wealth of subsurface data is available. This thesis used for the first time borehole cuttings data from the well DEL-03. DEL-03 is less then one kilometer away from the proposed drill site.

The aim of this thesis is to discover vertical heterogeneity within the Delft Sandstone Member with a sediment-petrographical analysis. With the use of thin slides of the cuttings of DEL-03 a sedimentary analysis has been made using a polarizing microscope. It goes more deeply into mineralogical content and cement types. Examination of the cuttings with fluorescent light and chloroform proved the absence of residual bitumen, which is a needed for the production of hot water. Also a grain size analysis has been made which was inconclusive.

The content of sandstone in the borehole cuttings analysis does not correspond with the results of the spontaneous potential log of DEL-03. Siderite present as cement in these sections is the cause of this contradiction. The siderite cement has a high influence on the porosity and permeability which is also concluded in the petrographical study of thin slides of plugs of MKP-11. Porosity is detected with the use of the software Image Analysis while the permeability is calculated with the Karman-Kozeny equation. The porosities in the upper part of the Delft Sandstone Member beneath Moerkapelle showed relatively high values and therefore a relative high permeability.

The results of this thesis can be used, together with the many images gathered, as a database for a heterogeneous reservoir model.

Chapter 1

Introduction

Sustainability is a word which roams the hallways of many technical institutes. A big focus area for sustainable development is the energy market. The whole world population and economic prosperity depend on it. One sustainable way of supplying the energy market is geothermal energy. The “Delft Aardwarmte Project” (DAP) is currently developing a project on geothermal energy.

DAP is a foundation which is initiated by students. For over two years they did research into the possibility of supplying TU Delft with geothermal energy by a geothermal doublet. This doublet consists of one well which produces hot water and another injector well which injects the cold water back into the formation. The use of composite drilling and the injection of CO_2 are studied and will be a part of the DAP project. All the research is done by students of Applied Earth Sciences as either a bachelor thesis, a research minor or a master thesis.

The target zone for the DAP project is the Delft Sandstone Member (Smits, 2008). It is identified as stacked distributary-channel deposits in a lower coastal plain setting (Wiggers, 2009). The formation is located in the West Netherlands Basin (WNB), an area in the southwestern part of the Netherlands (Figure 2.01 & 3.01). This basin knew initial Hercynian compressional tectonics with basin inversion in the Late Cretaceous.

The extensional and compressive forces that acted on the WNB during geological time left a tectonic footprint. Due to the tectonic history and the facies heterogeneity of the Delft Sandstone Member it is very difficult to correlate reservoir units between multiple boreholes. Data gathered closely to a project is therefore of great importance for a good understanding of the reservoir characteristics.

The aim of this thesis is to discover vertical heterogeneity within the Delft Sandstone Member with a sediment-petrographical analysis. Permeability baffles must be characterized in order to create a heterogeneous reservoir model. A cutting analysis has been done which reveals the sediment types of the borehole cuttings with their sorting, roundness and contacts just like cement types and mineralogical content. This can be correlated by depth to the spontaneous potential log to verify thoughts on vertical heterogeneities. With a petrographical analysis the porosity and permeability of different sections of the Delft Sandstone Member are calculated and these results can be linked to the results of the cutting analysis.

The well Delft 03 (DEL-03) was drilled west of the Delftse Schie and the railway, close to the Abtswoudseweg (Figure 1.01). DEL-03 is drilled in 1953 and is a vertically drilled borehole. Only two logs are available, a spontaneous potential (SP) log and a deep resistivity log. The cuttings were gathered every two meters. These cuttings have been at the core shed of the NAM in Assen ever since. It are these cuttings which hold, with their small relative distance to the proposed well sites for the DAP project, valuable information about the lithofacies heterogeneity within the Delft Sandstone Member.

The well Moerkapelle 11 (MKP-11) was drilled in between Zoetermeer and Moerkapelle in 1977 to evaluate hydrocarbons (Figure 1.02). It is a deviated well which is plugged and abandoned. The NAM was the drilling supervisor and the cores are stored in their core shed in Assen.

This paper will contribute to a dynamic model of the water flow through the Delft Sandstone Member in the area of the TU Delft that is to be constructed. The new materials gathered for this project are cuttings from DEL-03, thin slides of these cuttings and thin slides of plugs and chips from MKP-11. With this new information the search for permeability baffles can start. This thesis is also made as documentation for a correlation study between the DEL-03 and the MKP-11.

In chapter 2 and 3 the regional geology and stratigraphy are discussed. In chapter 4 the data and methods are described, where after a grain size analysis of the grains follows. Then the results of the cutting study will be discussed and also linked to the logs of the well DEL-03 in chapter 6 and 7. Furthermore, the petrographical analysis of the thin slides of well MKP-11 and its results are presented in chapter 8 and 9. The conclusions and recommendations form, together with the acknowledgements, the end of this thesis.

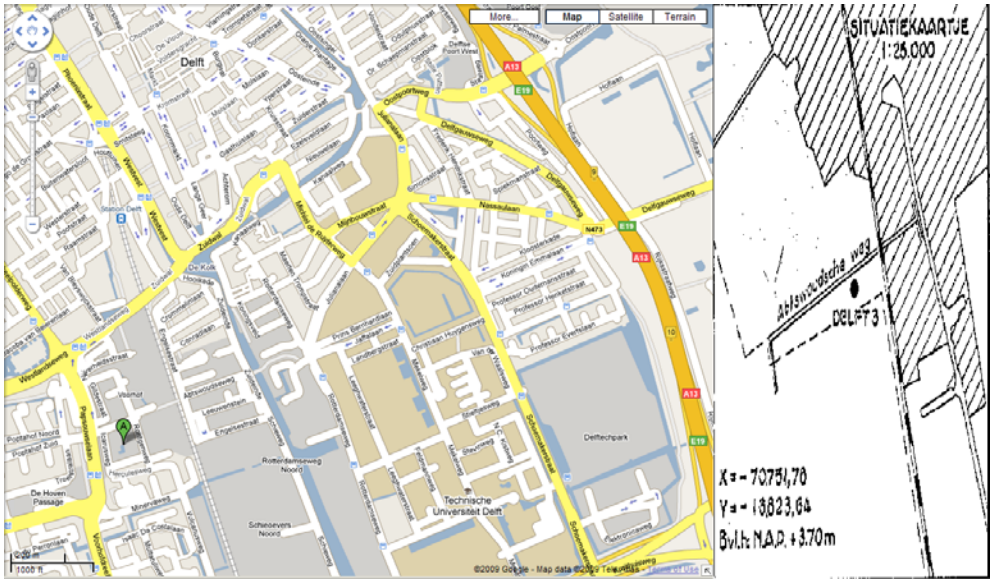

Figure 1.01: The green balloon is the location of DEL-03 (http://maps.google.nl/ & www.nlog.nl, 2009)

Figure 1.02: The red balloon is the location of MKP-11 (http://maps.google.nl/ & www.nlog.nl, 2009)

Chapter 2

Regional geology

Evolution of the West Netherlands Basin

The West Netherlands Basin (WNB) is located in the southwest of the Netherlands. It takes up an onshore area as well as an offshore area as can be seen on figure 2.01A. It is known as a gas province in the Netherlands and hydrocarbon accumulations *(figure 2.01B)* are mainly found in structural traps, formed by the reactivated faults, so called flower structures (De Jager, 2007) *(Figure 2.02, page 8).* To the south, the basin is bounded by the London-Brabant Massif and to the north the WNB is separated from the Central Netherlands Basin by the Zandvoort Ridge and Ijmuiden High (Van Adrichem Boogaeart & Kouwe, 1993 – 1997). Van Balen et al. (2000) have divided the history of the West Netherlands Basin into four stages from the Late Carboniferous to the Tertiary.

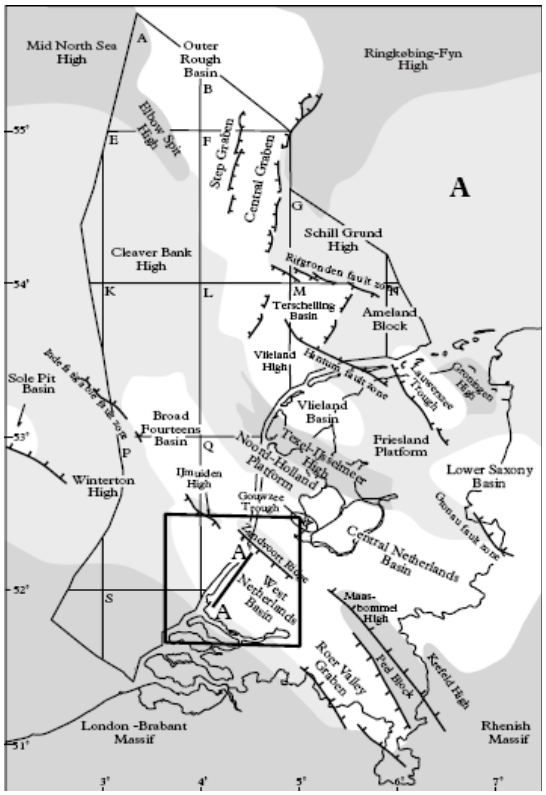

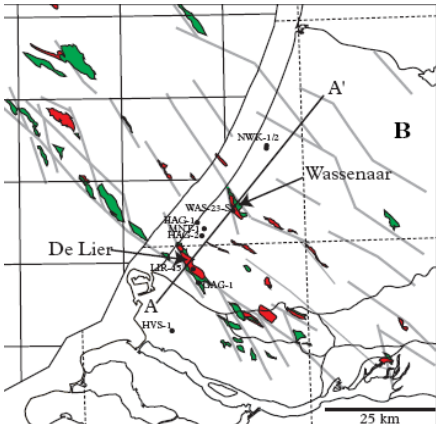

Figure 2.01:
A: Position on the map of the WNB. The box indicates figure 2.01B on the map and the line A-A' is the cross section shown in figure 2.01C.
B: Detailed view of the WNB. The green fields indicate gas, and the red fields indicate oil. Also are the main fault zones depicted by the grey lines.
C: This is a cross section through the WNB. The Rijnland Group and the Schieland Group are indicated with the green-blue colors. Horizontal scale is in kilometers, vertical in meters.
(NJG van Baalen, 2000 – modified after Van Adrichem Boogaert & Kouwe, 1993-1997)

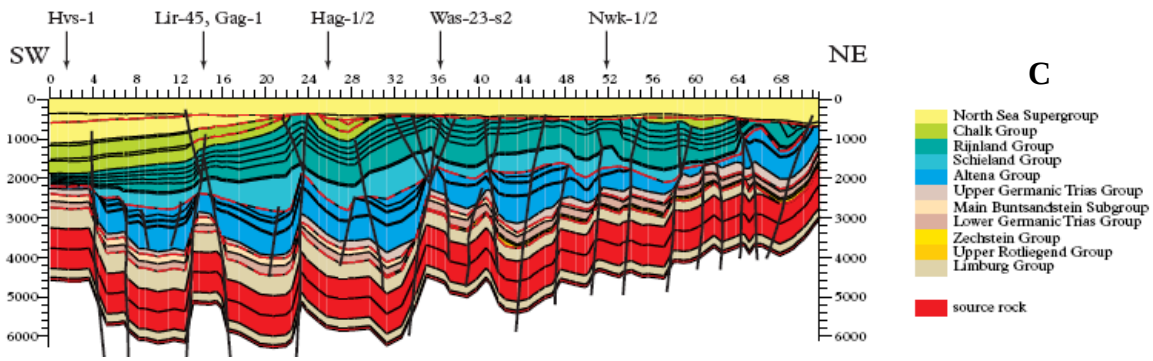

Late Carboniferous – Early Permian Stage
The southwest of the WNB was part of the Variscan basin during this period. During the Variscan orogeny (Westphalian – Early Permian) major faulting, uplift and erosion took place. In the northern part it removed 500 meter of sediments from the Zandvoort Ridge. The erosion of the southern part was much less, because of less uplifting (Van Balen, 2000).

Late Permian – Middle Jurassic 'pre-rift' stage
From the Late Permian onwards, the WNB formed a stable block. The basin was uplifted followed by regional thermal subsidence in the Early Triassic. It now was slightly dipping in northward direction. The sedimentary succession comprises mainly fluvial and aeolian sandstones of the Upper Rotliegend Group, followed by claystones, siltstones and carbonates of the Zechstein Group (Van Baalen 2000).
During the Early Kimmerian tectonic phase (Middle - Late Triassic) the WNB formed a structurally rather simple large - scale half - graben, bounded to the North by a major fault zone.

Late Jurassic – Early Cretaceous 'syn-rift' stage
The strongest rifting occurred during the Late Jurassic to Early Cretaceous, Late Kimmerian rifting. This caused the breaking-up of the basin in various subunits and large thickness variations in the Late Jurassic basin infill, which were locally more than 2500 meters thick sands and clays that belong to the largely continental Schieland Group (Figure 2.01C). Adjacent platforms were uplifted; resulting in a widely recognized unconformity. After this, a large open-marine basin formed in which the Rijnland Group was deposited (Figure 2.03). The Rijnland Group consists of up to 1400 meters of mainly fine-grained clastics with coastal sandstones (De Jager et al.)
The Late Jurassic-Early Cretaceous rifting was accompanied by repeated igneous activity, particularly in the southeastern part of the basin. The volcanism is indicative of deep crustal fracturing, which may have had a local impact on maturity. Rifting stopped into the Late Cretaceous, but the subsidence of the WNB continued into the Late Cretaceous (Wong, 2007).

Late Cretaceous – Quaternary 'post-rift' and inversion stages
After the rifting had ceased, compressive forces during the Alpine orogeny caused the inversion of the West Netherlands Basin (De Jager, 2007), which in its turn caused the oil bearing structures in the WNB. The whole basin was covered by sediments during the Maastrichtian Danian, when inversion movement temporarily ceased. Movement during the Paleogene caused more uplift in the basin and therefore hardly any sedimentation took place from that time onwards. The uplift was followed in the Neogene by again a subsidence (Van Balen et al., 2000).
During the syn-rift stage, the West Netherlands Basin filled with sediment from fluvial systems that came from the southeast and followed the southeast northwestern trend of the basin. In the northwest the sea had an entrance into the basin, and in this part of the basin, there was an interfingering of fluvial and marine sediments (Wong, 2007).
The different stress regimes through geological history imply that most of the faults have not only moved vertically, but also oblique. Because of this, it is almost impossible to reconstruct the type and amount of displacement of individual faults during the various evolutionary phases (De Jager, 2007).

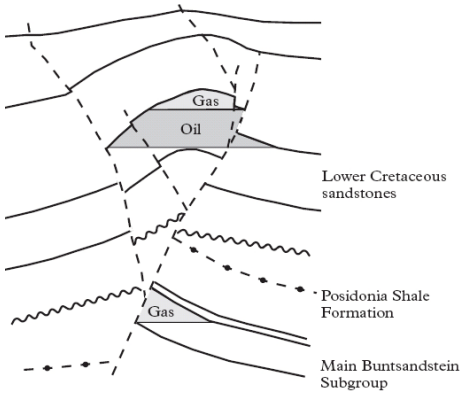

Figure 2.02: Flower structure as a characteristic trap situation in the WNB (Van Baalen et al., 2000)

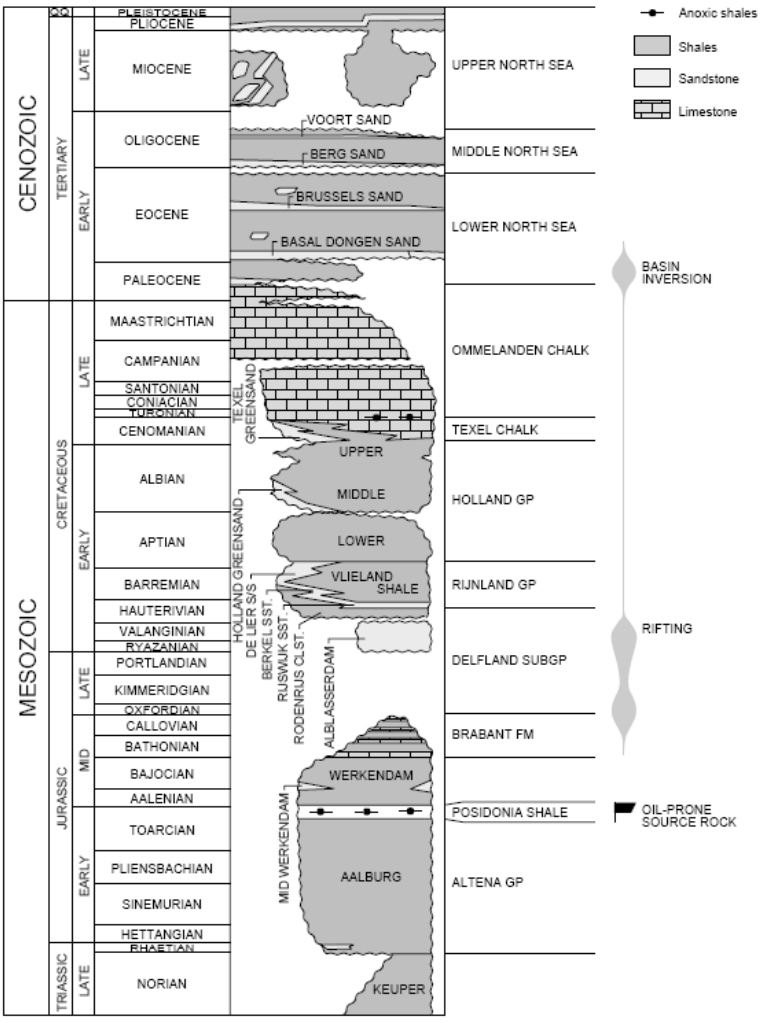

Figure 2.03: Stratigraphic column for the post-Triassic section in the WNB. (Jeremiah, 2002)

Chapter 3

Stratigraphy of the West Netherlands Basin

Several formations were deposited in the West Netherlands Basin (WBN). The significant formation for the Delft Aardwarmte Project (DAP) is the Nieuwerkerk Formation (SLDN), which lies beneath the TU Delft. The Nieuwerkerk Formation is part of the Delfland Subgroup (SLD) in the Schieland Group (SL). The Nieuwerkerk Formation contains three members: the Alblasserdam Member (SLDNA), the Delft Sandstone Member (SLDND) and the Rodenrijs Claystone Member (SLDNR) (Figure 3.01).

Schieland Group

The Schieland Group contains all deposits of the Upper Jurassic and Lower Cretaceous in the Central Graben Subgroup (SLC) and the Delfland Subgroup (SLD). The depositions in the Schieland Group consist of coaly to clayey sandstones, grey and colorful claystones and rare coal seams (Van Adrichem Boogaert & Kouwe, 1993).

Delfland Subgroup

The Delfland Subgroup contains all the formations found in the Vlieland Basin, Central Netherlands Basin, Broad Fourteens Basin, West Netherlands Basin and Roer Valley Graben.

Nieuwerkerk Formation

The deposits in the Nieuwerkerk Formation occur in the West Netherlands Basin or in the Roer Valley Graben. The Nieuwerkerk Formation contains a sequence of typically dark or light grey, red or colorful claystones, fine to medium grained sandstones (with a bed thickness of several meters) and coarse grained thick bedded sandstones. The grey claystones contains some coal (Van Adrichem Boogaert & Kouwe, 1993).

Alblasserdam Member

The Alblasserdam Formation consists predominantly of fluvial-plain deposits. Its thickness varies between less than 100 meters to more than 1300 meters, because of the syn-rift deposition and a rapid pinch-out in a southwesterly direction towards the London Brabant Massif (Figure 3.02). In the channels and crevasse splays sand is concentrated and on the floodplains swamps and soils were deposited. The dominant transport direction in the Alblasserdam Formation is from southeast to northwest (Van Adrichem Boogaert & Kouwe, 1993).
Sediments in the Alblasserdam Formation are of Portlandian to Hauterivian age and vary in color between dark gray to light gray, red and sometimes zones of multiple colors. They and consists of claystones, siltstones and fine to medium grained sandstones (with a bed thickness up to a few meters) and coarse grained sandstones (massive and thick bedded). The gray claystones consist of coal and lignite beds. This formation commonly consists of lignite matter, siderite spherulites and concretions.

Delft Sandstone Member

The Delft Sandstone Member is of Valanginian age and is distributed in the western and central parts of the West Netherlands Basin. The Member consists of a light-grey massive sandstone sequence which is fine to coarse gravelly, fining upward and contains lignite. It is interpreted as stacked distributary-channel deposits in a lower coastal plain setting (Wong, 2007).
The thickness of the Delft Sandstone Member varies between 0 and 130 meters and is, as the Alblasserdam Member, also influenced by syn-rift deposition of sediments.

Rodenrijs Claystone Member

The Rodenrijs Claystone Member is of Late Valanginian to Early Hauteverian age and occurs in the western and central part of the West Netherlands Basin. The Member consists of medium to dark gray, silty to sandy claystones in which laminated bedding, siderite spherulites, concretions and lignite or coal beds are common. Remains of mollusk shells are also found. It is interpreted as a lower coastal plain to lagoonal depositional setting (DeVault & Jeremiah, 2002).

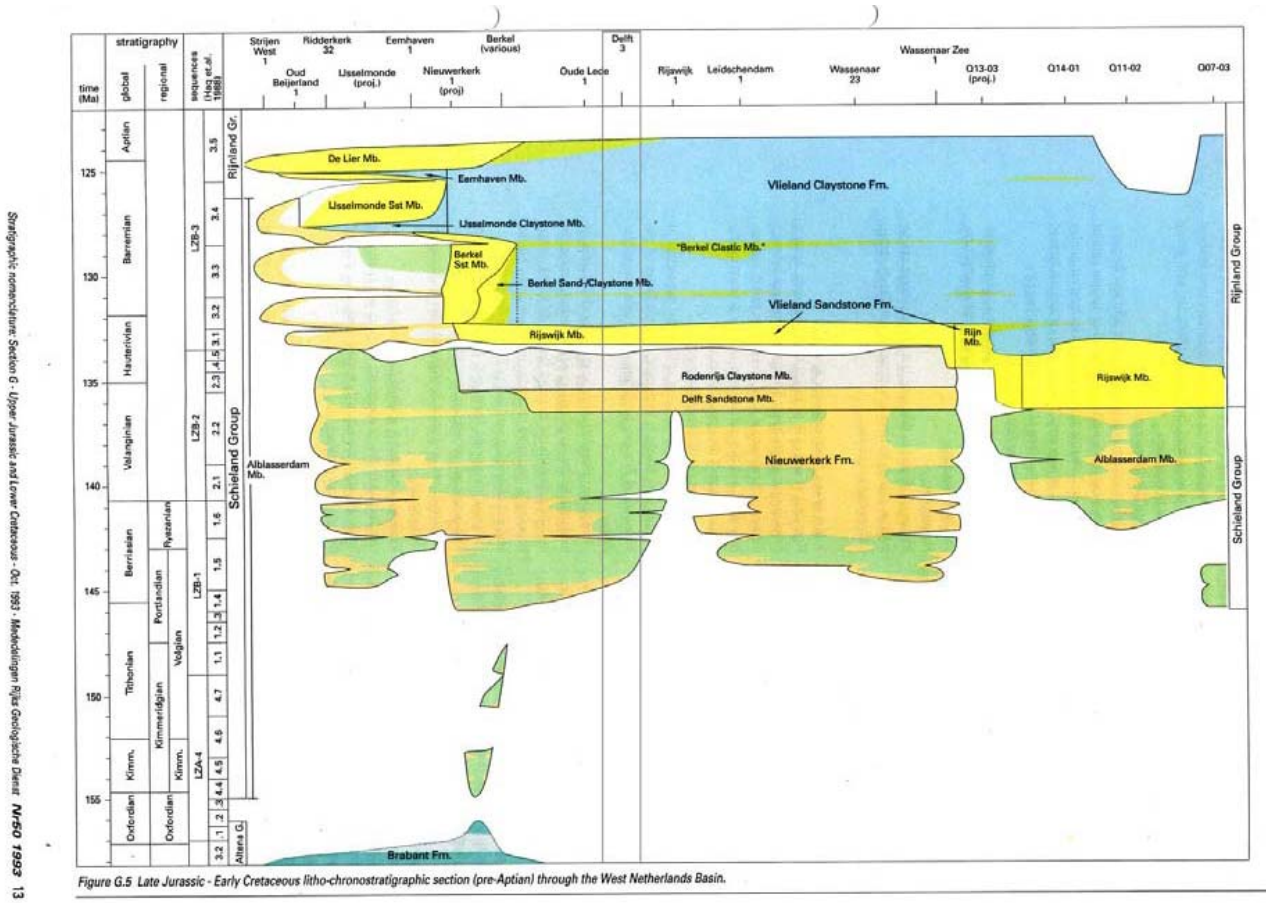

Figure G.5 Late Jurassic - Early Cretaceous litho-chronostratigraphic section (pre-Aptian) through the West Netherlands Basin.

Stratigraphic nomenclature: Section G - Upper Jurassic and Lower Cretaceous - Okt. 1993 - Mededelingen Rijks Geologische Dienst NR50 1993 13

Figure 3.01: Litho-Chronostratigraphic section through the West Netherlands Basin, where the stacking and stratigraphy of the different Members is shown (after Van Adrichem Boogaert & Kouwe, 1993). The Delft area is indicated by the rectangle.

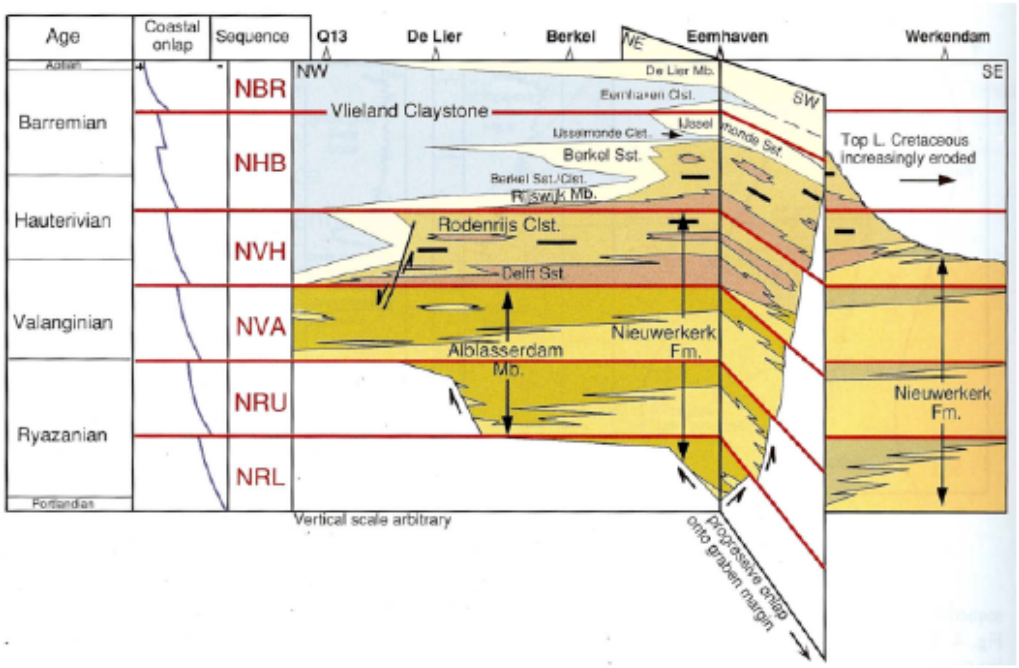

Figure 3.02: Sequence stratigraphic scheme for the Lower Cretaceous of the WBN (den Hartog Jager, 1996).

Chapter 4

Data & methods

For this project data was used from plugs and cuttings of respectively the MKP-11 and the DEL-03.

Company visits

PanTerra agreed to cooperate in the project by the production of thin slides. The material for these thin slides in the form of plugs, chunks and cuttings of MKP-11 and DEL-03 were provided by the NAM. Also a quick cutting study of two days has been performed at PanTerra with the use of stereomicroscopes to examine the contents of the cuttings. This is done one a fraction of the cuttings after sieving (1-2 mm) to safeguard consistency over the whole borehole. Subsequently it seemed that, besides the 1 – 2 mm fraction, the < 1 mm fraction is also very important. Coarse sand grains have a maximum diameter of 1 mm, so most sand grains could be found in the smallest fraction.

Determination of the grain size distribution

To examine the grain size distribution, the fine fraction of the cuttings (<1 mm) is chosen. This fraction contains in respect to the medium fraction more quartz grains. The study is performed in the depth range of 1800 to 1826 meters. From the SP-log, this section contains stacked fluvial channel sandstones. The sandstones with good reservoir qualities, high permeability, contain some or no cement. Therefore they will disintegrate in loose grains easily. The loose quartz grains of very fine to coarse sandstones are much smaller in diameter than 1 millimeter, which determines the reason for the fraction chosen.
The greatest diameter of fifteen quartz grains per interval was measured under a stereomicroscope. The image analysis method was employed to determine the porosity and permeability of the thin slides of the cuttings and plugs. This program is also used to measure diameters of the grains. For one interval the results were compared to the diameters determined with image analysis and the average lies within the boundaries of the standard deviations acquired with image analysis. A statistical analysis has been performed on the results of this study to verify them. The procedure for this analysis is described in chapter 5.

Cutting analysis

Besides the data gathered in the cutting study at PanTerra, each interval in the cutting analysis contains some figures. Photos of the cuttings are made at PanTerra. The overall photo of the thin slides is a scanned image, made in Delft in the image analysis room. The detailed photos of single cuttings were also made there. The data which is given with each cutting is gathered by microscopic research in Delft with a polarization microscope.

Image Analysis

The thin slides of the MKP-11 plugs are analyzed with a polarization microscope in Delft. Of all samples the mineral content, grain sizes, cement type and grain contacts are determined. Overall photos and detailed photos of the thin slides are made in the Image Analysis room and the detailed photos are used for the image analysis process. A detailed step by step description of the image analysis procedure is shown in the flow sheet on the next page.

For the calculation of the permeability the Karman-Kozeny formula for a 2D and 3D method is used. The 2D method is based on a model of grains in a 2D view which are in contact with each other. The perimeter and the area of the pore space used in the 2D formula are calculated with Image Analysis. The following formula is used:

$$k = \frac{\varphi}{\tau * \frac{\pi}{4} * \left(\frac{Perim.}{A} \right)^2}$$

The 3D method is based on a model of grains in a 3D view which are not in contact with each other. The area of the pores and the volume of the grains are calculated with Image Analysis. The following formulas are used:

$$s_{vg} = \frac{A_p}{V_g}$$

$$k = \frac{1}{5 * s_{vg}{}^2} * \frac{\varphi^3}{(1-\varphi)^2}$$

Because some thin slides contain a large amount of clay cement the porosity and permeability could not be calculated of all slides. To check the calculated permeability, a porosity-permeability graph is used which also depends on grain size and sorting (figure 4.01).
A cumulative distribution of the grain size is made for all samples. The description and results can be found in chapter 9.

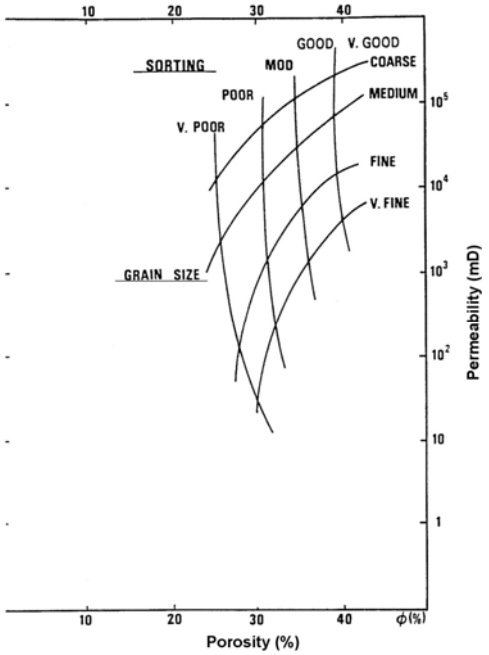

Figure 4.01: Porosity-permeability graph

Flow sheet of Image Analysis procedure

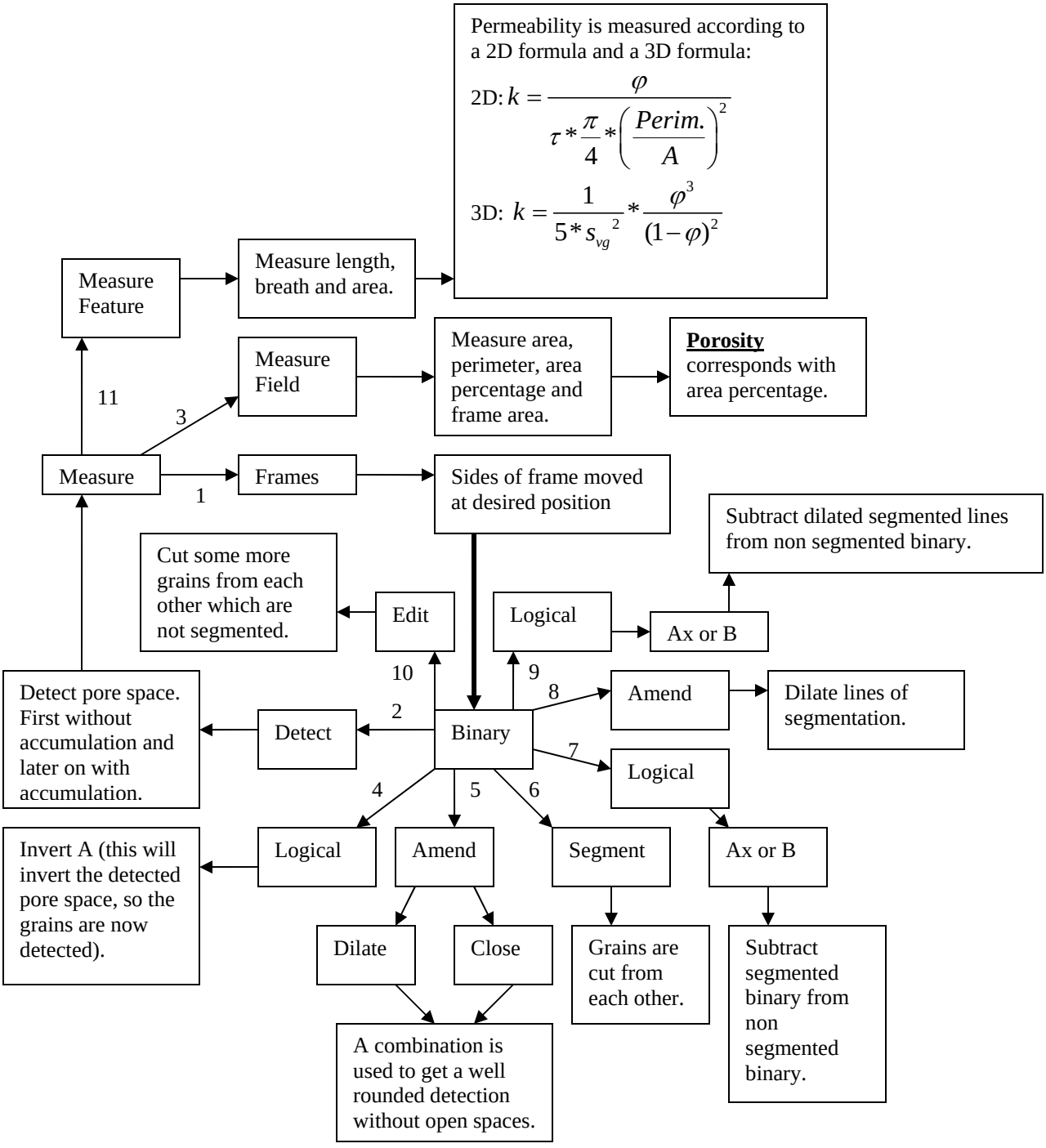

Chapter 5

Grain size analysis

In a study on regional geology is concluded that the Delft Sandstone Member is a fluvial deposit in a lower coastal plain setting where meandering rivers are common (Van Adrichem Boogaeart & Kouwe, 1993 – 1997). The grain size distribution within this Delft Sandstone Member is still unknown. To get more knowledge about this, the following statistical analysis on the grain size distribution is performed.

The grain sizes of fifteen quartz particles per cutting sample are measured. All these cutting samples are in the depth interval of 1798 – 1826 meter. This is the top part of the Delft Sandstone Member which is believed to contain thick sandstone beds. The quartz particles came all from the fraction below 1 mm and were chosen as mean sized particles for that fraction. The arithmetic mean of the diameter is plotted against the depth.

Run tests are based on a sequence of observations arranged in order of occurrence. The observations can only have one of two states. One would assume the observations appear in a random order. The randomness can be tested by examining the number of runs. Runs are defined as uninterrupted sequences of the same state. In our case we have state A which is an increase in grain size and state B which is a decrease in grain size. For the expected mean number of runs and the expected variance in the mean number of runs, only the amount of increases and decreases has to be known, as can be seen in formula 1 & 2. (Davis, 1986)

Formula 1: $$\overline{U} = \frac{2n_1 n_2}{n_1 + n_2} + 1$$

Formula 2: $$\sigma_{\overline{U}}^2 = \frac{2n_1 n_2 (2n_1 n_2 - n_1 - n_2)}{(n_1 + n_2)^2 (n_1 + n_2 - 1)}$$

Formula 3: $$Z = \frac{U - \overline{U}}{\sigma_{\overline{U}}}$$

With:

$\overline{U}$ = expected mean number of runs
U = observed number of runs
σ = expected variance in the mean number of runs
n_1 = runs up in grain size
n_2 = runs down in grain size

Now these two values are known, the Z-factor can be determined. The meaning of the Z-factor is: “the number of runs in the sequence is this many times the standard deviation away from the mean of all runs possible in such a sequence.”

When a horizontal graph segment occurs, one must look at the adjacent line segments. If they have both the same direction, the horizontal segment is a part of this run. Do they have a different direction; one may choose whether it belongs to the upward or the downward run. For the total amount of runs it is obviously negligible and therefore allowed.

- A smaller diameter than the previous meting
+ A bigger diameter than the previous meting

0 A difference in diameter with the previous meting less than 2.5%

Remember, a fining upwards sequence is a relatively high amount of – followed by one +. The data shows us the following sequence:
[- - + - - - + - - + - 0 -]

The diagram gives a graphic representation of the grain size distribution.

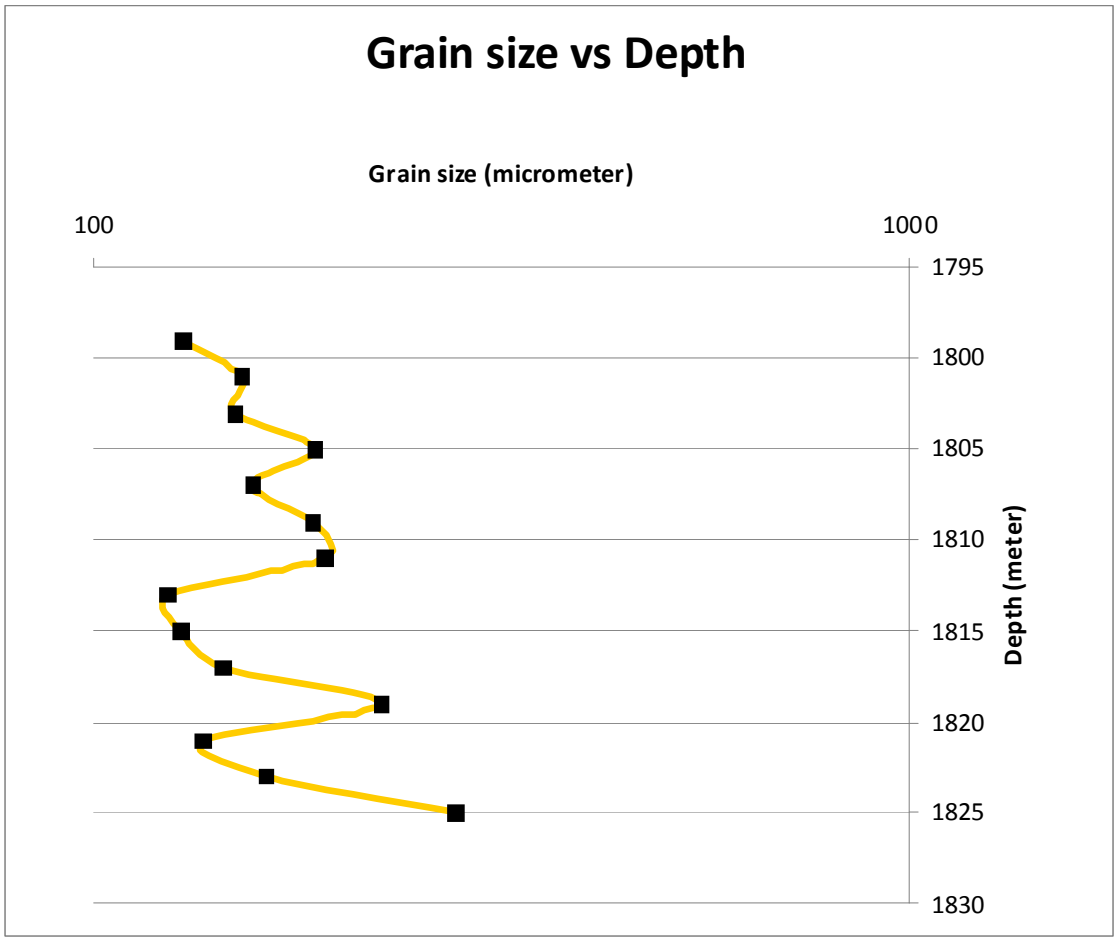

Figure 5.02: Diagram that shows grain size versus depth.

With formula 1, 2 & 3 the following parameters can be calculated:

$\overline{U}$ = 5.6
σ = 1.2
n_1 = 3
n_2 = 4
Z-factor = 1.2

A two-tailed test can be used to check if the value for Z, which follows a normal distribution N(0,1), is either sufficiently small or sufficiently large. The hypotheses stated are as follows:

Null hypothesis $H_0 : U = \overline{U}$

Alternative hypothesis $H_1 : U \neq \overline{U}$

Using a 5% level of significance, the critical regions are bounded by -1.96 and +1.96. The Z-factor of 1.2 does not fall in the critical region, so the null hypothesis is not rejected. The conclusion is that the number of runs is random. Therefore, it cannot be said that there is a stacking of fining upward sequences or any other succession of grain sizes.

Why is it impossible to show a trend in the grain sizes in the Delft Sandstone Member underneath Delft?

First of all, each cutting sample is a representation of an interval of two meters. The calculated vertical thickness of the sandstone bodies in the core vary from 1.8 to 9.5 meters with an average thickness of 5 meters. On average there are only two data points per individual sand body. This data is derived from MKP-11 cores. Exact thicknesses are reported in the thesis of Loerakker (2009). Secondly, the amount of data per interval is too low. The amount of fifteen measurements per cutting sample is too low for a statistical analysis. However, to achieve hundred grain diameters by hand per cutting sample is too time-consuming. At last is the grain size distribution of sediments skewed. This is the case with all sediments in every geological setting (Davis, 1986). If the logarithmic value of the grain sizes is plotted instead of the real grain sizes, the distribution becomes nearly normal. These variables are called lognormal.

Sadly, there is no statistic significant result which concludes that we deal with a series of stacked fining upward sequences. These fining upward sequences would have represented one point bar each. The section of the borehole would show a river with a changing course where point bars cut into each other. The overall fining upward trend of figure 5.02 represents a continuing rise of the sea level. The transgression is also observed in the slabs of the MKP-11 at the core shed of NAM. So the sediments were deposited relatively close to the coast, and therefore smaller in grain size.

Further and far more detailed research has to be done to scientifically prove the fining upward sequences in the Delft Sandstone Member underneath Delft. However, the fining upward sequences have been closely looked at in the Moerkapelle oil field and the Delft Sandstone Member in Moerkapelle can be linked by many other parameters to the Member underneath Delft.

Chapter 6

Sample description Delft Sandstone Member DEL-03

How does this chapter work?
This chapter is divided in several intervals. These intervals correspond with a cutting interval from the well DEL-03 of which all information is gathered. Each interval contains the following:

- An estimation of the content on the fraction of 1-2 mm of the cuttings
- At least two photos of the fraction of 1-2 mm and the fine fraction of <1 mm or some rarities.
- A photo of the whole thin slide of the cuttings of that section. These cuttings were randomly picked by hand.
- A description of every single cutting in the thin slide.
- Some close-up pictures of special or characteristic cuttings.

Some photos of cuttings are made with crossed nichols, this is a view with the polarizer and the analyzer enabled. All cuttings are numbered so it is easy to refer to them.

As accessorial minerals tourmaline is spotted most frequently. It is mostly present in sandstone, but has also been observed in claystones. Also chert, microcrystalline quartz, has been seen a lot. Furthermore, zircon has been present in numerous thin slides. Sporadically some other high relief minerals have been spotted. Most likely these have been titanite and rutile.

Many untwined feldspars were observed. Much of them looked very much like orthoclase. Twinning has been, with exception of a very few cases, absent.

In the cuttings and the thin slides are some artifacts present, as can be seen on the two pictures on the bottom of this page. Some thin slides were badly polished or were not filled up correct with the blue epoxy. This resulted in loss of a couple of thin slides or parts of thin slides which cannot be described anymore. The photo on the right shows some metal pieces which were separated from the sediments with a magnet. Some other obscurities in the cuttings were leaves, twigs and plastics.

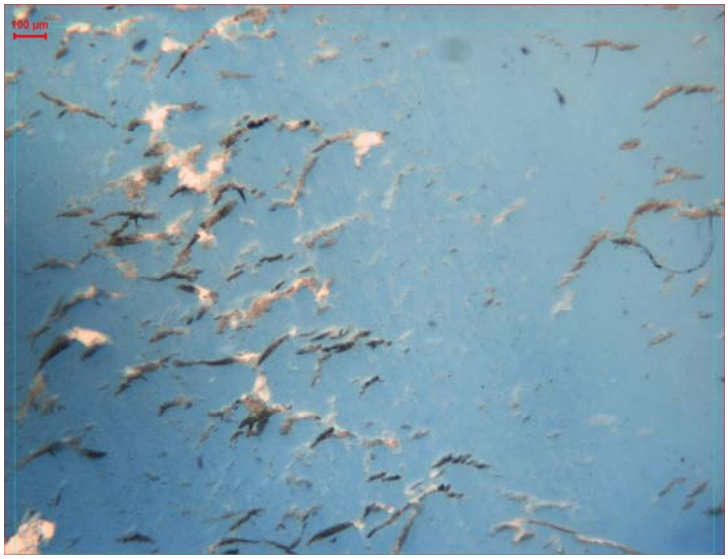

Figure 6.01
Cracks in the epoxy due to bad casting or a bad solidification process.

Figure 6.02
A collection of metal pieces which broke of the drill bit during drilling and came to surface with the cuttings and ended up in the cutting samples.

1770 – 1772 m

	Sandstone	Claystone	Lignite	Quartz	Other
Content (%)	20	72	3	5	Trace
Color	Yellowish grey	Dark grey to dark reddish brown	Grayish black	Grayish yellow to pale green	Flaky calcite
Porosity (%)	15-20	0-5	5-10	0	

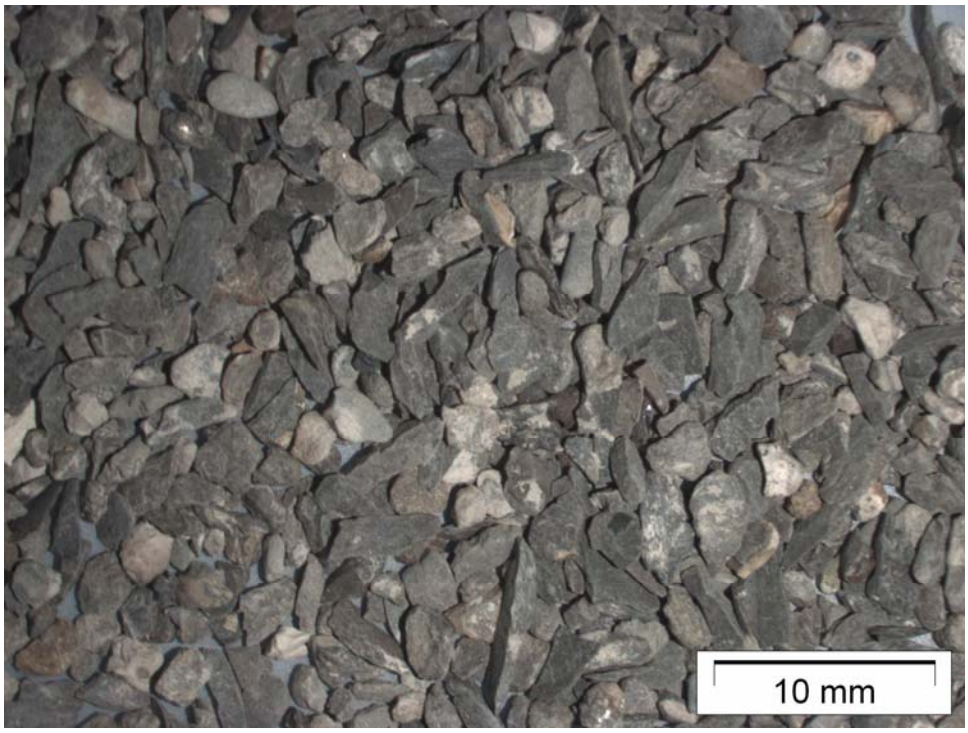

Figure 1770a
This is an overview of the sample. It can be clearly seen that the claystone is in the majority, also the fraction <1 mm contains a lot of claystones.

Figure 1770b
1- Dark grey claystone
2- Laminated calcite
3- Loose quartz grain
4- Dark red claystone, typical for the Rodenrijs Claystone Member
5- Lignite particle

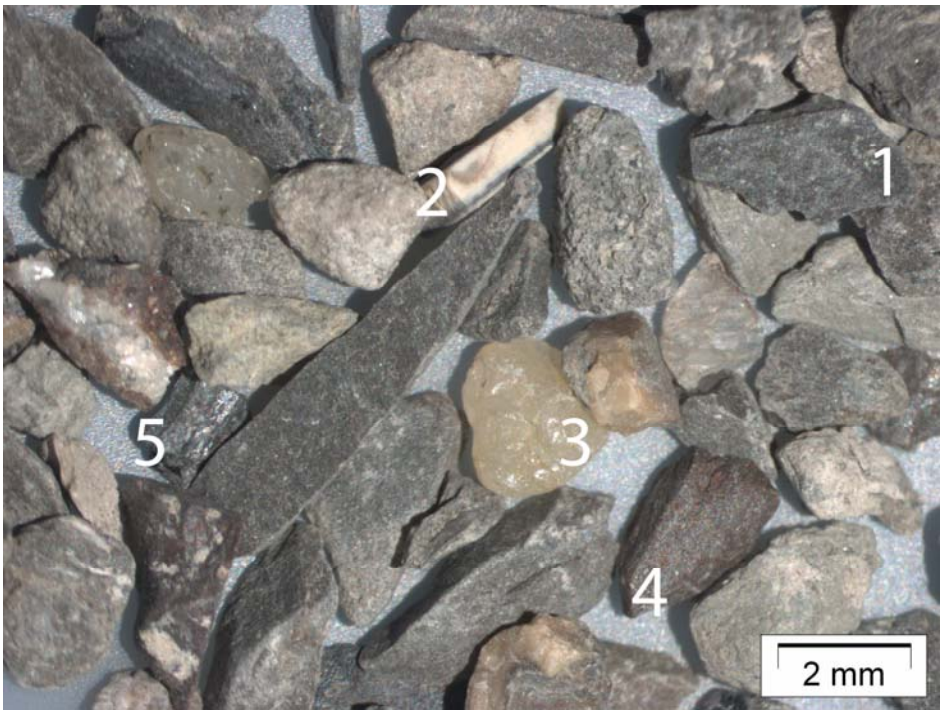

3 siderite cuttings (2, 6 & 7)
Up to 30% mono crystalline quartz, poorly sorted, quartz grains float in a matrix of siderite, 10-50% calcite, very fine grains
2 coal cuttings (5 & 10)
Up to 10% quartz and 20% lignite
1 carbonate rich claystone cutting (11)
Up to 25% siderite and calcite, 5% lignite particles, lots of micaceous clay present which holds everything together, 10% sub angular quartz grains
1 siltstone cutting (3)
50% quartz, silt sized
30% micaceous clay
10% muscovite grains
10% pyrite spherulites
3 sandstone cuttings (8, 9 & 12)
Very much alteration, at least 10% feldspars, 5% pyrite
85% quartz, well sorted, no cementation, one cutting does have zones with clay cementation, longitudinal contacts
1 calcitic sandstone cutting (4)
65% quartz, point to concave-convex contacts, sub angular, moderately sorted
10% feldspar, alteration clearly visible
25% calcite, appears more as replacement than as cement, no diamond shapes spotted, some clay cement present in the pores
1 micaceous claystone cutting (1)
35% sub angular quartz grains in a matrix of micaceous clay
1 badly sliced cutting (13)
Some quartz grains visible, the rest must be clay, probably micaceous, cutting is sliced too thin and epoxy penetrates minerals

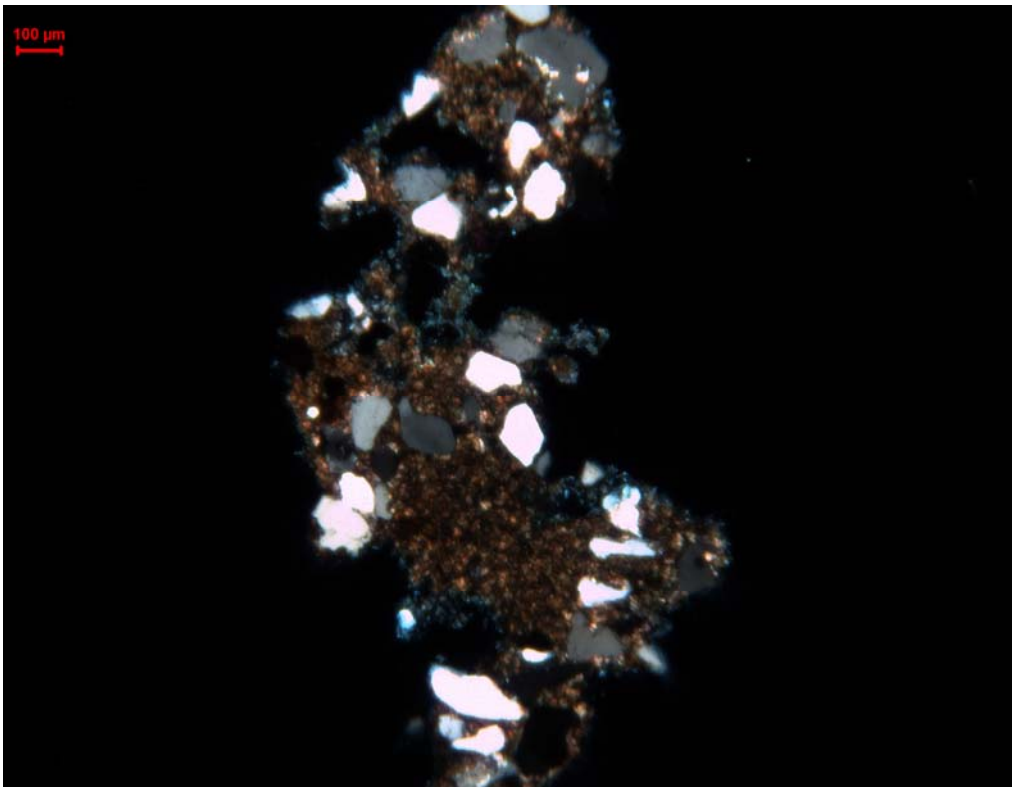

Figure 1770c; cutting no. 7
Siderite cemented sandstone, view with crossed nichols.

Figure 1770d; cutting no. 8
Altered sandstone

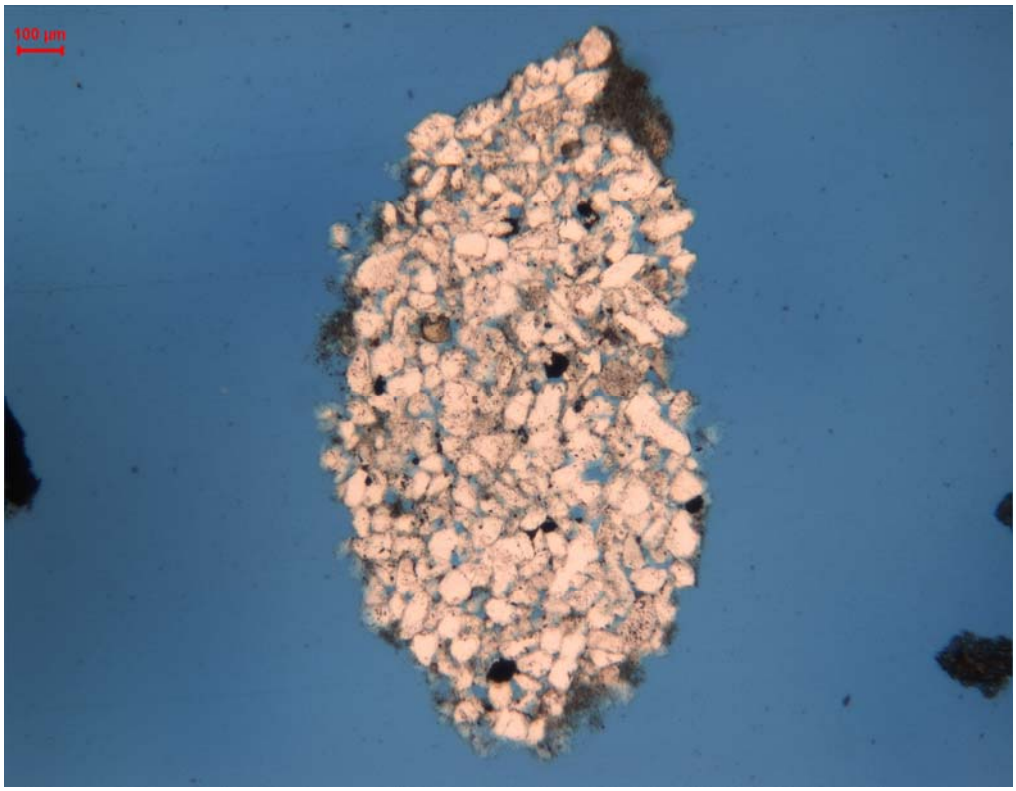

1780 - 1782 m

	Sandstone	Claystone	Lignite	Quartz	Other
Content (%)	45	50	Trace	-	5
Color	Yellowish grey	Grayish black			White clay
Porosity (%)	15-20	0-5			

Figure 1780a
This is an overview of the fraction 1-2 mm. Remarkably, there is no red claystone visible.

Figure 1780b
This is an overview of the fraction <1 mm, a lot of loose quartz grains are visible. This is in contrast with the medium fraction where loose quartz grains are absent. The brown, rusty particle in the center on the upper half of the picture is a part of a drill bit which has not been removed.

3 claystones cuttings (7, 9 & 14)
5-20% quartz
5-20% lignite particles
70% clay, often with high interference colors, only in one particle clearly muscovite
1 siderite cutting (1)
Typical brown (iron) color in combination with high interference colors of a carbonate, small round grains with vague boundaries
10 sandstone cuttings (2 - 6, 8 & 10 - 13)
A lot of weathered grains, some feldspars present, 90% quartz grains, most of the time polycrystalline, sutured grain contacts means pressure solution, on some grain boundaries calcite can be seen, only one cutting fiercely cemented with quartz cement, rest has cementation in some zones
1 quartz/lignite cutting (15)
A couple of quartz grains with a big lignite particle, surrounded with some clay

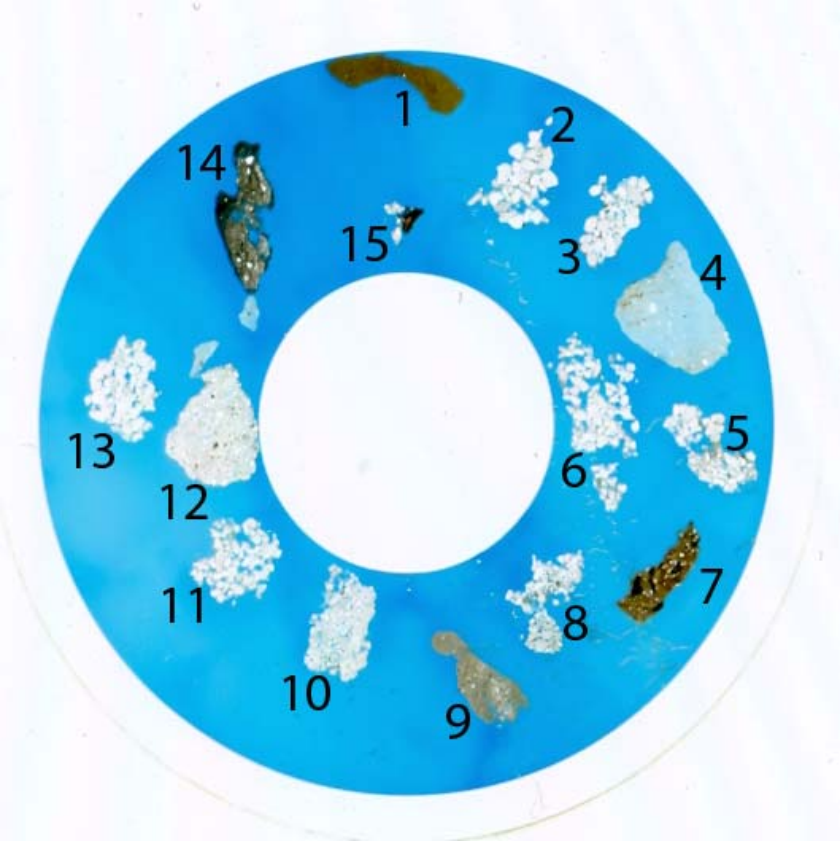

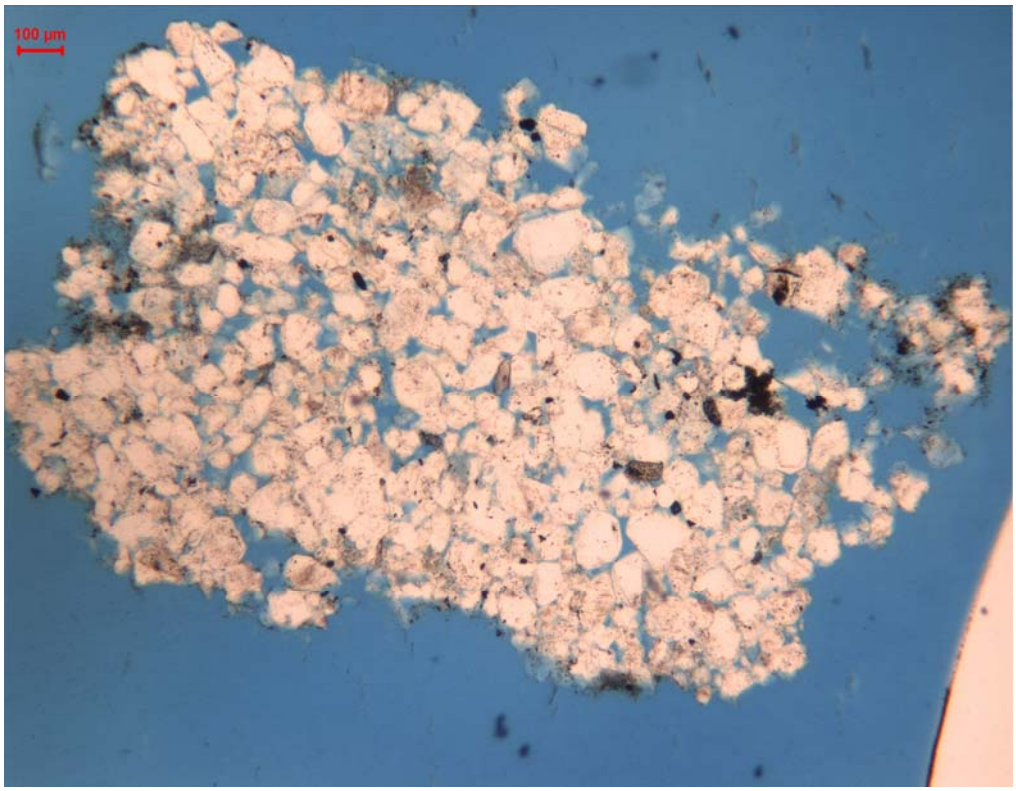

Figure 1780c; cutting no. 10
Sandstone with some porosity visible

Figure 1780d; cutting no. 12
Fiercely cemented sandstone

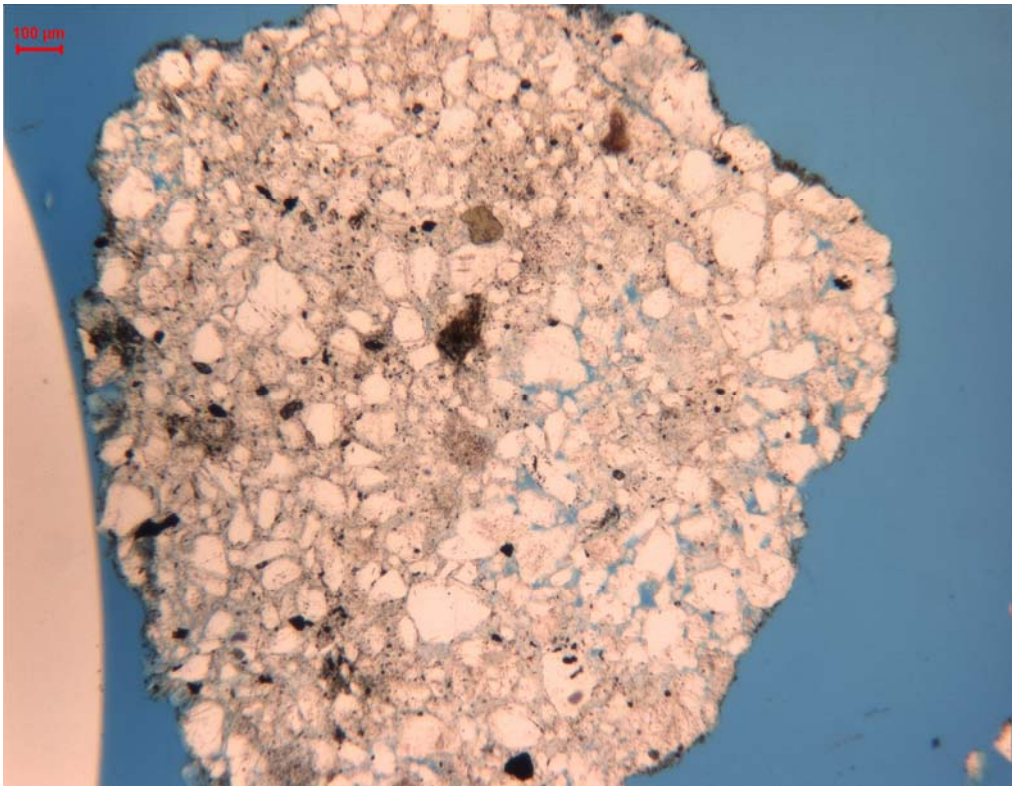

1788 – 1790 m

	Sandstone	Claystone	Lignite	Quartz	Other
Content (%)	50	40	5	Trace	5
Color	Yellowish grey	Medium dark grey	Grayish black		White clay
Porosity (%)	15-20	0-5	0-5		0-5

Figure 1788a
Mix of sandstones, cemented with white clay mineral cement, and claystones from the fraction 1-2 mm.

Figure 1788b
The fraction <1 mm with a lot of loose quartz grains.

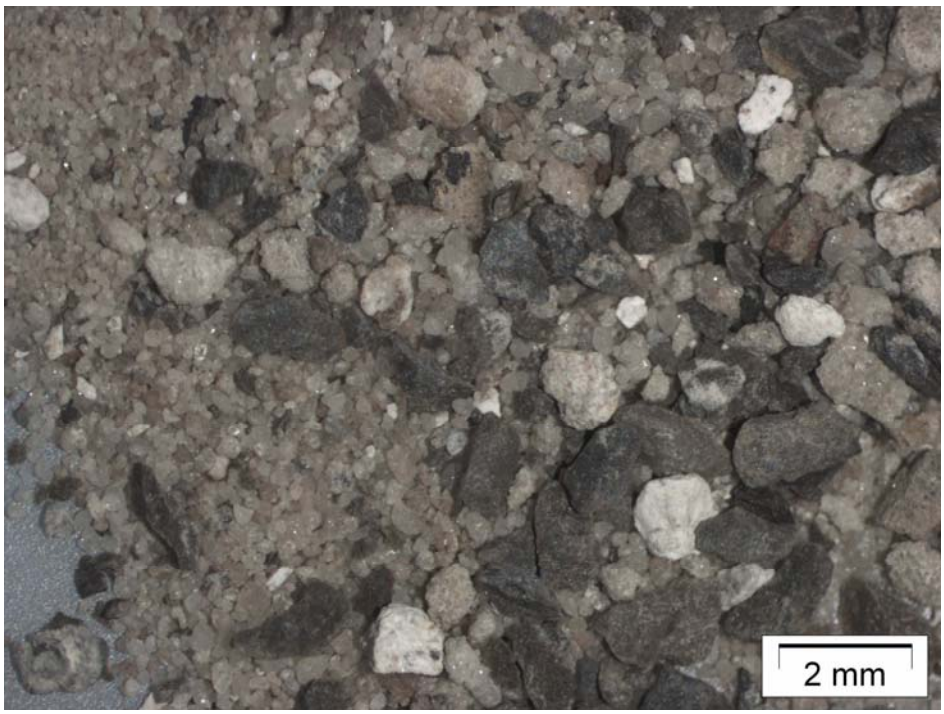

9 sandstone cuttings (1, 2, 4, 7-10, 16 & 17)
Non-cemented, quite a lot alteration, 5% feldspars, 95% mono crystalline quartz, point to concave-convex grain contacts, sub rounded, moderate to good sorting

8 cemented sandstone cuttings (3, 6, 11-15 & 18)
Same content as the other cuttings in this sample, 5% big claystone grains present, clay cement binds the grains, accessorial big muscovite grains

1 micro crystalline quartz cutting (5)
Light blue-green in color, very small quartz grains, close packing, 5% lignite

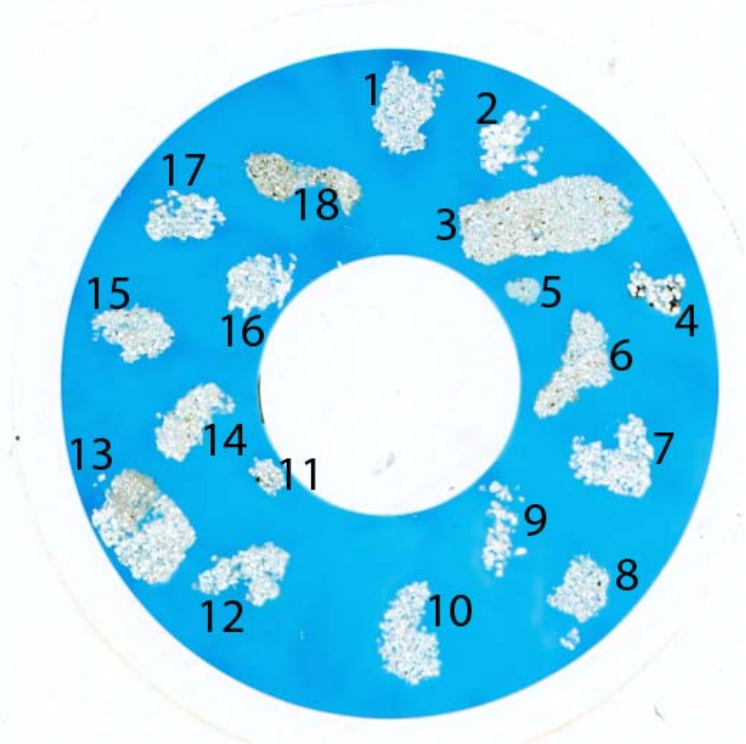

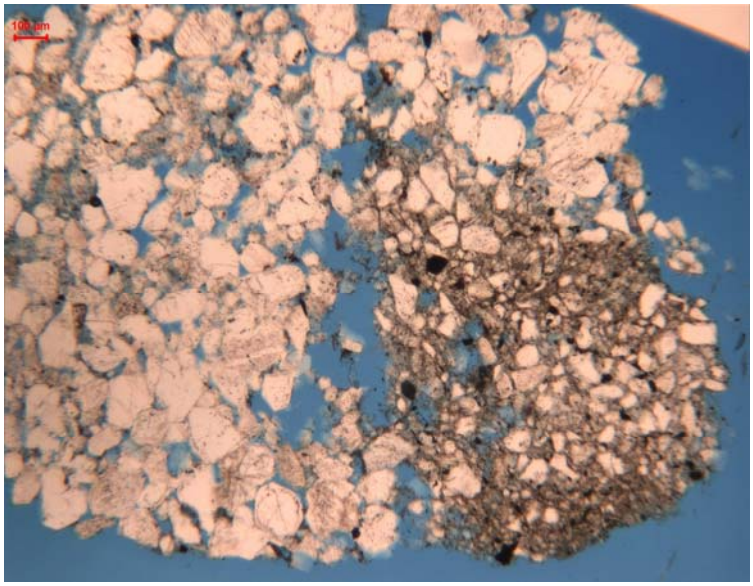

Figure 1788c; cutting no. 13
Sandstone with a zone that contains a high amount of clay cement

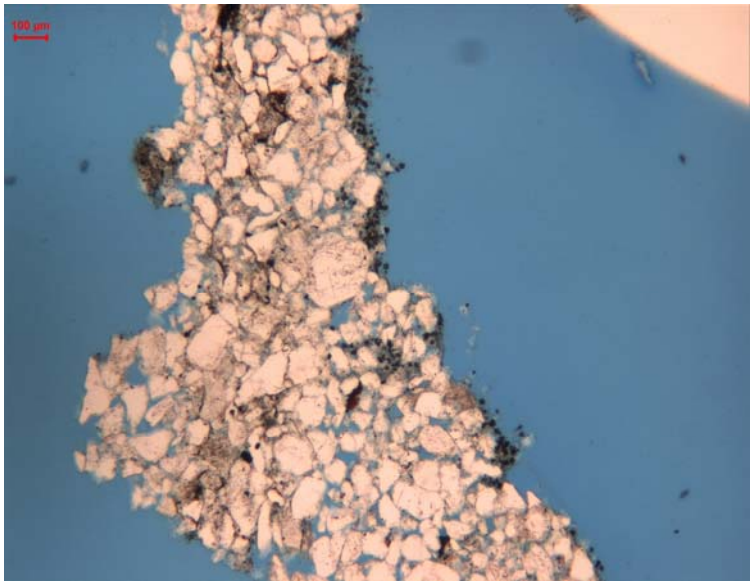

Figure 1788d; cutting no. 6
Dolomite crystals with a diamond shape and a very high interference color as brown dots on the right edge of the cutting.

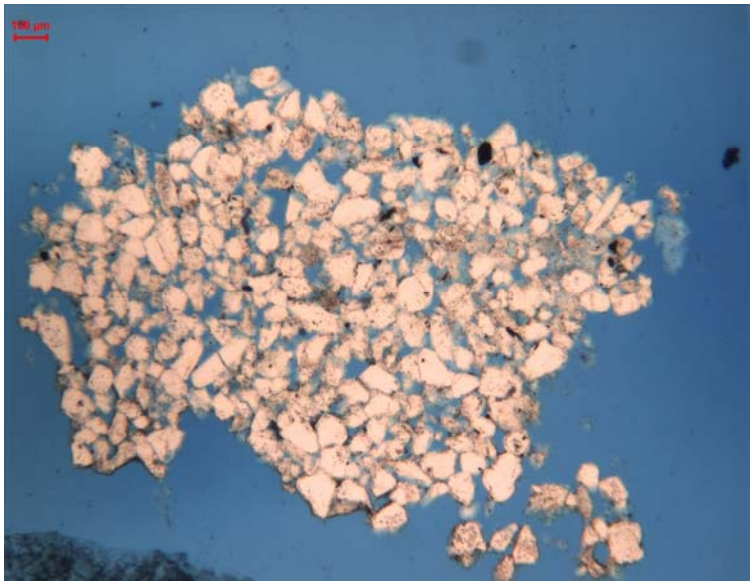

Figure 1788e; cutting no. 1
Nice, clean sandstone with a lot of pore space

1798 – 1800 m

	Sandstone	Claystone	Lignite	Quartz	Other
Content (%)	50	47	3	-	-
Color	Yellowish grey	Grayish black to dark reddish brown	Grayish black		
Porosity (%)	10-25	0-5	0-5		

Figure 1798a
This is an overview of the 1-2 mm fraction. It is evenly divided in sandstone and claystone cuttings. Some sandstone cuttings do have very high porosities.

Figure 1798b
< 1 mm fraction, containing a high amount of loose quartz grains and elongated claystone cuttings.

1 coal cutting (8)
Some well rounded quartz grains present
3 siderite cuttings (10, 11 & 18)
2-10% quartz
Calcite film around quartz particles
Brown-orange color is more intense near fractures and the edge of the cutting.
Two of the particles are bright orange-brown, the other is darker brown. High interference colors can be seen.
1 cemented sandstone cutting (15)
Completely cemented with siderite spherulites, sub angular quartz grains with point contacts almost 'float' in the matrix of siderite
8 sandstone cuttings (4, 5, 7, 9, 12, 13, 16 & 17)
Closely packed and poor sorting, only a small amount of cement present, sub angular, point to concave-convex contacts, some micaceous clay in between the quartz grains (example cutting no. 9)
5 micaceous claystone cuttings (1 - 3, 6 & 14)
0-10% lignite particles
2-5% quartz
In cutting no. 2 there is up to 40% of the total are quartz and lignite present

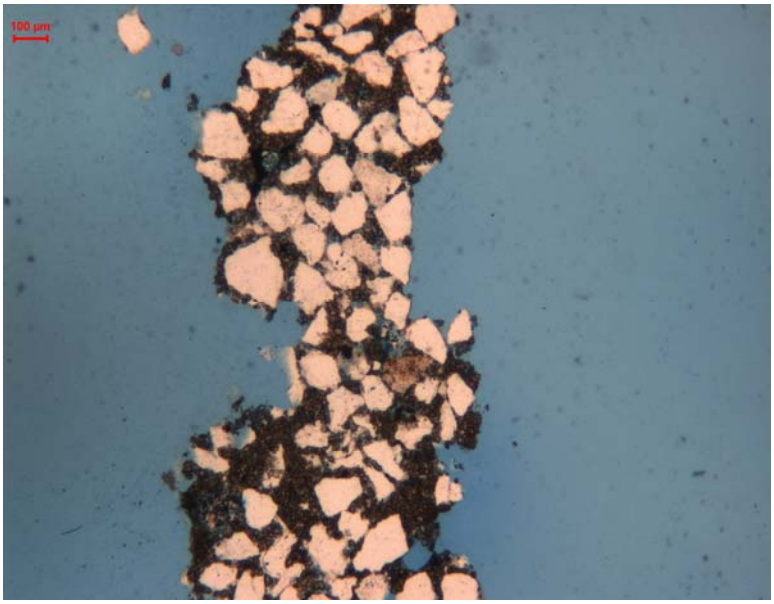

Figure 1798c; cutting no. 15
Sandstone completely cemented with siderite

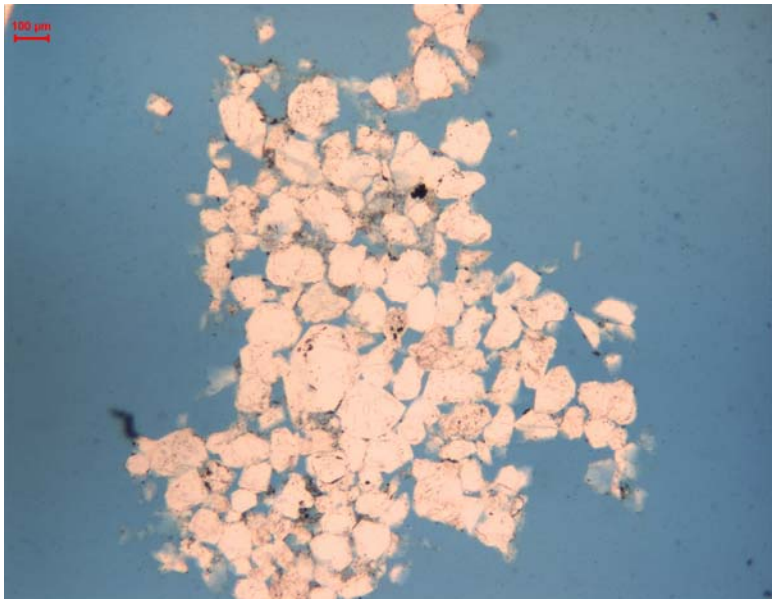

Figure 1798d; cutting no. 13
Sandstone cutting

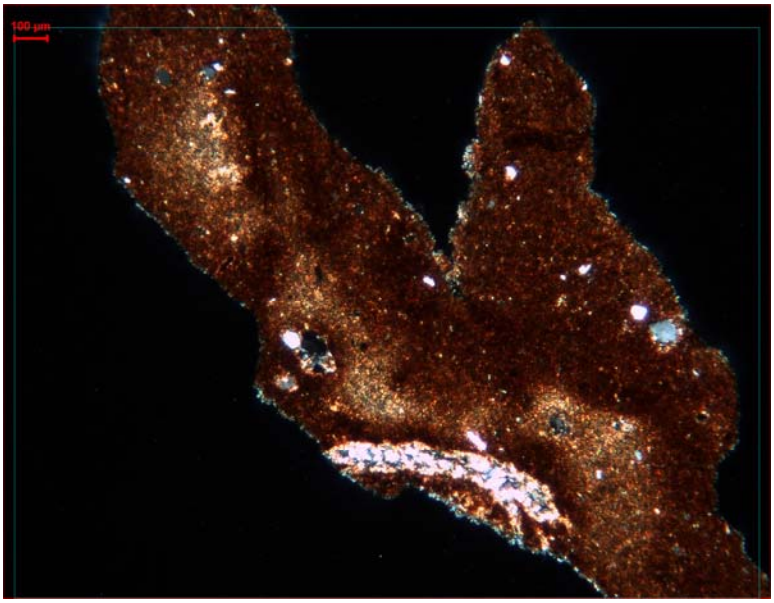

Figure 1798e; cutting no. 18
A view with crossed nichols of a siderite cutting with calcite films around quartz enclosures.

1806 – 1808 m

	Sandstone	Claystone	Lignite	Quartz	Other
Content (%)	62	35	3	-	-
Color	White to yellowish grey	Dark grey	Black		
Porosity (%)	10-15	0-5	0-5		

Figure 1806a
This is an overview of the fraction 1-2 mm

Figure 1806b
Big siderite spherulites on sandstone cuttings

12 sandstone cuttings (1, 2, 4 – 9 & 11 – 14)
Very poorly sorted, lots of little quartz grains fill up the pore space of bigger quartz grains, sub rounded, sutured grain contacts, accessorial muscovite. This all is prove for consolidation, cutting no. 8 contains micaceous clay mineral cement
2 micaceous claystone cuttings (3 & 10)
1-5% lignite particles

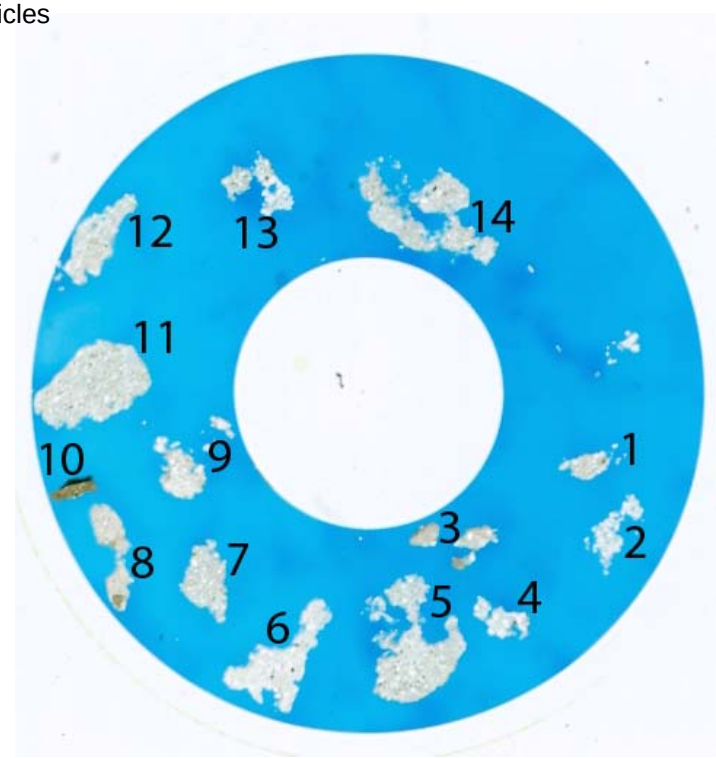

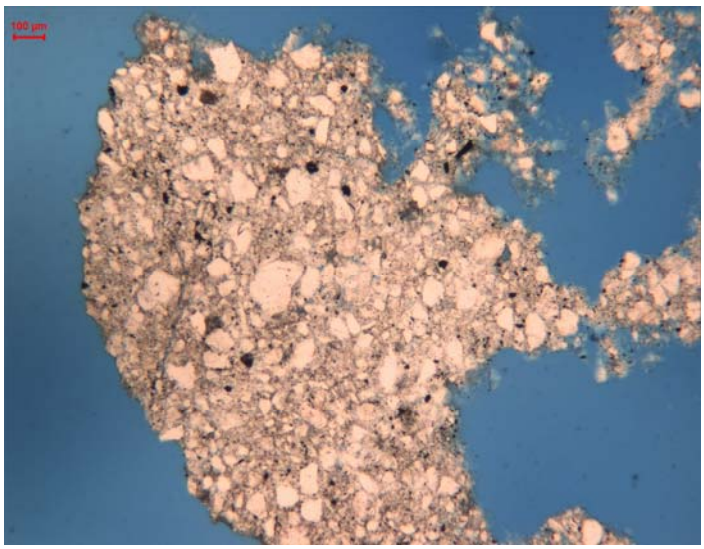

Figure 1806c; cutting no. 5
Fiercely cemented sandstone

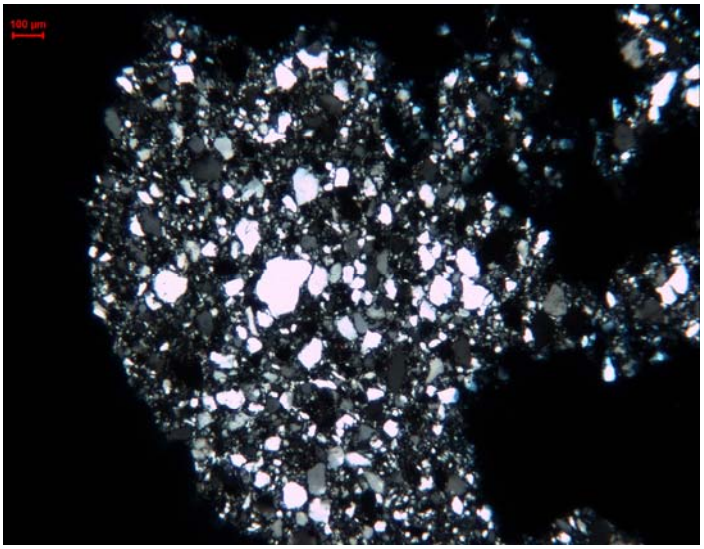

Figure 1806d; cutting no. 5
This is the same sandstone as on figure 1806c, but this time photographed with crossed nichols. From this figure it can be clearly seen that the cement is quartz.

1820 – 1822 meter

	Sandstone	Claystone	Lignite	Quartz	Calcite	Other
Content (%)	60	35	Trace	Trace	Trace	-
Color	Very light grey to yellow	Medium dark grey				
Porosity (%)	10-25	0-5				

Figure 1820a
This is an overview of the fraction 1-2 mm

Figure 1820b
Overview of the sample from the fraction <1 mm. A very high amount of loose quartz grains in this fraction indicates a friable sandstone and gives a wrong image of the sandstone content in the studied fraction.

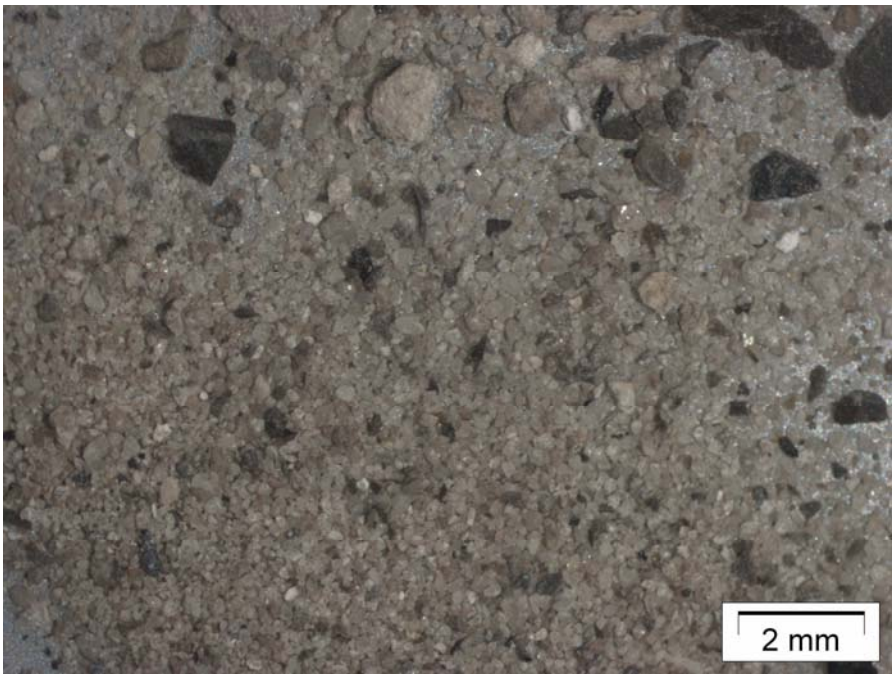

1 micaceous claystone cutting (2)
3 loosely packed sandstone cuttings (1,3 & 8)
Films of clay around the particles containing a high interference color, accessorial chert, lots of porosity visible, sub rounded, moderate to good sorting, point to longitudinal contacts
4 cemented sandstone particles (4 – 7)
Accessorial tourmaline, micaceous clay cement, very poorly sorted, quartz cement, small quartz grains fill up the pores between the bigger quartz grains, sub rounded, not much alteration, some orthoclase, point to longitudinal contacts, the big grains almost 'float' in the matrix of small quartz grains.

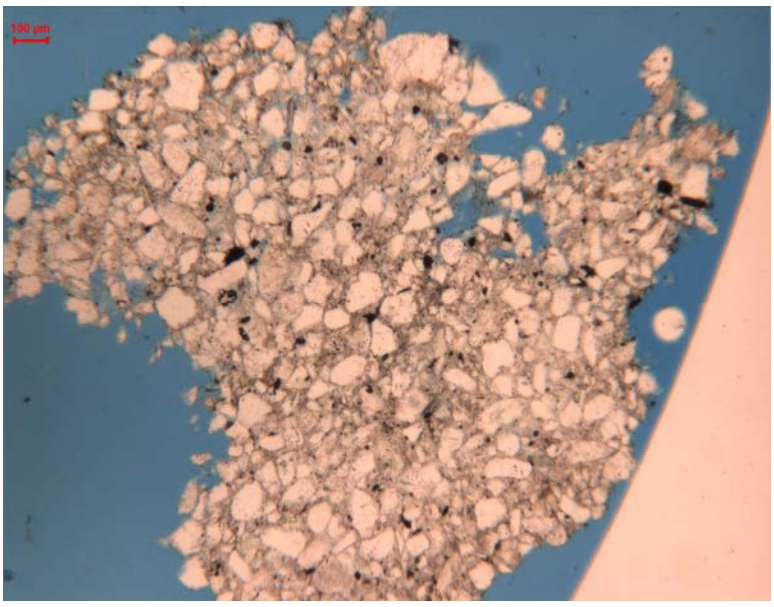

Figure 1820c; cutting no. 5
A cemented sandstone cutting with clay cement, almost no porosity and some lignite particles

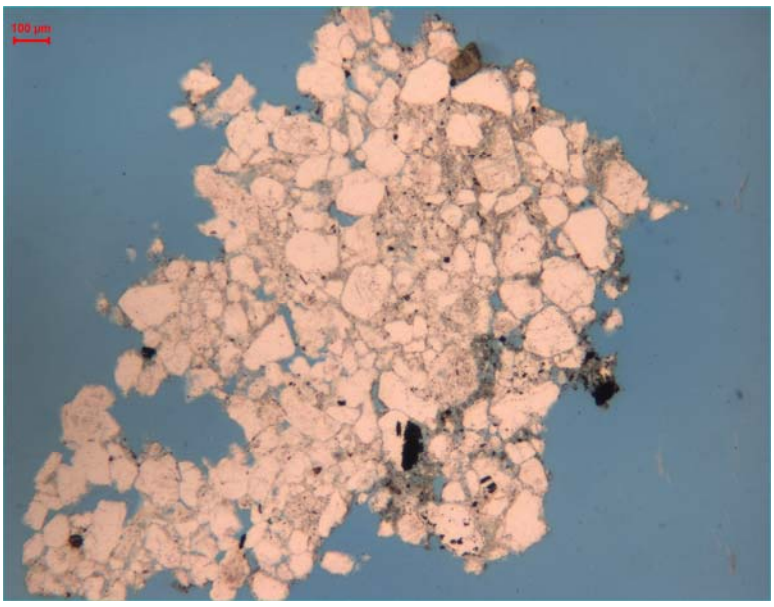

Figure 1820d; cutting no. 7
A sandstone with dominating quartz cement, little porosity visible

1832 – 1834 m

	Sandstone	Claystone	Lignite	Quartz	Calcite	Other
Content (%)	65	30	Trace	Trace	5	Trace
Color	Yellowish grey	Medium dark grey	Grayish black	Yellowish grey		Pyrite and siderite
Porosity (%)	15-20	0-5	0-5	0	0-5	

Figure 1832a
Course fraction (>2 mm), in the lower right corner is a sandstone cutting with small siderite spherulites.

Figure 1832b
1- Pyrite-rich cutting
2- Calcite cutting, possible shell remain
3- Sandstone with white clay mineral cement

Poor quality thin slide, some cuttings cannot be studied.

1 claystone cutting (1)
5% silty quartz grains sub angular
95% clay with colorless minerals with a preferred direction and a very low bireflectance, this may have happened because of the bad preparation of the thin slide, cutting no. 1 lies close to the bad zone, shell fragment present
6 sandstone cutting (2 – 7)
5% orthoclase
95% quartz, sub rounded, poorly sorted, point to concave-convex contact.
Shell fragment, quartz cement, micaceous clay cement, accessorial tourmaline, alteration, calcite replacement, almost no porosity shown

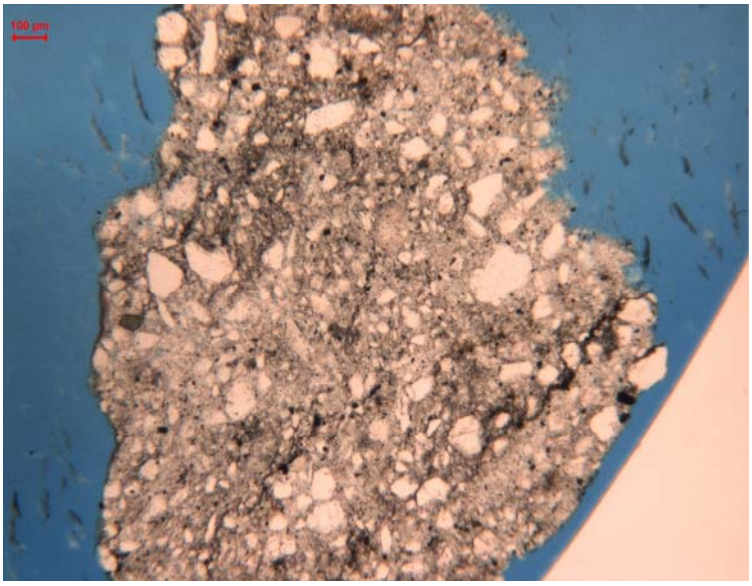

Figure 1832c; cutting no. 6
Fiercely cemented sandstone

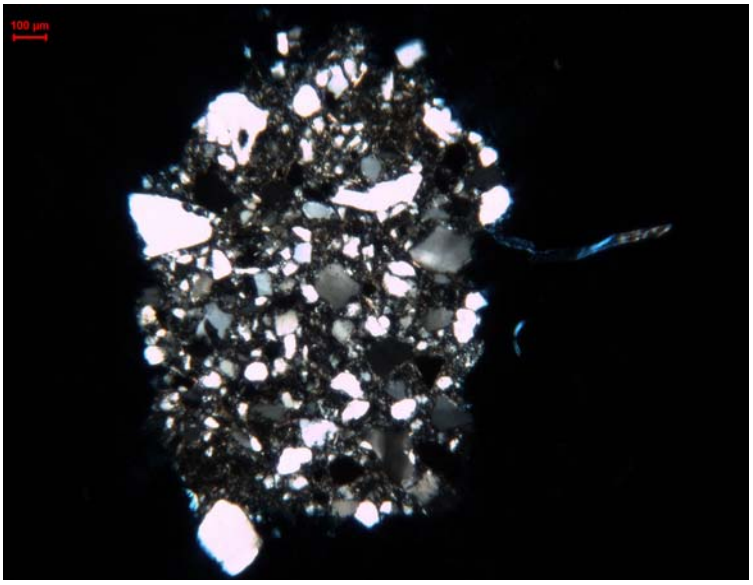

Figure 1832d; cutting no. 5
Cemented sandstone, view with crossed nichols

1840 – 1842 m

	Sandstone	Claystone	Lignite	Quartz	Calcite	Other
Content (%)	65	30	Trace	Trace	5	Trace
Color	Yellowish grey	Medium dark grey	Grayish black	Yellowish grey		White clay
Porosity (%)	15-20	0-5	0-5	0	0-5	

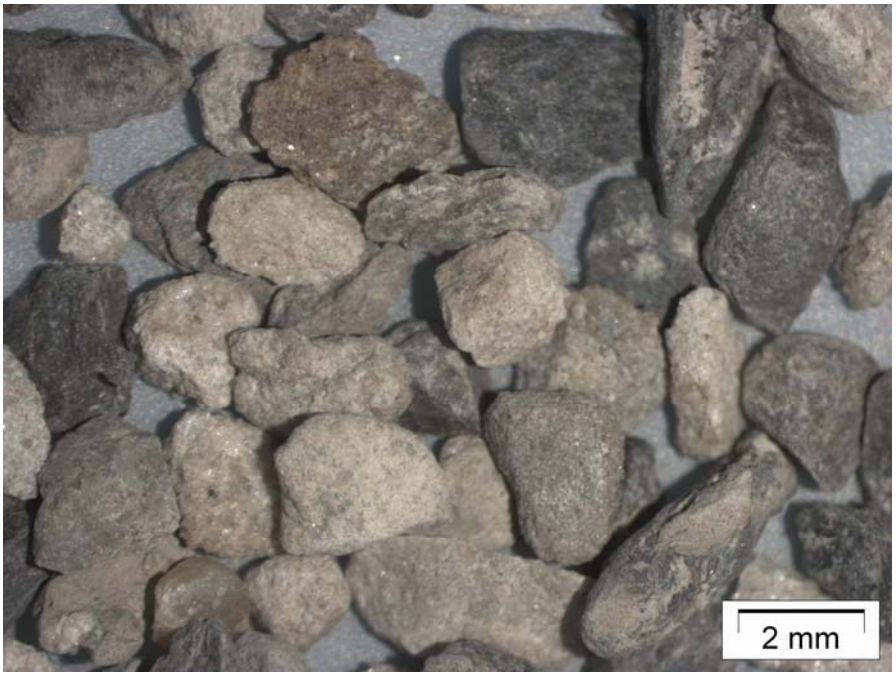

Figure 1840a
This is an overview of the fraction 1-2 mm

Figure 1840b
Fraction < 1 mm with very small loose quartz grains

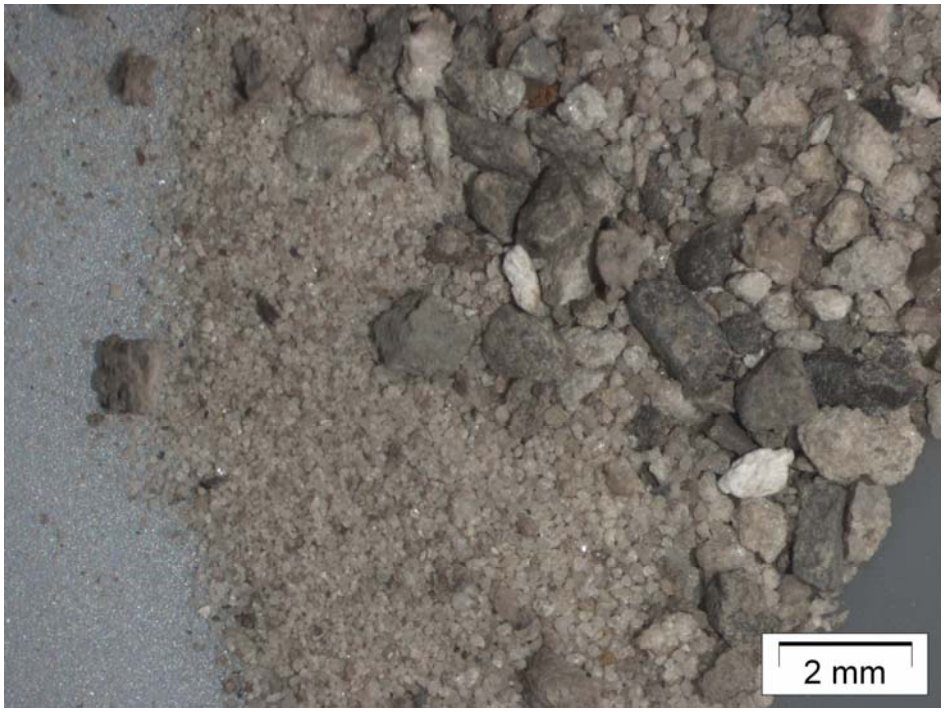

1 coal cutting (6)
1 sandstone cutting (11)
Fiercely cemented with siderite, quartz grains do not have any contact.
8 sandstone cuttings (3 – 5, 7, 8, 10, 13 & 14)
High amount of alteration, accessorial chert and tourmaline,
1% lignite
5% orthoclase
94% quartz (mono- & polycrystalline), sub rounded, poorly sorted, longitudinal to concave-convex contacts, not to poorly cemented with clay, quite a lot porosity visible.
1 claystone cutting (2)
Slightly micaceous, 35% quartz grains, no contact between the quartz grains.
1 claystone cutting (1)
Very fine material, strong brown-orange color.
1 siderite nodule (12)
Occasionally calcite particles, but predominantly brown color of ferric rich siderite, accessorial quartz grains, microcristalline
1 dark blue cutting (9)
Unknown content, probably the epoxy was sucked in the mineral due to wrong preparations

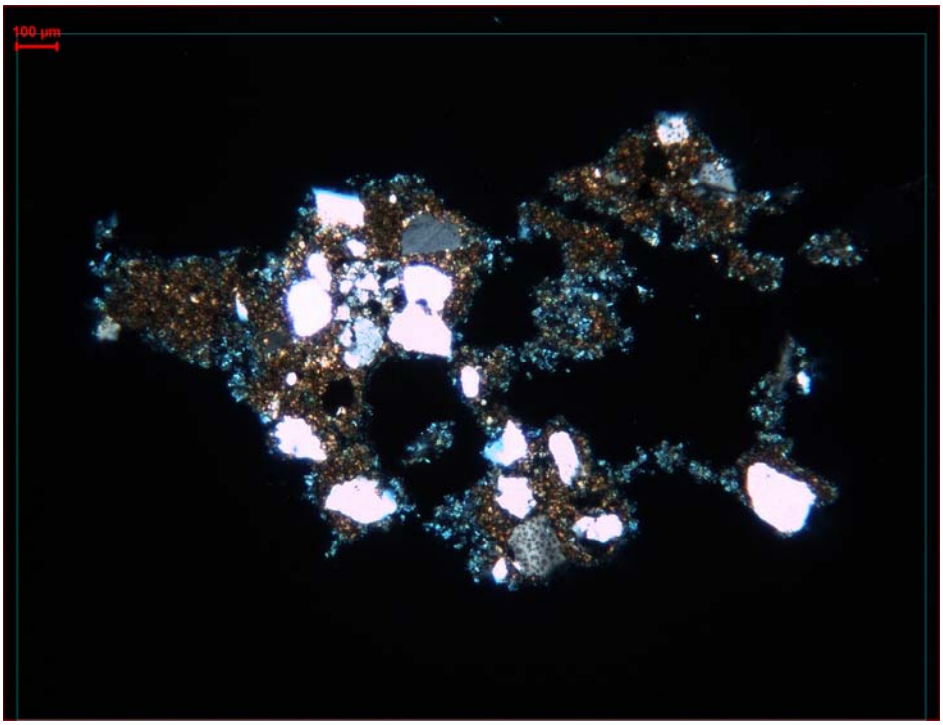

Figure 1840c; cutting no. 11
Disintegrated sandstone with a high amount of siderite cement, view with crossed nichols

Figure 1840d; cutting no. 13
Non-cemented sandstone with a lot of alteration

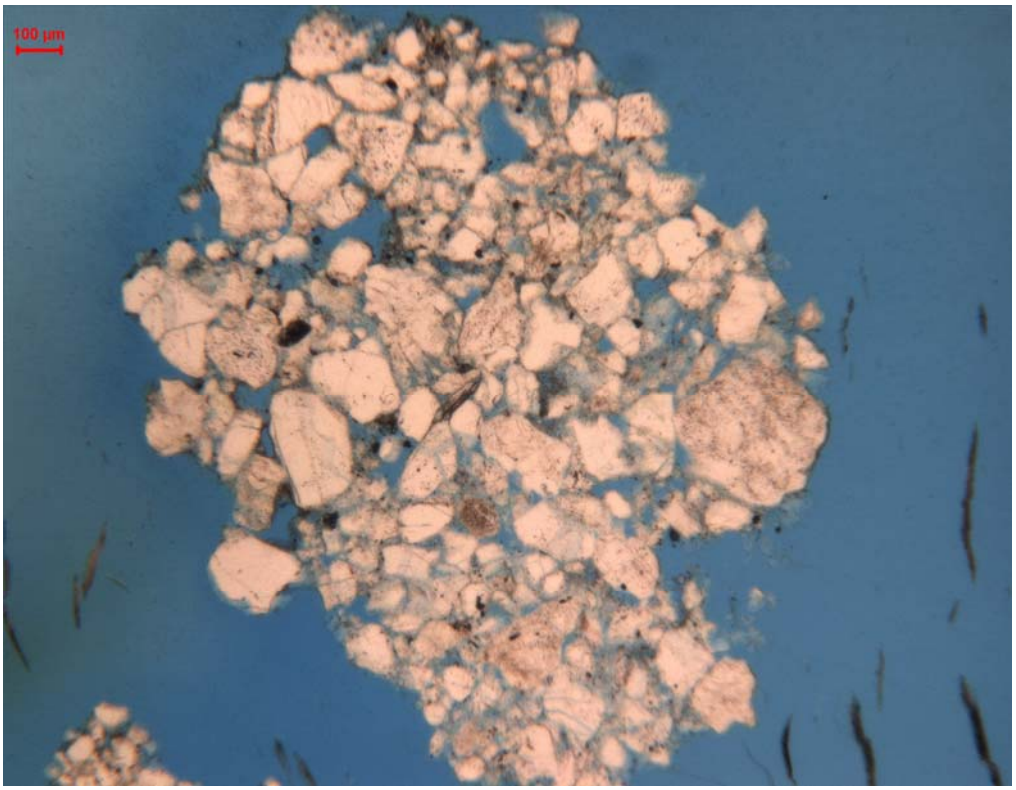

1850 – 1852 m

	Sandstone	Claystone	Lignite	Quartz	Calcite	Other
Content (%)	60	35	5	Trace	-	Trace
Color	Yellowish grey	Medium dark grey	Grayish black	Yellowish grey		White clay
Porosity (%)	15-20	0-5	5	0		

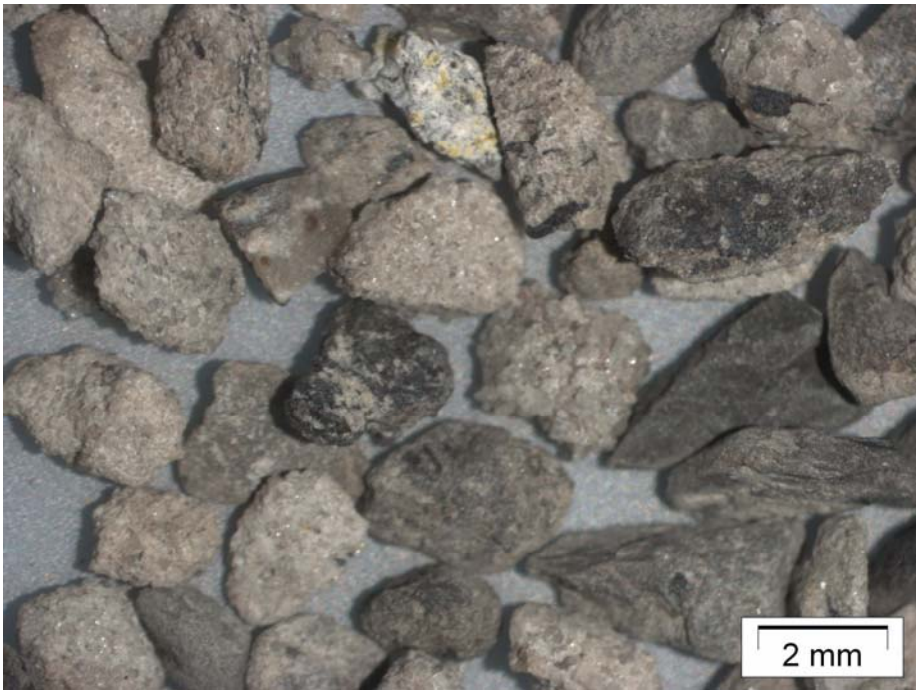

Figure 1850a
A high amount of sandstone with white clay mineral cement is present in the fraction 1-2 mm.

Figure 1850b
Picture of the small fraction (< 1 mm) where you can see the amount of returns is quite low

1 claystone cutting (4)
Brownish tint on most spots, very rich in mica, some lignite particles, 10% quartz grains, rich in biological components.
3 sandstone cutting with more than 10% lignite (7, 8 & 11)
Accessorial chert and tourmaline, little porosity visible, high amount of alteration, some orthoclase, 90% quartz grains, sub angular, moderate sorting, poorly cemented but some clay present in the pores, concave-convex contacts.
11 sandstone particles (1 – 3, 5, 6, 9, 10 & 12 – 14)
Lots of porosity visible, only some zones show micaceous clay cement, accessorial tourmaline and chert, sub rounded, moderately sorted, longitudinal to concave-convex contacts.

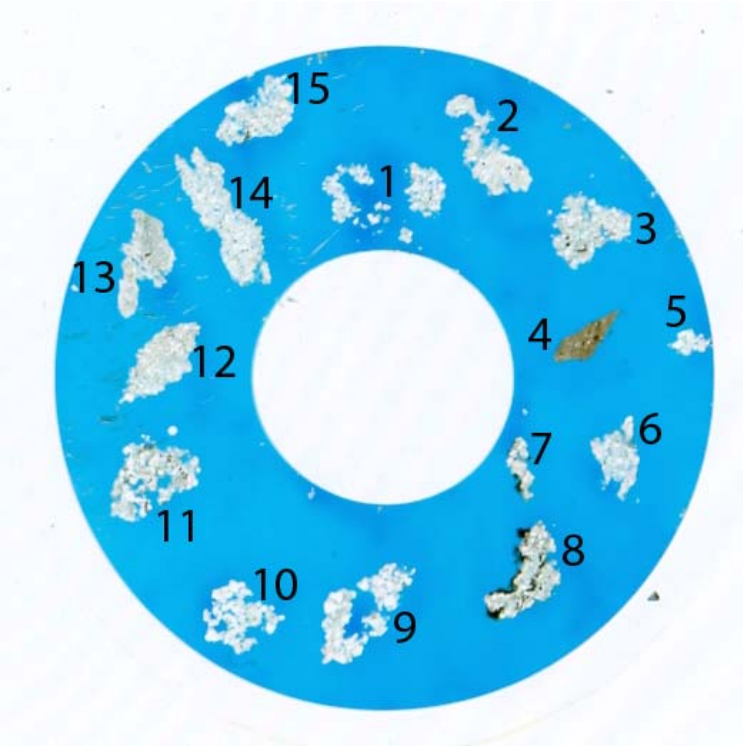

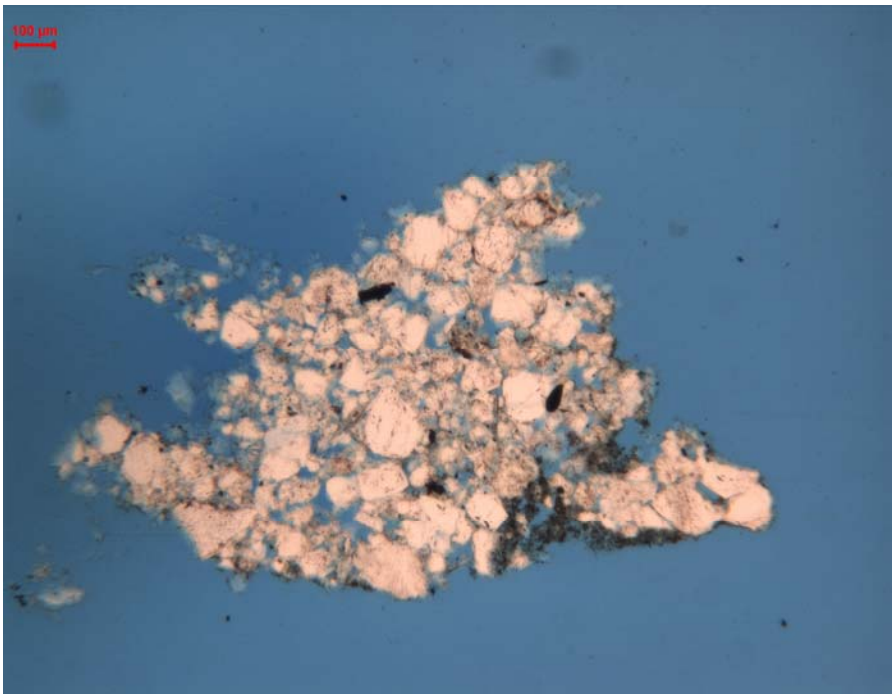

Figure 1850c; cutting no. 6
Typical sandstone cutting for this depth interval

Figure 1850d; cutting no. 14
Typical sandstone cutting for this depth interval

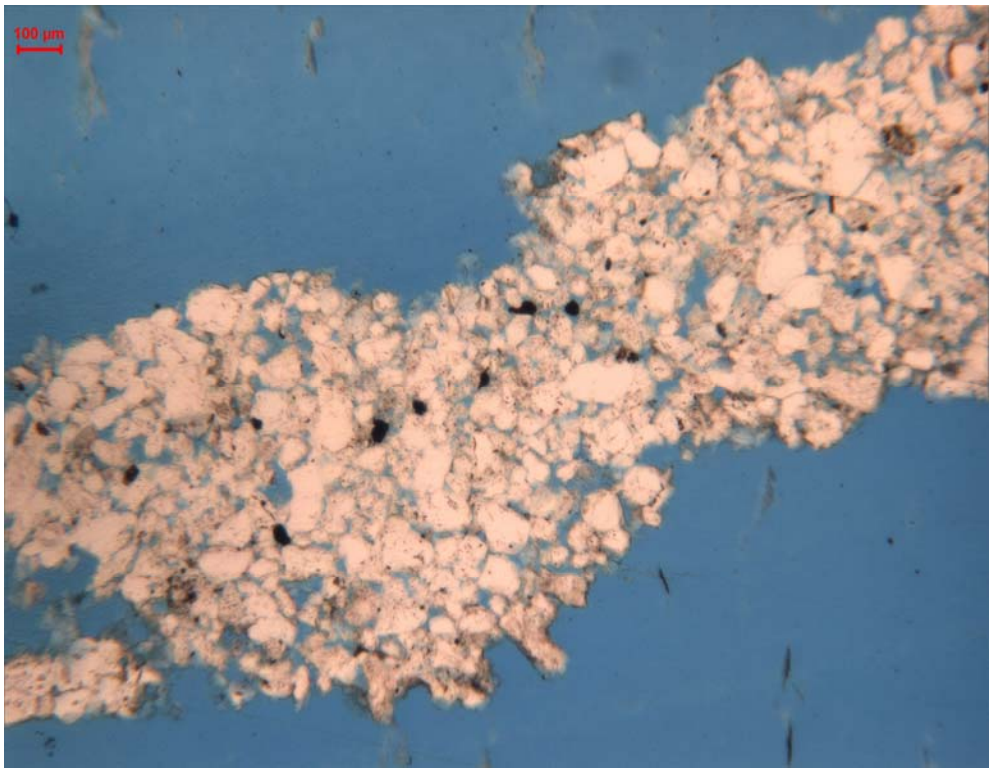

1860 – 1862 m

	Sandstone	Claystone	Lignite	Quartz	Calcite	Other
Content (%)	40	60	Trace	Trace	-	Trace
Color	Yellowish grey	Medium grey	Grayish black	Yellowish grey		White clay
Porosity (%)	10-20	0-5	0-5	0		0-5

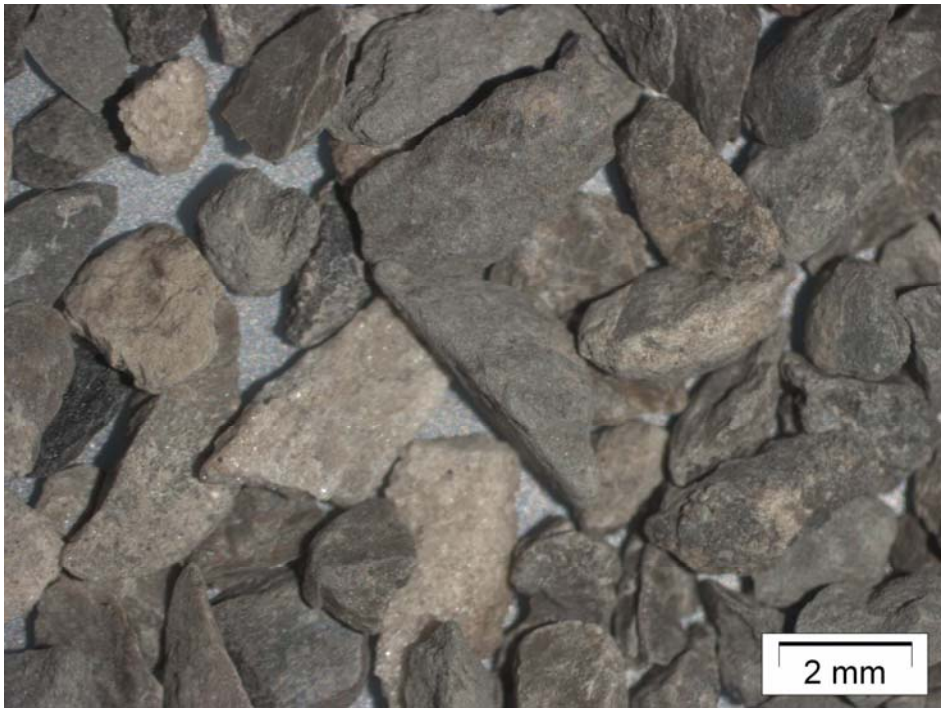

Figure 1860a
This is an overview of the fraction 1-2 mm

Figure 1860b
This is an overview of the fraction < 1 mm

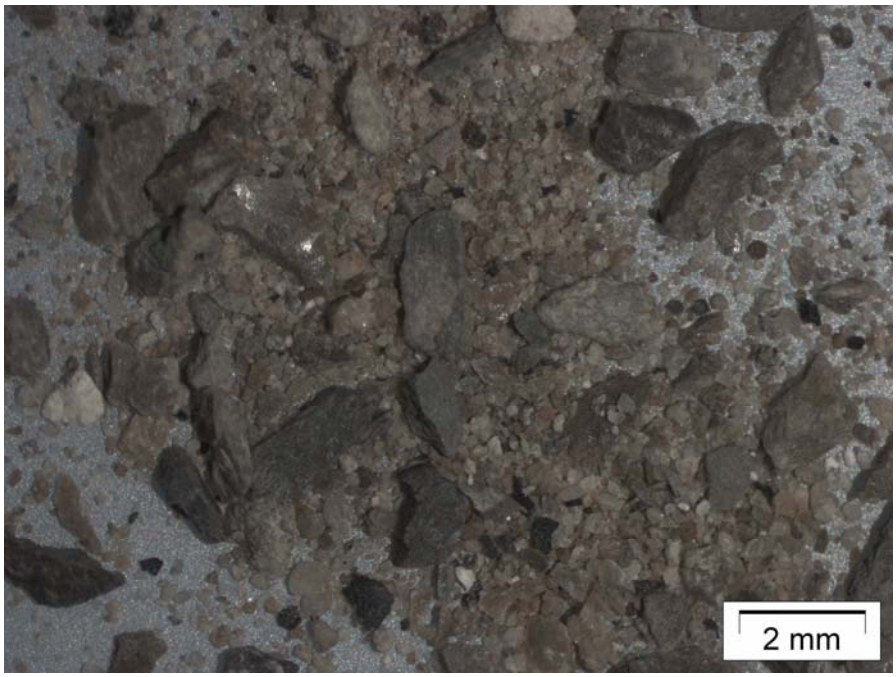

6 micaceous claystone cuttings (4, 5, 8, 9, 13, 14)
In some cuttings up to 5% quartz grains.
1 sandstone cutting with a siderite nodule (10)
Surface of siderite is half the surface of the cutting, accessorial big mica grains, shell remain, some pore space visible, light orange-brown clay in between the quartz grains.
1 siderite cutting (1)
25% quartz, broad film of calcite around the quartz grains, floating in a matrix of dark brown siderite
10 sandstone cuttings (2, 3, 6, 7, 11, 12 & 15 – 18)
Accessorial mica grains, quartz cement, very little to no porosity visible, very poor sorting, angular, concave-convex contacts, some alteration

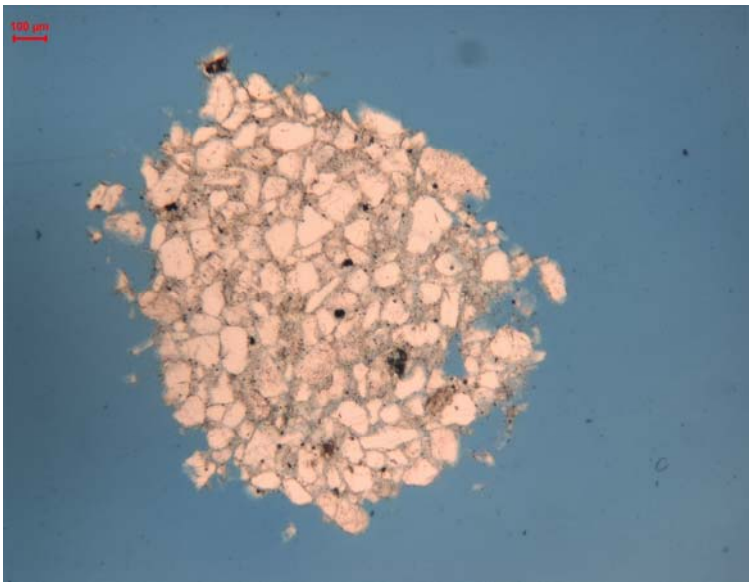

Figure 1860c; cutting no. 6
Typical non-porous sandstone cutting

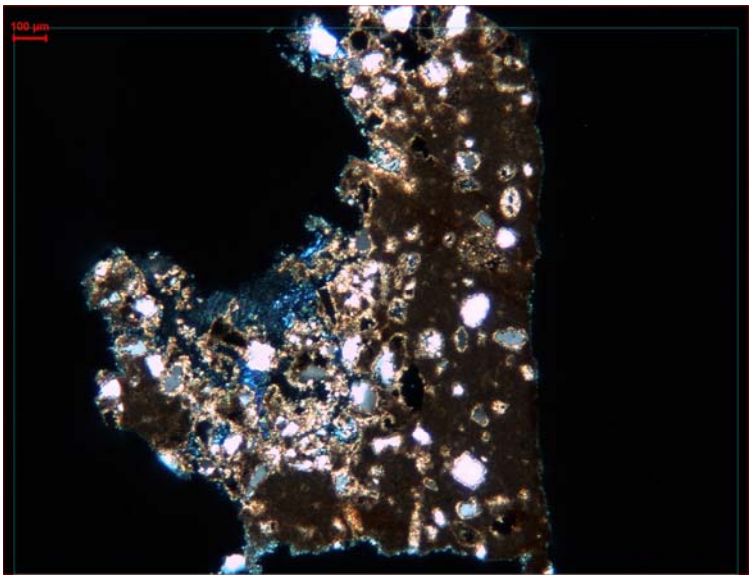

Figure 1860d; cutting no. 1
Calcite films around quartz enclosures in a siderite matrix

Figure 1860e; cutting no. 8
A micaceous claystone cutting

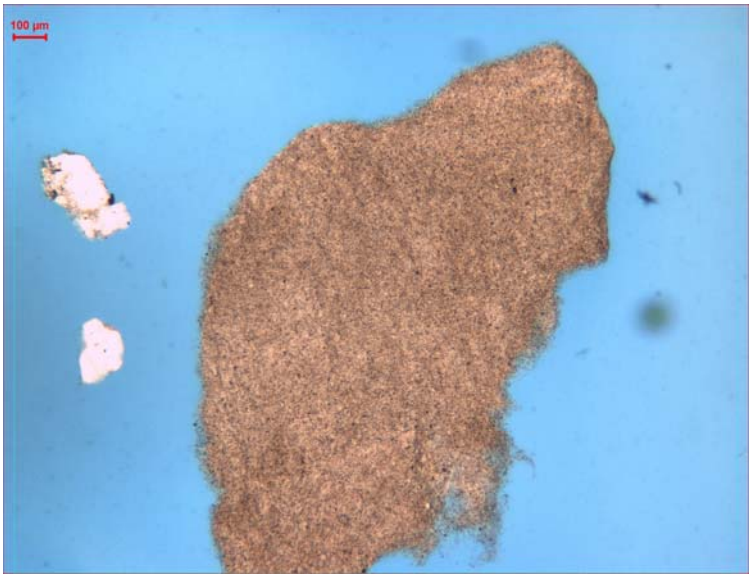

Figure 1860f; cutting no. 8
Mica minerals show high interference colors with on this crossed nichols view from figure 1860e

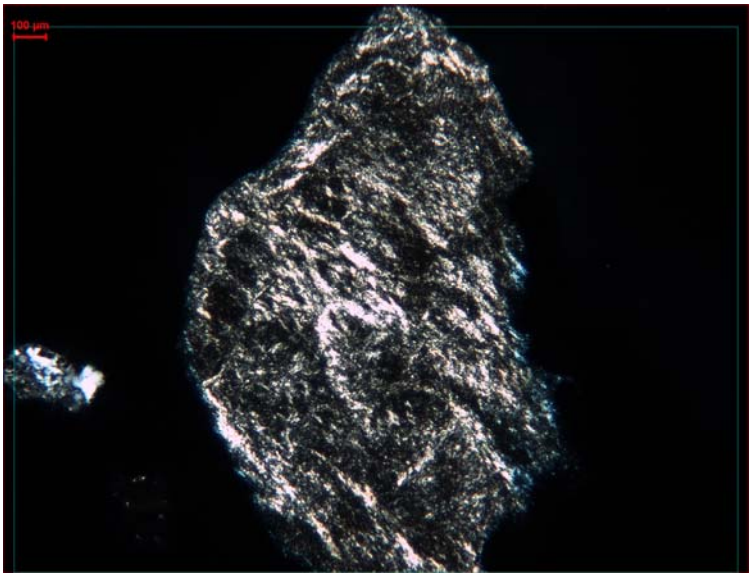

1870 – 1872 m

	Sandstone	Claystone	Lignite	Quartz	Other
Content (%)	40	50	5	5	Shell remain
Color	Yellowish grey	Medium grey	Grayish black	White to very light grey	Pyrite
Porosity (%)	10-20	0-5	0-5	0	

Figure 1870a
This is an overview of the fraction 1-2 mm

Figure 1870b
This is an overview of the sample < 1 mm

3 coal cuttings (3, 5, 16)
1 cutting with organic matter (12)
1 big shell remain (4)
13 sandstone particles (1, 2, 6 – 11, 13 – 15, 17 & 18)
5% untwinned feldspars
95% quartz, loosely packed, lots of porosity visible, much alteration, longitudinal contacts, rounded, moderate sorting, no cementation.

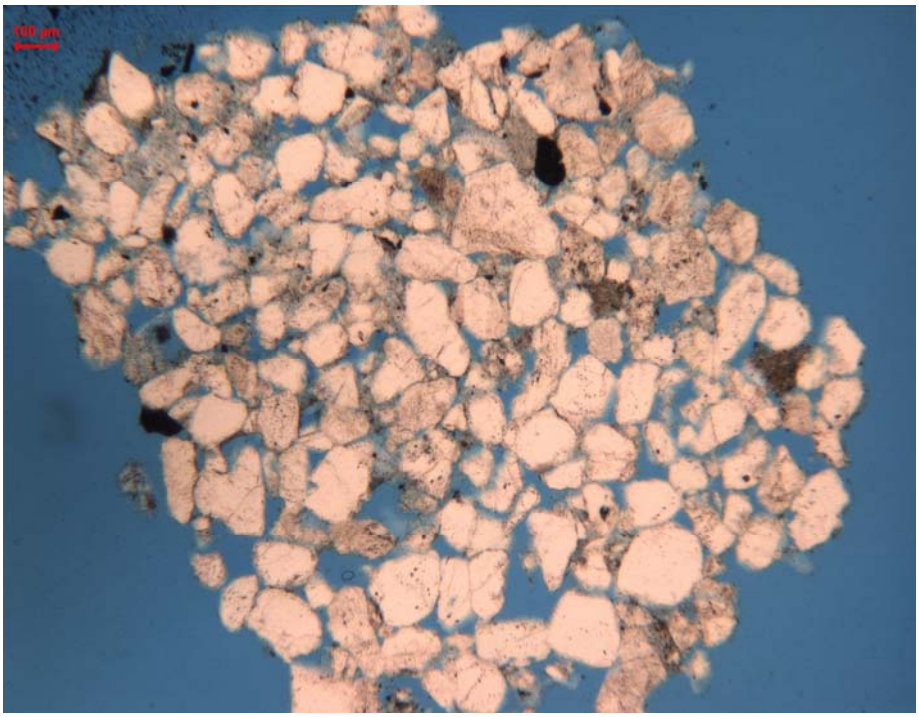

Figure 1870c; cutting no. 1
Porous sandstone

Figure 1870d; cutting no. 4
View with crossed nichols of a shell remain, lots of high interference colors of carbonates are visible, mainly calcite

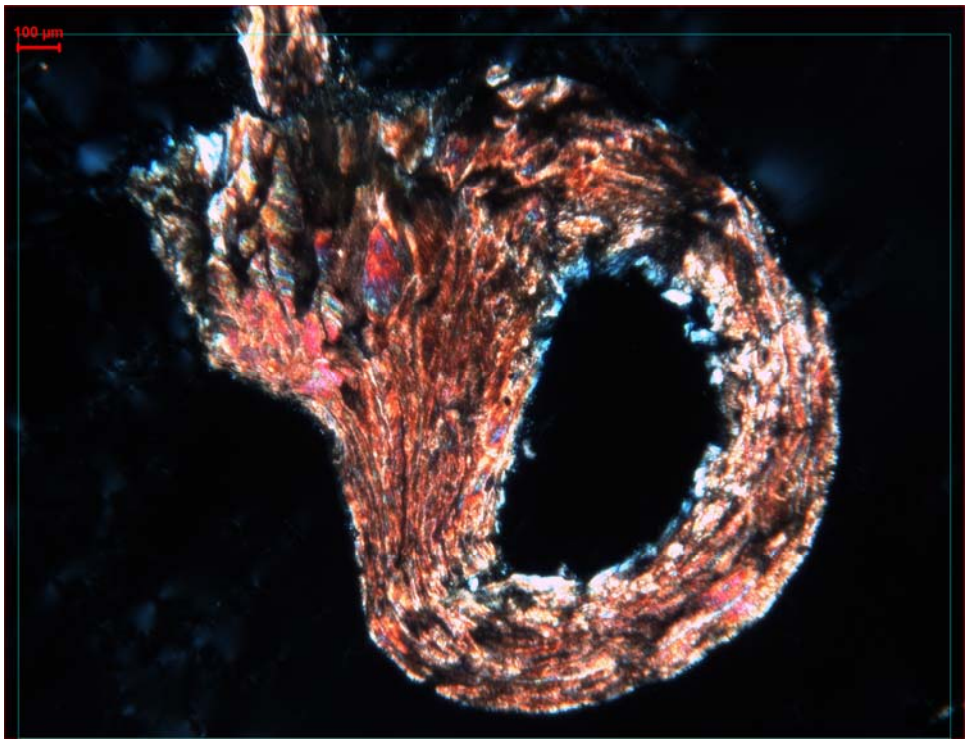

1880 – 1882 m

	Sandstone	Claystone	Lignite	Quartz	Other
Content (%)	20	40	Trace	40	-
Color	Yellow to white	Medium grey	Grayish black	Yellowish grey	
Porosity (%)	10-15	0-5	0-5	0	

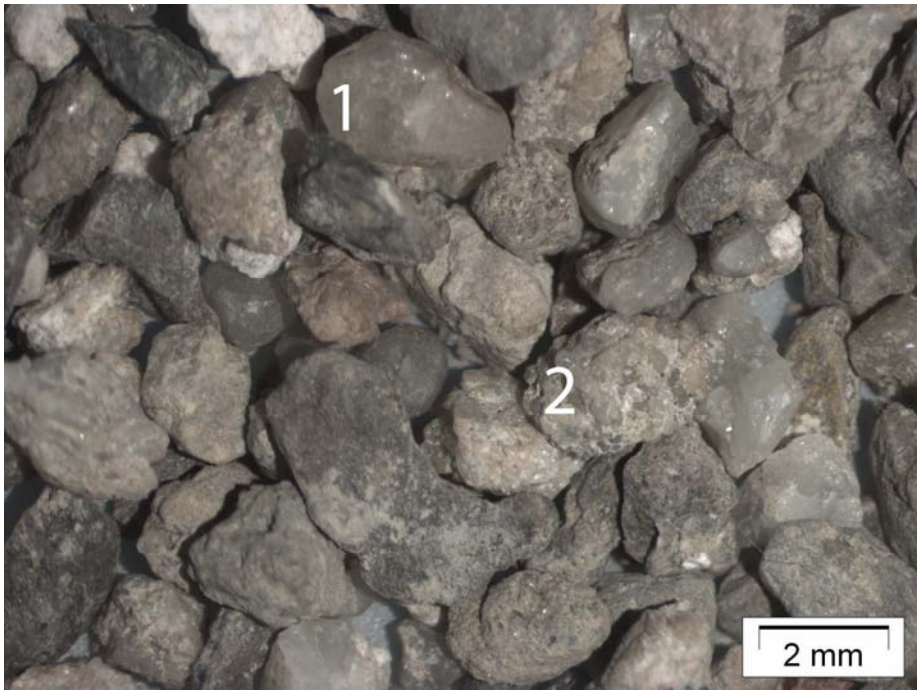

Figure 1880a

1- There are a lot of these big quartz grains present in the fraction 1-2 mm

2- Sandstone cutting with white mineral cement

Figure 1880b

This is an overview of the fraction < 1 mm with a lot of well rounded quartz grains

12 sandstone cuttings (1-12)
5% feldspars
95% quartz, sutured grain boundaries noticed, occasionally very big, elongated quartz minerals, sorting is very poor, sub angular, concave-convex contacts, no to little porosity visible, clay cement on many places present, high interference colors visible, possibly of calcite origin, lots of alteration present, little pieces of lignite

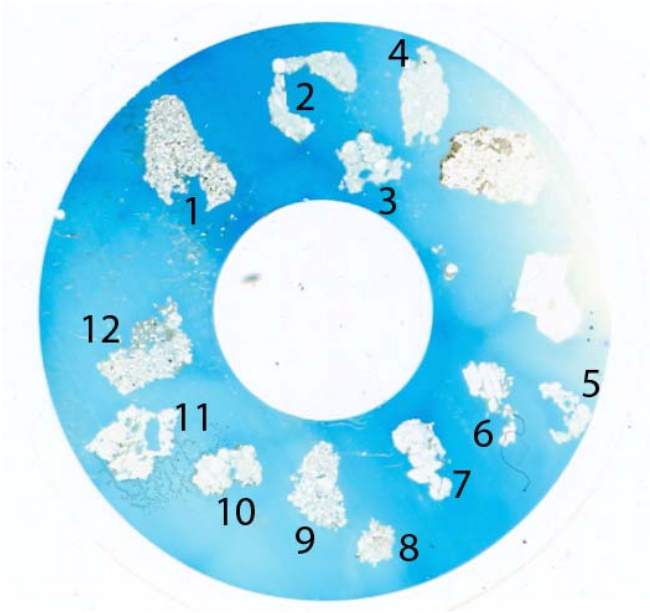

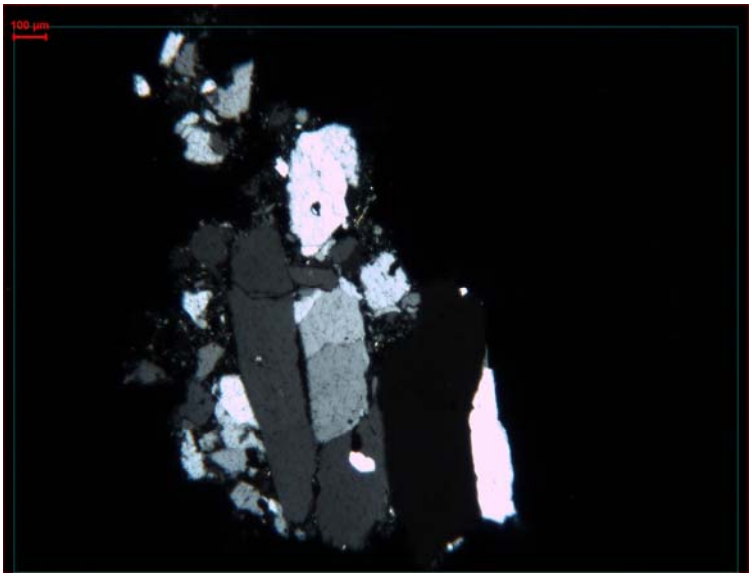

Figure 1880c; cutting no. 6
Elongated quartz minerals

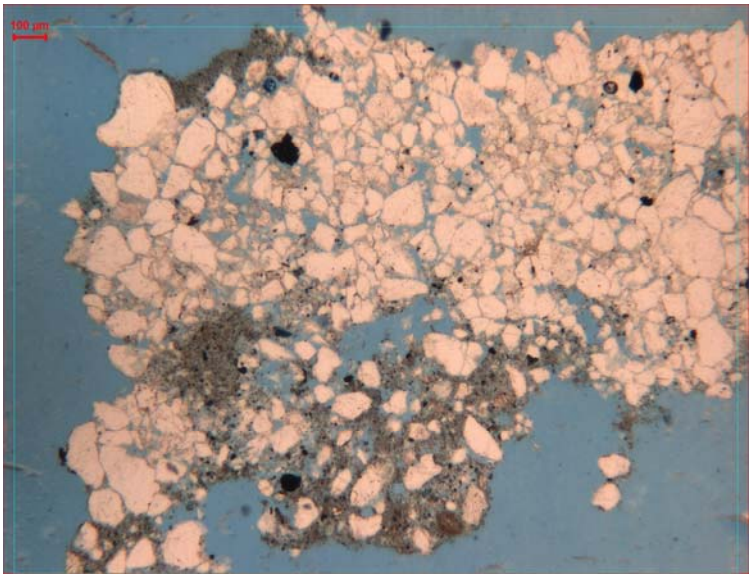

Figure 1880d; cutting no. 12
Clean sandstone with zones which contain clay mineral cement

1890 – 1892 m

	Sandstone	Claystone	Lignite	Quartz	Other
Content (%)	40	40	Trace	20	Trace
Color	Yellow to white	Medium grey	Grayish black	Yellowish grey	White clay
Porosity (%)	5-20	0-5	0-5	0	0-5

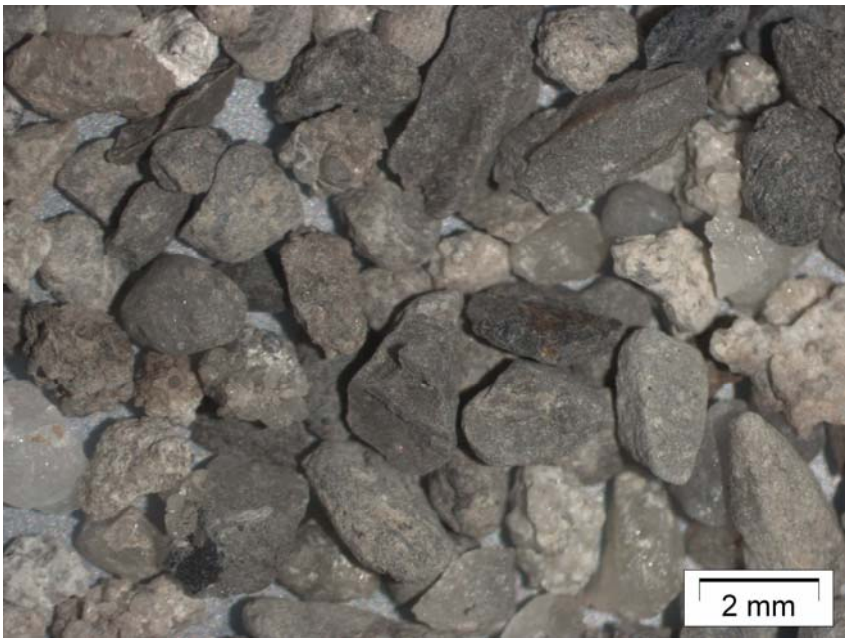

Figure 1890a
This is an overview of the fraction 1-2 mm

Figure 1890b
An overview of the fine fraction, with a relative high amount of loose quartz grains in respect to the medium fraction in figure 1890a.

2 coal cuttings (17 & 19)
2 siltstone cuttings (6, 11)
10% organic matter
One with 35% siderite, brown spots which create together with the quartz a matrix, high interference color with a high magnification.
The rest of the grains are quartz grains, silty size, almost no visible porosity, very well sorted
3 siderite cuttings (8, 23 & 24)
Variation in color from reddish brown to dark brown
1 micaceous claystone cutting (25)
4 claystone cuttings (7, 14, 15 & 22)
Up to 30% quartz grains, some contain mica's, small amounts of coal present, areas with influence of siderite, dark brown, iron rich carbonates,
2 loose quartz grains (1 & 13)
1 sandstone cutting with sutured grain boundaries (16)
no visible porosity, no cement
12 sandstone cuttings (2 - 5, 9, 10, 12, 18, 20, 21, 26 & 27)
All quartz, not a lot alteration, little porosity visible, quartz cement, little amount of clay cement, very poor sorting, sub rounded, concave-convex contact.

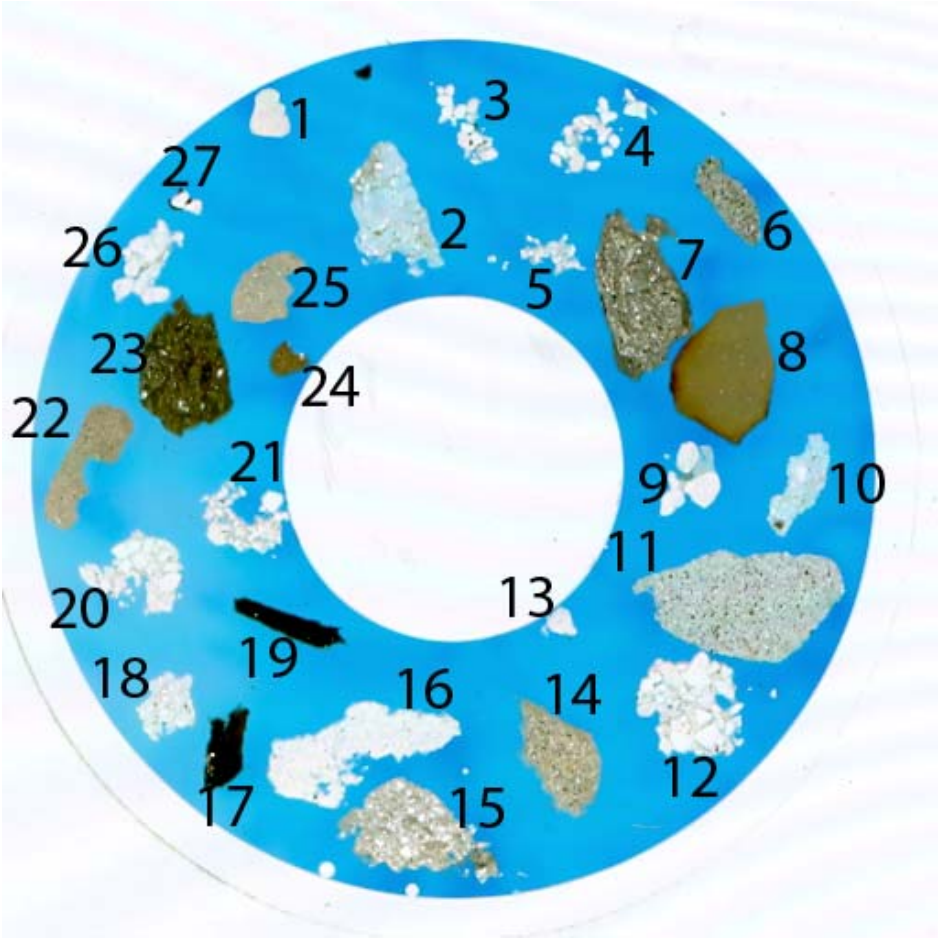

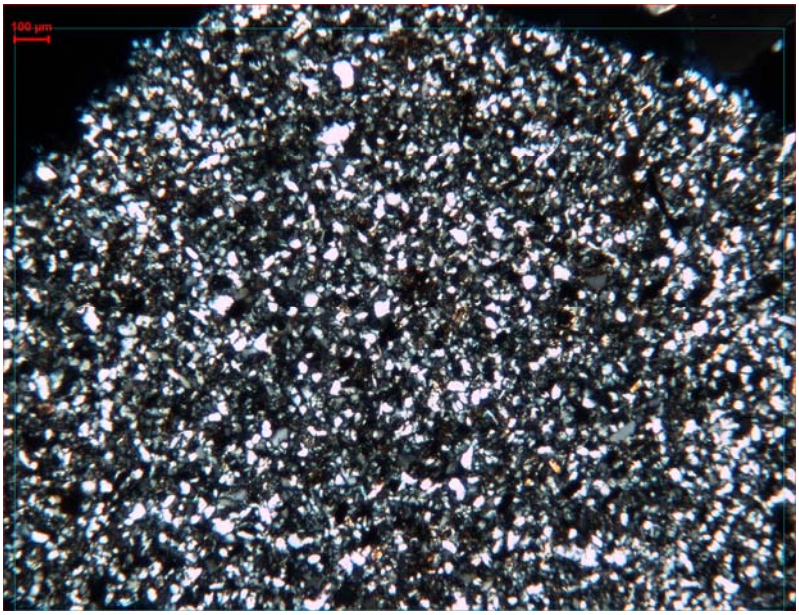

Figure 1890c; cutting no. 11
A photo of a part of a cutting containing silt. The photo is taken with crossed nichols.

Figure 1890d; cutting no. 1
Loose quartz grain

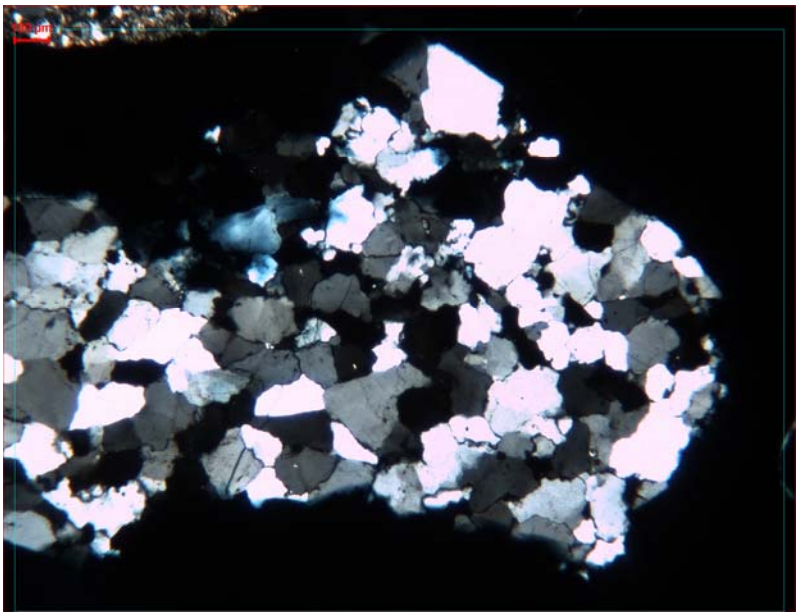

Figure 1890e; cutting no. 16
Sutured grain boundaries can be observed on this photo which was taken with crossed nichols.

1902 – 1904 m

	Sandstone	Claystone	Lignite	Quartz	Other
Content (%)	70	25	5	-	Trace
Color	Yellowish grey to light grey	Light to medium grey	Grayish black		White clay
Porosity (%)	10-20	0-5	0-5		0-5

Figure 1902a
This is an overview of the fraction 1-2 mm.

Figure 1902b
This is an overview of the sample < 1 mm.

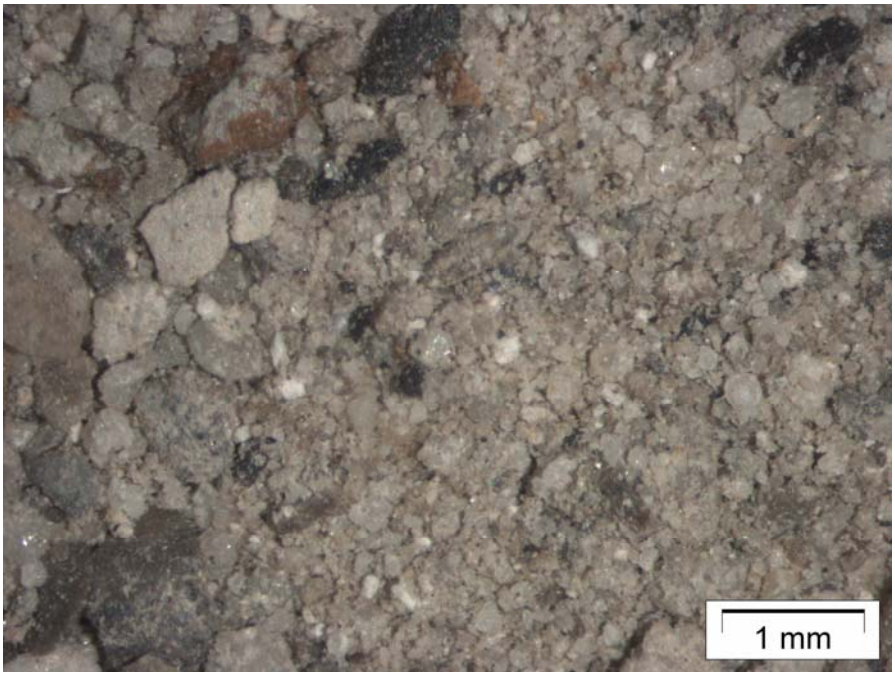

4 micaceous claystone cuttings (2, 3, 6 & 7)
1 coal cutting (1)
1 claystone cutting (8)
5% quartz grains
20% muscovite
20% siderite, dark brown, well rounded
55% clay
1 completely cemented sandstone (14)
No porosity visible, high amount of well rounded siderite, accessorial muscovite, clay and quartz cement.
11 sandstone cuttings (4, 5, 9 -13 & 15 – 18)
Much alteration,
5% untwined feldspars
95% quartz, some visible porosity, low amounts of coal present, traces of siderite, no cement present, longitudinal contacts, moderately sorted, sub rounded,

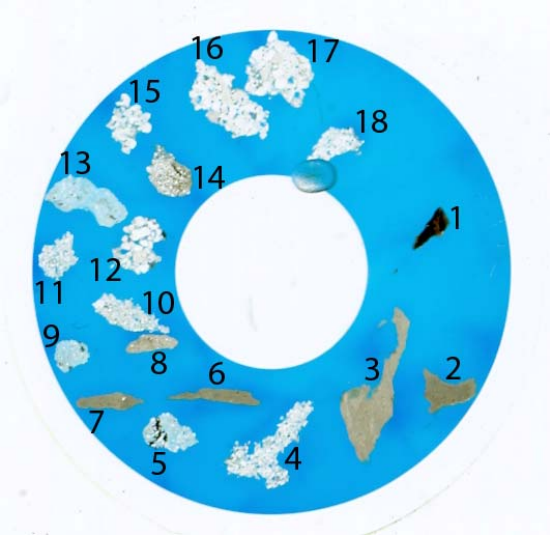

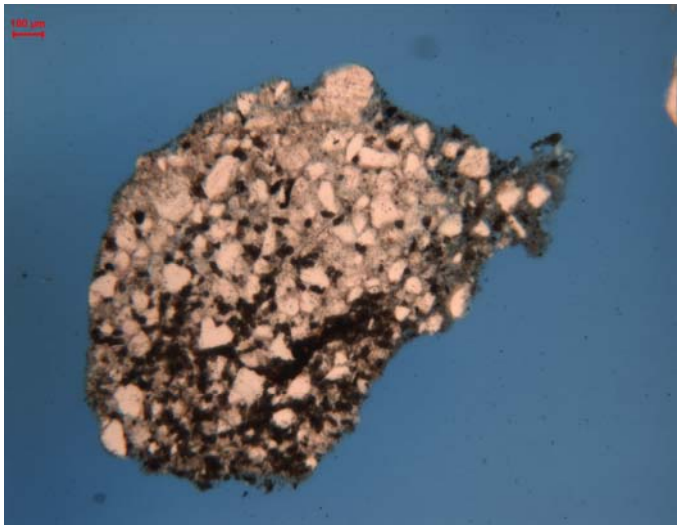

Figure 1902c; cutting no. 14
Siderite spherulites are easy to see.

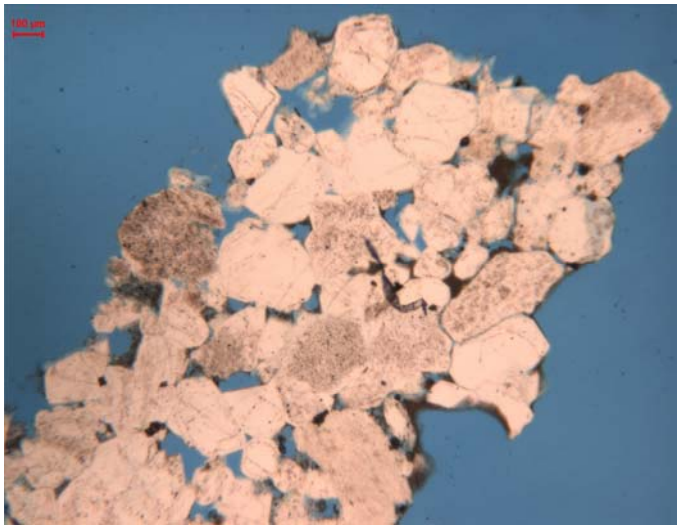

Figure 1902d; cutting no. 16
Grains are not completely cemented, but films of siderite are present.

1910 – 1912 m

	Sandstone	Claystone	Lignite	Quartz	Calcite	Other
Content (%)	25	70	5	Trace	Trace	Trace
Color	Light grey	Light grey	Grayish black and laminated	Pale white		Pyrite and shell remains
Porosity (%)	5-20	0-5	5		0-5	

Figure 1910a
This is an overview of the 1-2 mm sample

Figure 1910b
This is an overview of the sample < 1 mm

1 calcareous cutting (7)
Lots of calcite crystals present, together with a cross section of a shell
3 quartz-rich claystone cuttings (4, 10 & 12)
30% quartz in a matrix of micaceous clay
1 micaceous claystone cutting (5)
8 sandstone cuttings (1 – 3, 6, 8, 9, 11 & 13)
Accessorial muscovite minerals, some alteration spotted, no to moderate porosity visible, traces of calcite, clay mineral cement, concave-convex contacts, sub rounded, poorly sorted

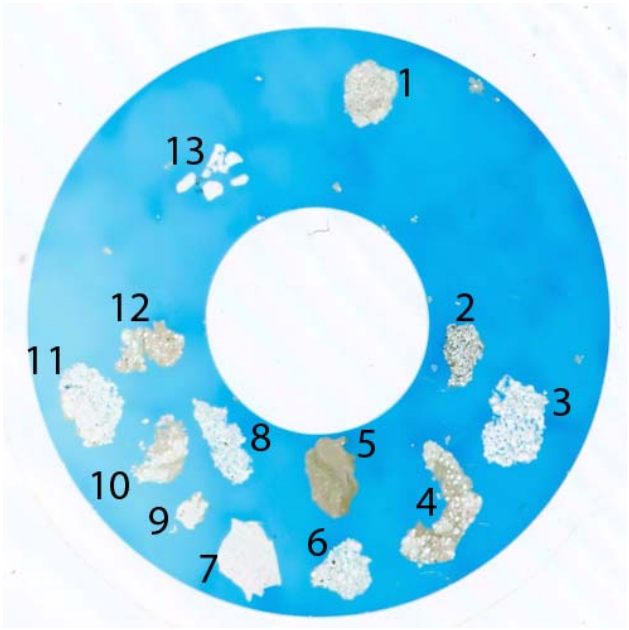

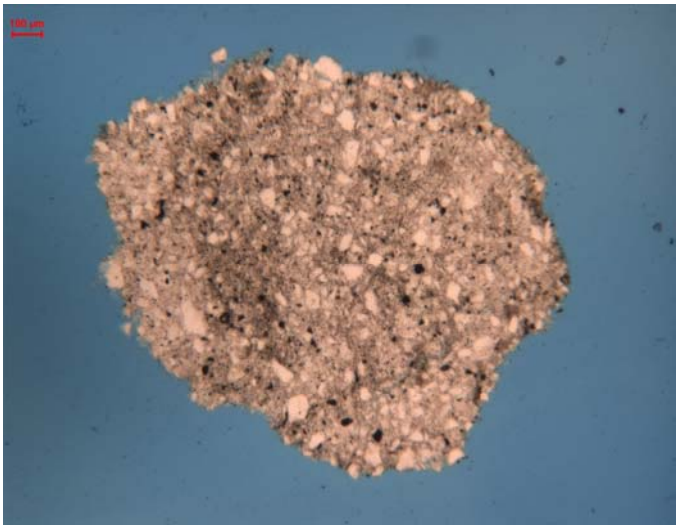

Figure 1910c; cutting no. 1
Photo with the analyzer disabled.

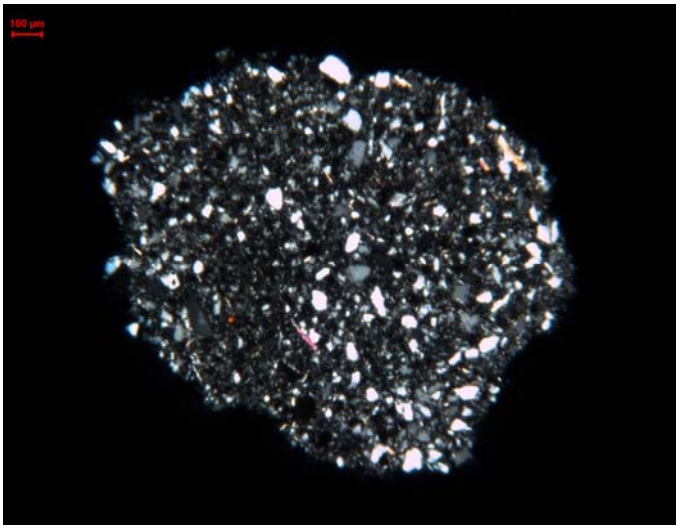

Figure 1910d; cutting no. 1
Elongated minerals with a high interference color light up when the analyzer is enabled. In the upper right corner is a big yellow muscovite mineral and in the center there is a muscovite mineral with a pink interference color.

1918 – 1920 m

	Sandstone	Claystone	Lignite	Quartz	Calcite	Other
Content (%)	20	75	Trace	Trace	5	Shell remain
Color	Light grey	Medium grey and red	Grayish black	Pinkish white		
Porosity (%)	10-15	0-5	0-5		0-5	

Figure 1918a
This is an overview of the fraction 1-2 mm. In the left bottom corner, a shell remain can be seen. In the bottom middle a bright red piece of plastic differs from the other particles. It is probably a part of the sachets in which the cuttings were contained.

Figure 1918b
This is the fine fraction (<1 mm).
- *1- Pink well rounded quartz grain*
- *2- Layered calcite particle (very fizzy)*
- *3- Lignite particle*
- *4- Red claystone*

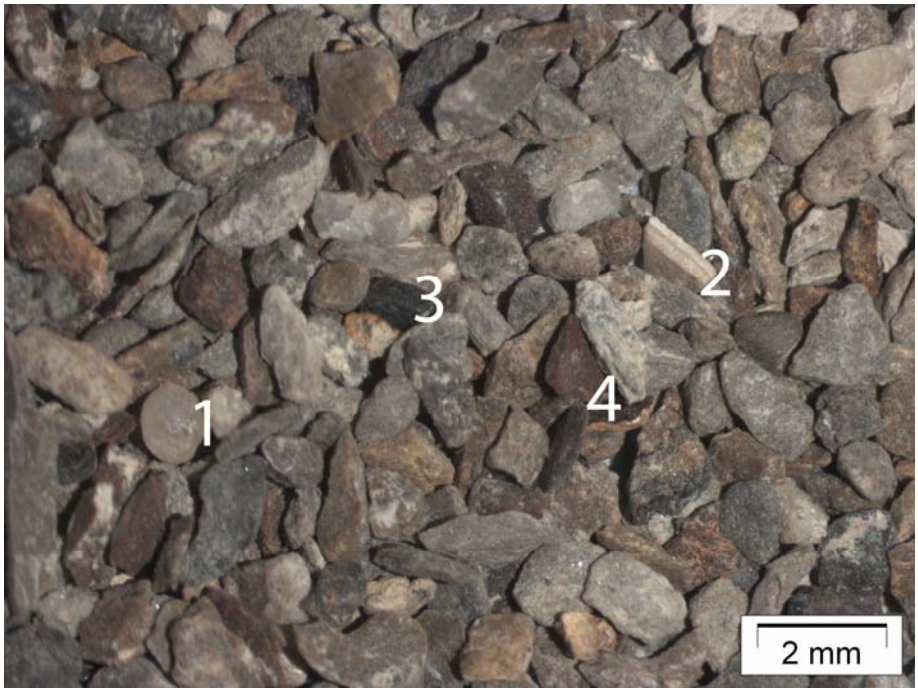

Quality of the thin slide is bad, due to this two cuttings cannot be analyzed
11 siderite cuttings (1 -4, 6, 7, 11, 12 & 14 – 16)
Containing none up to 20% of quartz, lots of traces of calcite, color varies between light and dark brown.
1 loose quartz grain (8)
1 micaceous claystone cutting (10)
3 sandstone cuttings (5, 9, 13)
100% quartz, longitudinal contacts, some alteration, little clay mineral cement present, small amount of porosity visible, sub angular, sorting is good, accessorial feldspars

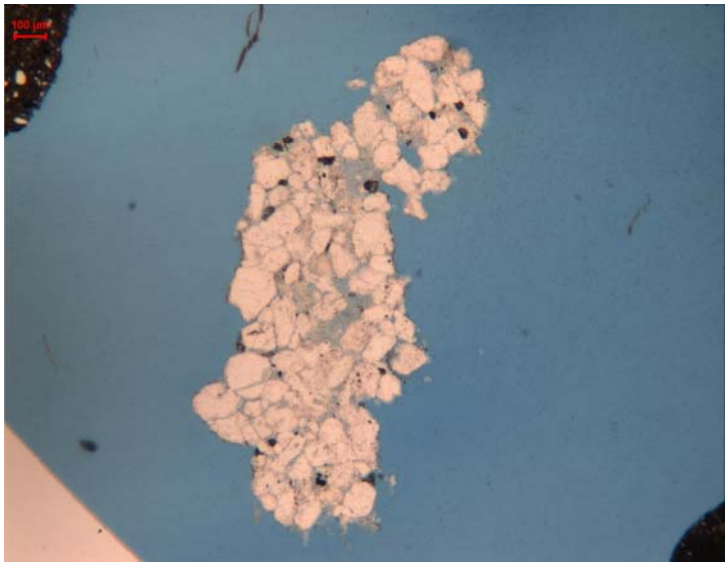

Figure 1918c; cutting no. 13
A typical sandstone cutting for this depth interval.

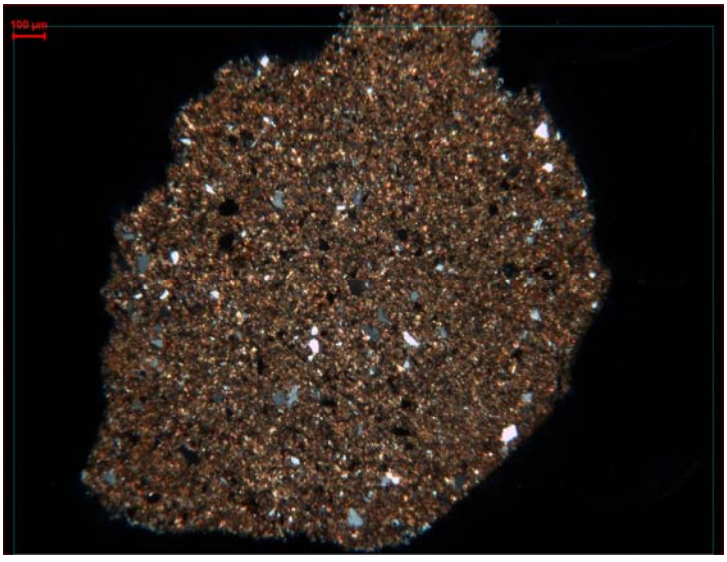

Figure 1918d; cutting no. 14
A photo of a siderite cutting with enabled analyzer.

Chapter 7

Cutting to log correlation

The cuttings of well DEL-03 are not the only information available of that area. Back in 1953, two logs were taken. A spontaneous potential (SP) log and a deep resistivity log. In figure 7.02 the depths of all intervals of which the thin slides are prepared are indicated. This way, the type of deposition can be seen with respect to the rest of the sand and clay bodies within the Delft Sandstone Member. Both the deep resistivity and the spontaneous potential log are used to interpret the type of sediments at the relevant depth, but only the spontaneous potential log is used to plot the thin slide locations along the borehole axis. The depth of the logs is measured with reference to the rotary table which is positioned 4.06 meters above NAP (www.nlog.nl, 2009). This way, the data gathered from the cuttings can be linked to the spontaneous potential measurements.

In permeable zones, the SP deflection is controlled by the mud and the salinity of the formation water. With increasing amounts of shale in the sandstone, the SP deflection will move towards the shale line and show smaller amplitudes. Also hydrocarbons can suppress the SP readings, but since the Delft Sandstone Member underneath Delft does not contain any hydrocarbons it cannot influence our readings. If the SP curve moves left, it indicates a high permeable formation which can be interpreted as sandstone. Parallel to that, the SP curves moves towards the shale base line if there are any impermeable zones. This results in straight angular lines (Hilchie, 1979). Impermeable zones in the DEL-03 are mostly caused by clay mineral cement or siderite cement.

In figure 7.02 it can be seen that the first two thin slides are taken from the Rodenrijs Claystone Member. This corresponds with the shale contents of 50 to 70 percent as described in chapter 6. The numbers (1-16) indicate the depths of the cuttings which are used for the preparation of the thin slides. SLDND_T is the top of the Delft Sandstone Member. From 1808 up to 1860 meters the result of the cutting study show sandstone contents in between 50 and 65 percent. However, the SP curve shows a lower amplitude (closer to the shale base line) starting at 1820 meters depth. A good explanation is an increase in cement between the particles at this depth. This conclusion is also supported by results in the cutting analysis where the first siderite cement is found at a depth of 1832 meters. Quartz and clay mineral cement is found in the whole formation. By accident, many of the thin slides are made in a part of the formation where the SP deflection is relatively far away from the shale base line, this might be deceiving.

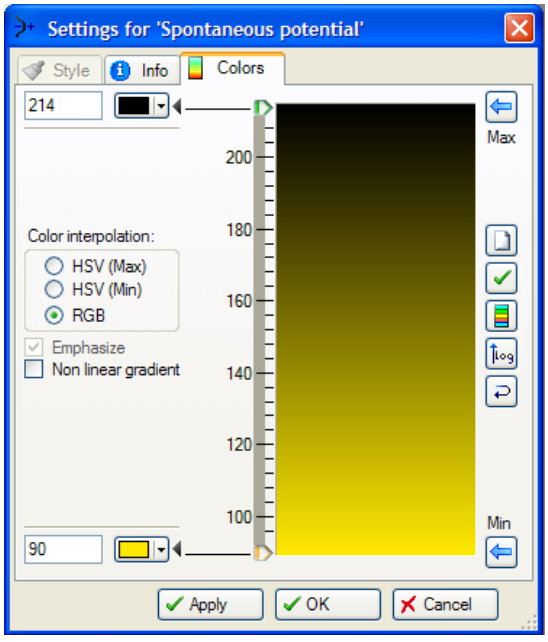

Figure 7.01:
This is the color range used in figure 7.02. The brightest yellow color will appear at a SP reading of 90, while a dark color appears at 214. A low SP reading indicates a permeable formation and is interpreted as sandstone while high SP readings indicate shales and clay.

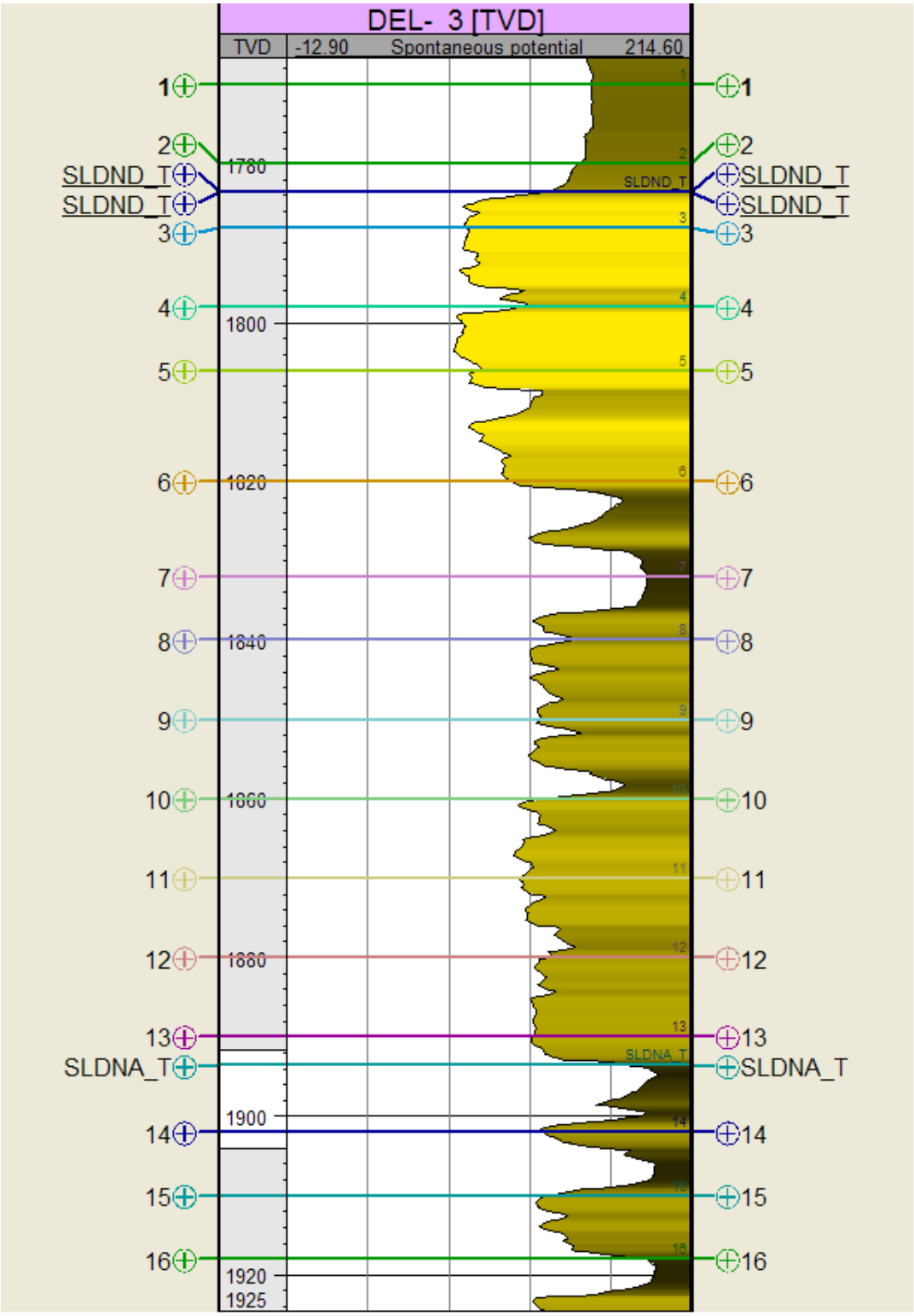

Figure 7.02
Petrel image of the Delft Sandstone Member with all depth locations of the thin slides, 16 in total.
SLDND_T is the top of the Delft Sandstone Member.
SLDNA_T is the top of the Alblasserdam Member and therefore the bottom of the Delft Sandstone Member.

Chapter 8

Petrographical analysis Delft Sandstone Member MKP-11

Introduction

This chapter is subdivided in several depths corresponding with a sample found at that depth. Each depth contains a photograph of the original plug, a mineralogical description and porosity and permeability calculation of the thin slides of the plug. Because the plugs were taken from three different depth intervals (Appendix A), each depth interval has a different character:

- Samples A: depth interval 907 – 901 meter
- Samples B: depth interval 883 – 881 meter
- Samples C: depth interval 873 – 868 meter

Because some parts of the original core of the MKP-11 were more friable than other parts, the number of samples per depth interval is not the same.

The mineralogical description is done by microscopical analysis. The following properties of the thin slides are determined:

- Type of minerals
- Roundness of minerals
- Content of minerals
- Sorting
- Cement type
- Grain contact

Some obscurities found in thin slide sample are mentioned, like a remarkable bitumen content or clay content.

The porosity and permeability calculation is done with Image Analysis. Of every interval a photograph of the thin slide is made and the porosity and permeability is calculated if possible. In chapter 'Data and Methods' the method is described and a detailed flow sheet of the image analysis process is inserted. There are some samples by which it was not possible to calculate the porosity and permeability because of the high matrix infill of small minerals (sample C01 and A04.2)) or high clay cement content (sample B02 and A03). There also are some samples where the grains are very large and the plug samples contain a lot of bitumen. During the preparation of the thin slides the bitumen flushed away and as a consequence the thin slides of these samples do not contain any bitumen. Most grains in these thin slides are not in contact with each other and therefore it is reliable that the plugs broke during the preparation of the thin slides. As a result, the calculated porosity and permeability of the thin slides are not that reliable. It seems that the bitumen in the original plugs sticked the grains together, although the plug is very friable. This can be seen at the samples C02 and B01.

Sample C04
861.15 m

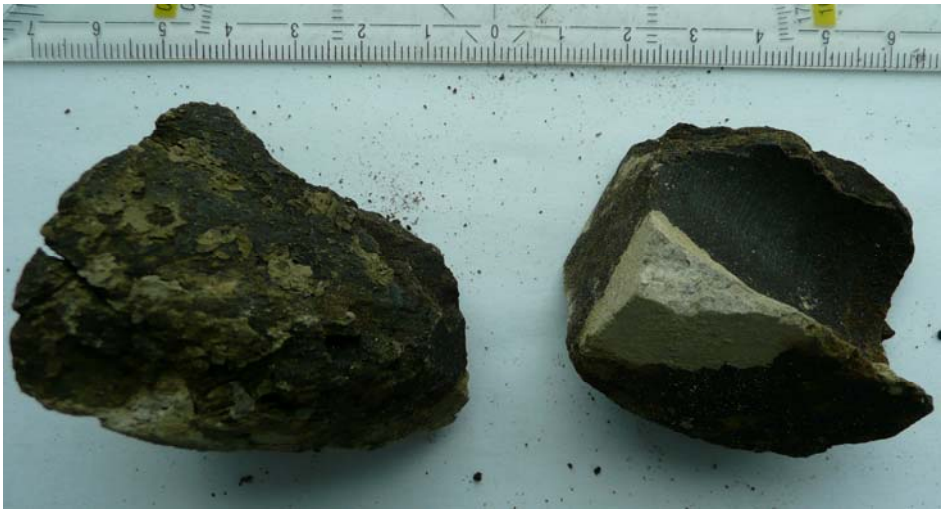

Figure 8.01: Photo of plug

Mineral type	Roundness	Content
Quartz	Subangular	80%
Clay cement	-	8%
Hornblende	Subangular	4%
Chert	Subangular	4%
Quartzite	Subangular	2%
Accesory minerals: Tourmaline, Zircon, Rutile, Microcline, Clay minerals	-	2%

Sorting	Cement type	Grain contact
Bad	Clay cement	Point contact Long contact Concavo convex contact

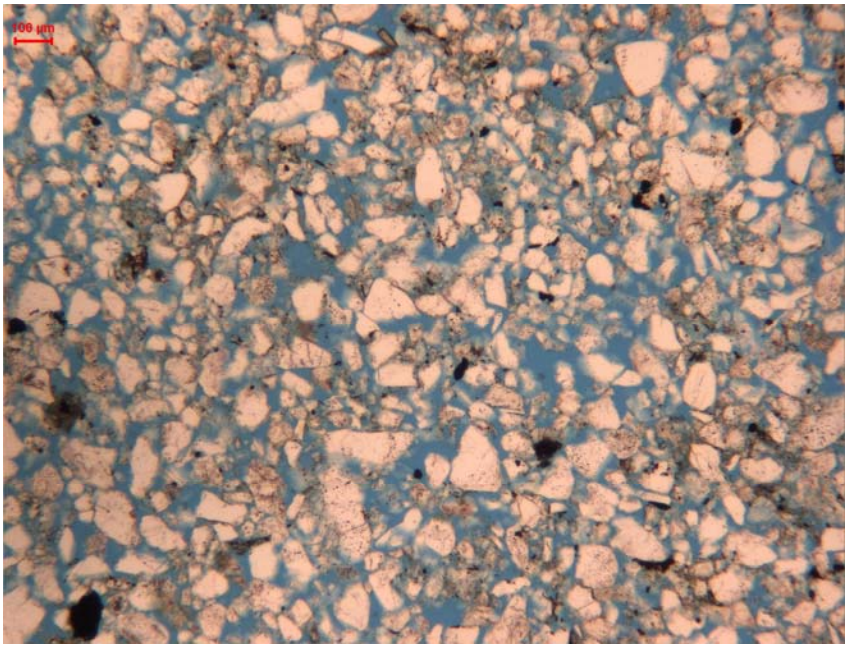

Figure 8.02: Image Analysis photo

Figure 8.03: Thin slide overall photo

Porosity	35.81 %
Permeability 2D	7.31 D
Permeability 3D	63.58 D
Mean length	> 56.66 µm
Grain size	Fine to medium
Sorting	Moderately

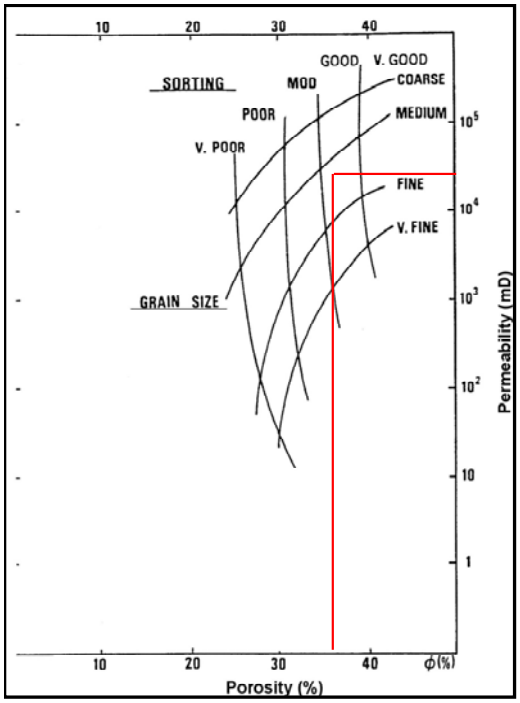

Figure 8.04: Porosity-permeability graph

According to the porosity-permeability graph the permeability of the thin slide is around 45 D. This given is in agreement with the calculated 2D and 3D permeabilities and lies in between them as can be seen in above table.

Sample C03
862.00 m

Figure 8.05: Photo of plug

Mineral type	Roundness	Content
Quartz	Subangular	72%
Hornblende	Subangular	8%
Quartzite	Subangular	8%
Chert	Subangular	5%
Clay minerals	-	4%
Accesory minerals: Muscovite, Tourmaline, Zircon, Titanite	-	3%

Sorting	Cement type	Grain contact
Bad	-	Point contact Long contact Concavo convex contact Free floating

This thin slide almost contains no clay. Loose clay minerals on the other hand are found in the slide. There are also some bitumen parts found.

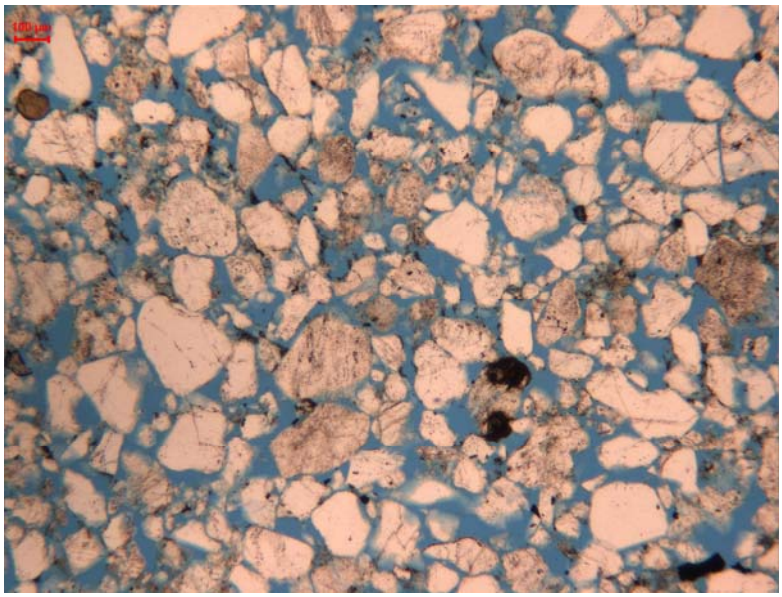

Figure 8.06: Image Analysis photo

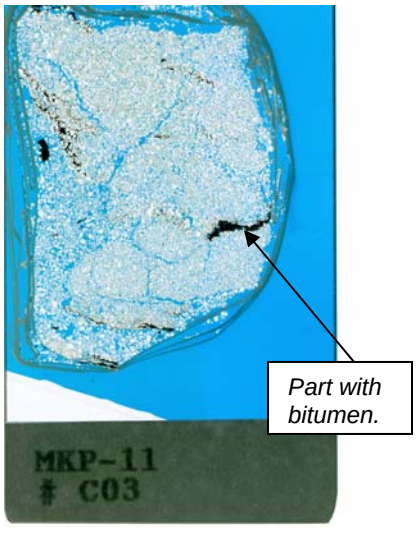

Figure 8.07: Thin slide overall photo

Porosity	30.35 %
Permeability 2D	17.66 D
Permeability 3D	173.35 D
Mean length	> 71.39 µm
Grain size	Medium to coarse
Sorting	Poor

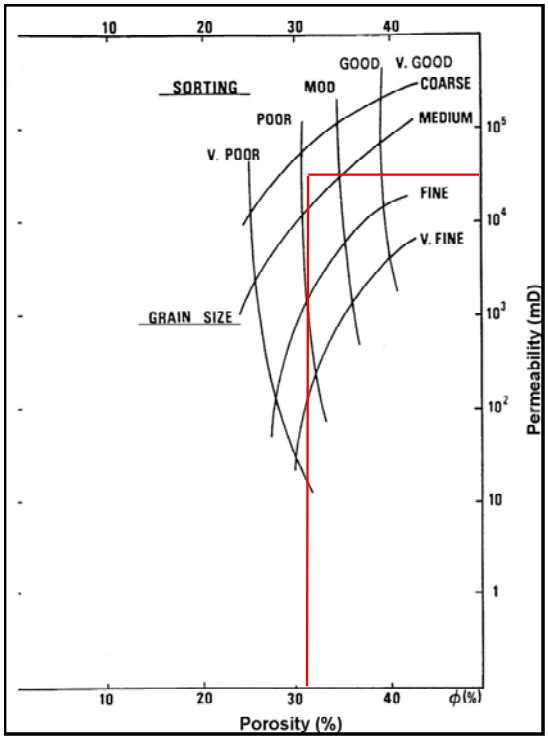

Figure 8.08: Porosity-permeability graph

According to the porosity-permeability graph the permeability of the thin slide is around 50 D. This given is in agreement with the calculated 2D and 3D permeabilities and lies in between them as can be seen in above table.

Sample C02

868.15 m

Figure 8.09: Photo of plug

Mineral type	Roundness	Content
Quartz	Subrounded	63%
Hornblende	Subangular	12%
Quartzite	Subangular	12%
Chert	Subangular	7%
Clay minerals	-	5%
Accesory minerals: Muscovite, Rutile	-	1%

Sorting	Cement type	Grain contact
Good	-	Point contact Free floating

The grains in this slide are large. The slide seems to be very porous which can be seen at the photograph of the slide made in Image Analysis (figure 8.10) and the overall photo (figure 8.11). The photograph of the plug (figure 8.09) shows the porosity before the slides were made; it has a very friable appearance. The plug also contains a lot of bitumen as can be seen on the photograph. It seems that the grains of the plug are sticked together by the bitumen and it is flushed away during the preparation of the slides. As a result the grains in the thin slide are hardly making any contact with each other (figure 8.10).

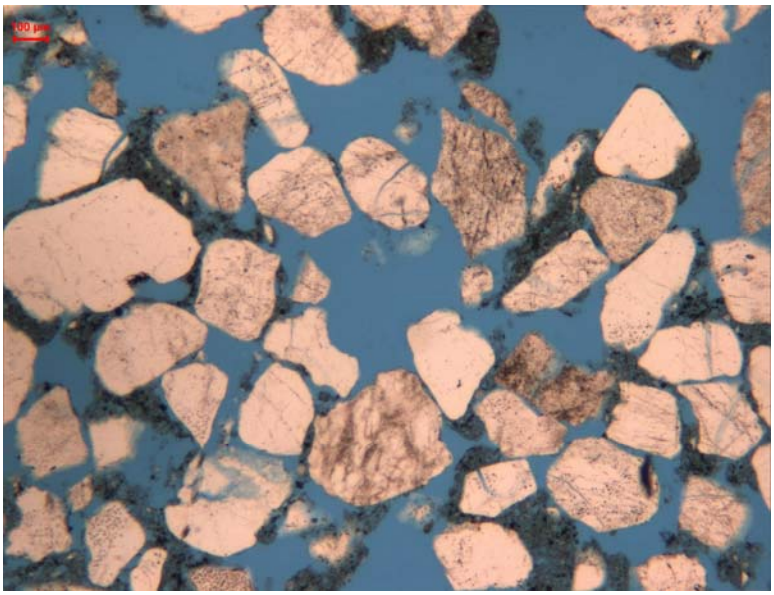

Figure 8.10: Image Analysis photo

Figure 8.11: Thin slide overall photo

Porosity	32.79 %
Permeability 2D	23.79 D
Permeability 3D	2384.86 D
Mean length	> 79.73 µm
Grain size	Coarse
Sorting	Moderately

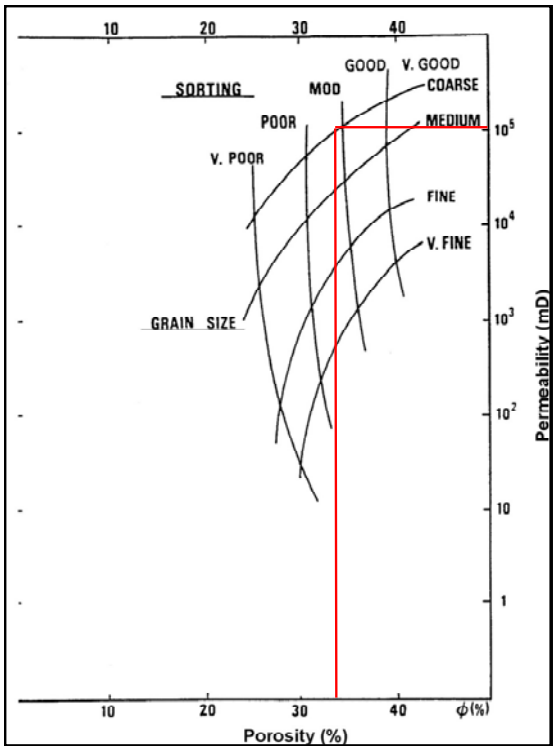

Figure 8.12: Porosity-permeability graph

The permeability according to the porosity and permeability graph is around 100 D. The calculated 3D permeability is not realistic because the amount is too large. The plug (figure 8.09) contains a lot of bitumen which is flushed away during the preparation of the thin slide (figure 8.10). Because the grains are hardly making any contact with each other the Image Analysis photo is not a realistic view of the plug.

Sample C01

872.85 m

Figure 8.13: Photo of plug

Mineral type	Roundness	Content
Micaceous clay	-	73%
Quartz	Subangular	15%
Muscovite	Angular	5%
Clay minerals	Angular	5%
Accesory minerals: Zircon, Tourmaline	-	2%

Sorting	Cement type	Grain contact
Very bad	-	-

This sample contains a lot of clay as can be seen on the photograph of the plug (figure 8.13). On the photograph of the thin slide of the plug (figure 8.14), hardly any grain is visible. The thin slide mostly consists of clay cement and neither grains nor free space in the slide could be detected. Because of this, it was not possible to calculate the porosity and permeability with image analysis.

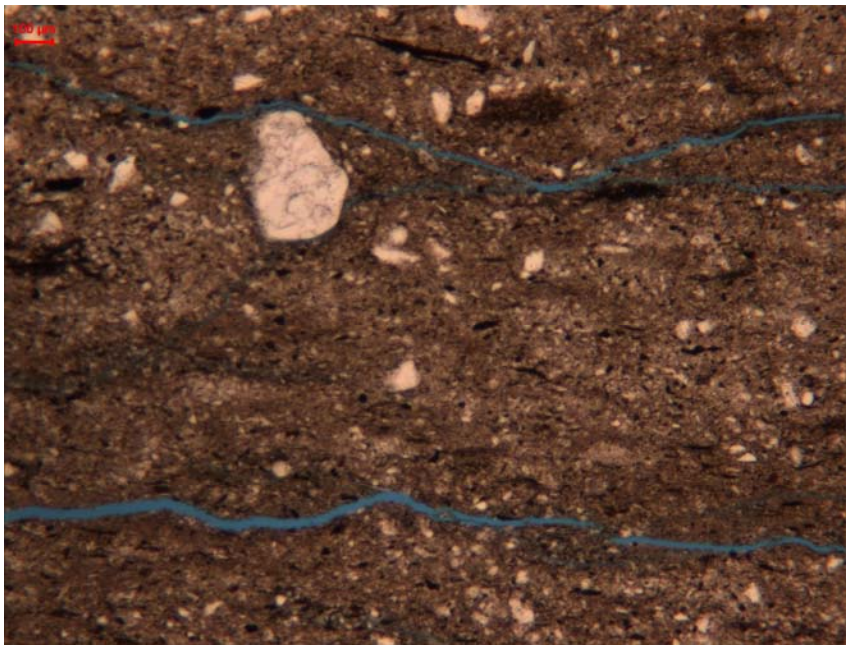

Figure 8.14: Image Analysis photo

Figure 8.15: Thin slide overall photo

Sample B02

881.70 m

Figure 8.16: Photo of plug

Mineral type	Roundness	Content
Quartz	Subangular	48%
Micaceaous clay	-	45%
Hornblende	Subangular	4%
Muscovite	Angular	3% (content of clay cement)
Accesory minerals: Tourmaline, Chert, Rutile, Quartzite, Calcite	-	3%

Sorting	Cement type	Grain contact
Very bad	Micaceaous Clay	-

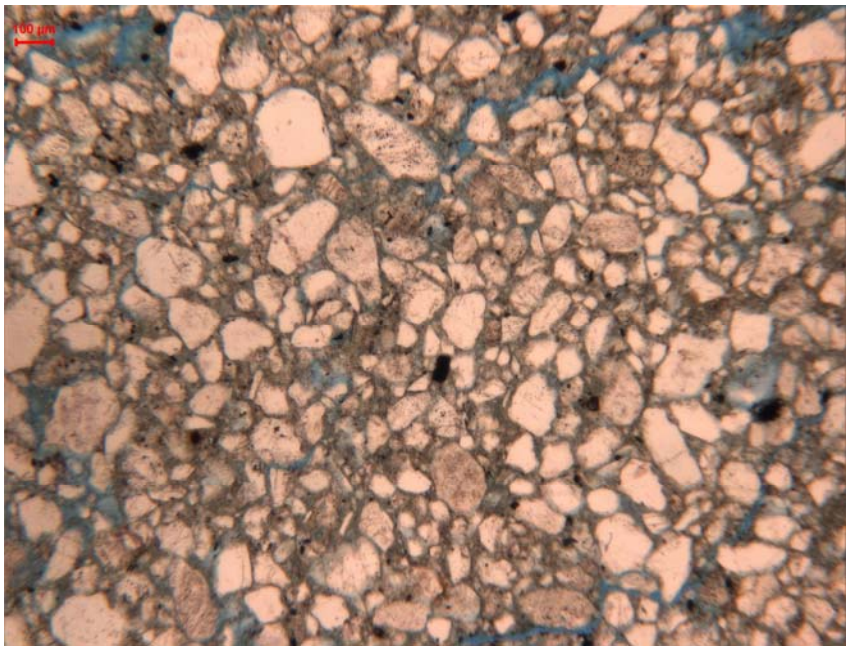

Figure 8.17: Image Analysis photo

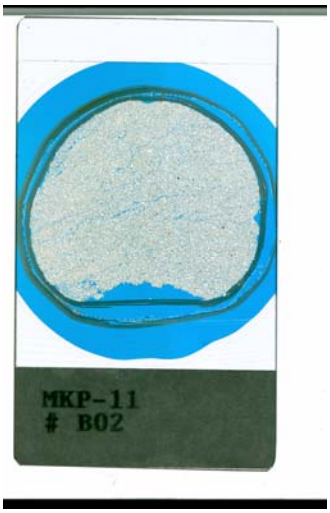

Figure 8.18: Thin slide overall photo

Porosity	7.07 %
Permeability 2D	2.79 D
Permeability 3D	0.44 D
Mean length	> 65.95 µm
Grain size	Fine to medium
Sorting	Very poor

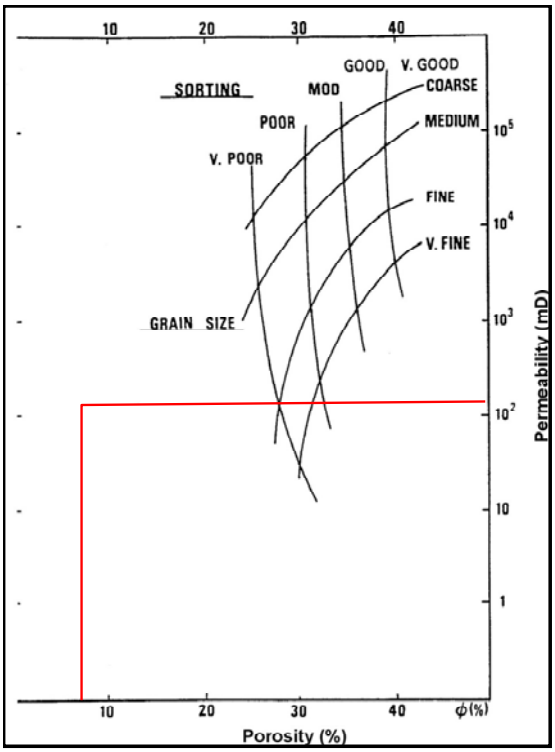

Figure 8.19: Porosity-permeability graph

The permeability of the sample according to the porosity-permeability graph is around 0.15 D. This amount is in agreement with the calculated 2D and 3D permeabilities as can be seen in the table above.

Sample B01
882.63 m

Figure 8.20: Photo of plug

Mineral type	Roundness	Content
Quartz	Subrounded	85%
Quartzite	Subangular	5%
Hornblende	Subangular	5%
Chert	Subangular	3%
Clay minerals	-	2%

Sorting	Cement type	Grain contact
Good	-	Free floating Point contact

This sample shows similarities with sample C02. The thin slide (figure 8.21) consists of large grains which are hardly making any contact with each other. The plug (figure 8.20) contains a lot of bitumen by which the grains are sticked together. The sample has a very porous appearance and as can be seen on the photograph (figure 8.20) the plug is very friable. During the preparation of the thin slide the bitumen is flushed out of the plug and as a result no bitumen is found in the slide (figure 8.22).

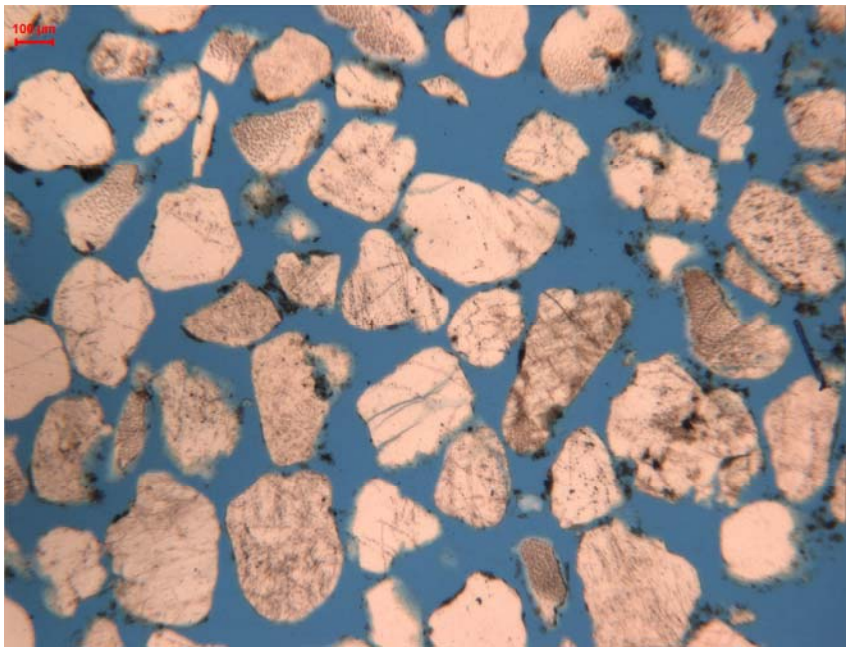

Figure 8.21: Image Analysis photo

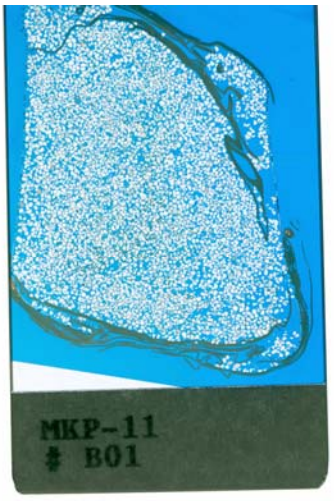

Figure 8.22: Thin slide overall photo

Porosity	40.83 %
Permeability 2D	24.89 D
Permeability 3D	1520.90 D
Mean length	> 61.55 µm
Grain size	Medium to coarse
Sorting	Very good

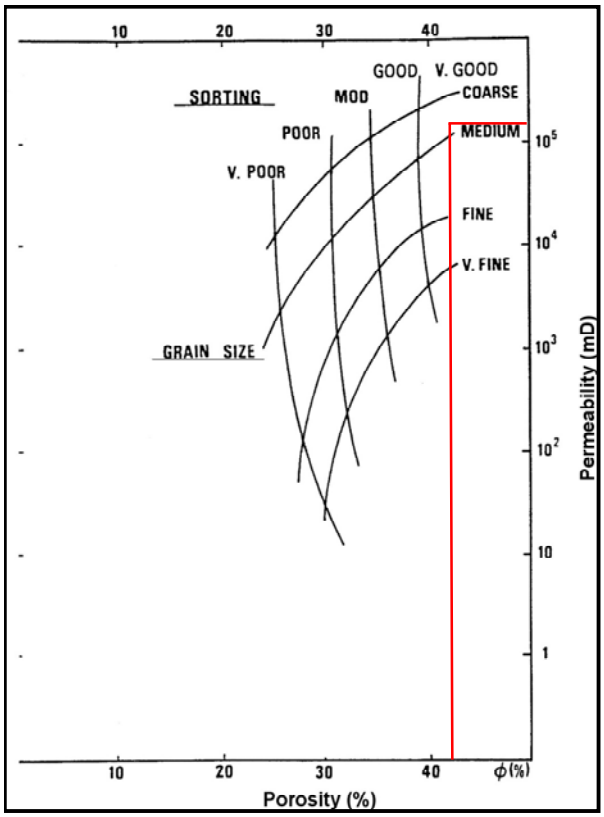

Figure 8.28.1: Porosity-permeability graph

The permeability according to the porosity-permeability graph is around 115 D. The calculated 3D permeability is not reliable because of its large amount. In this thin slide the grains are hardly making any contact with each other which is not a reliable image of the original material.

Sample A08

901.82 m

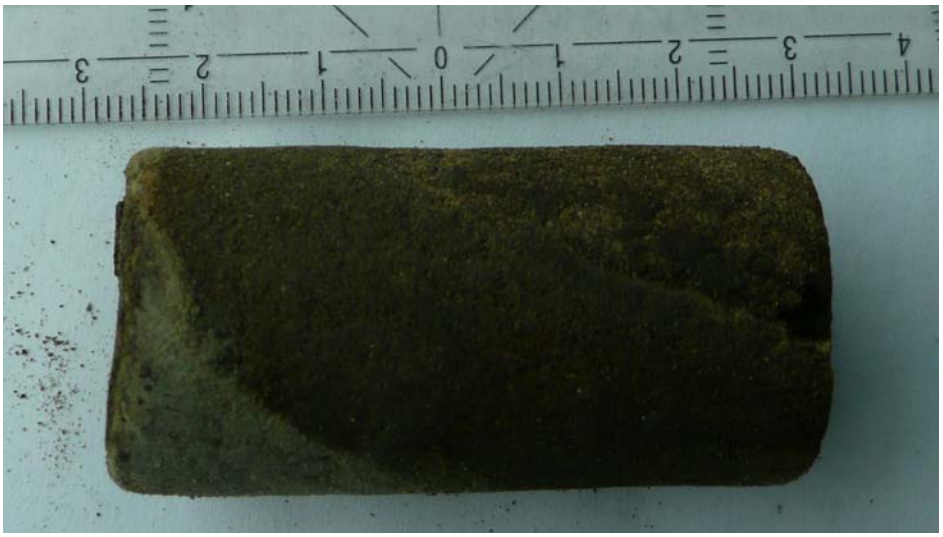

Figure 8.24: Photo of plug

Mineral type	Roundness	Content
Quartz	Angular	50%
Clay cement	-	40%
Muscovite	Angular	4%
Orthoclase	Subangular	3%
Tourmaline	Subangular	2%
Accessory minerals: Quartzite, Zircon, Rutile, Titanite	-	1%

Sorting	Cement type	Grain contact
Bad	Clay minerals	Point contact Long contact Concavo convex contact

This sample contains several cement bands in the thin slide (figure 8.25). The cement bands mainly consist of clay minerals, with all clay minerals pointing in the same direction. The cement bands are straight and perpendicular to each other. One cemented band as shown in figure 8.25 can also be seen on the Image Analysis photograph (figure 8.27).

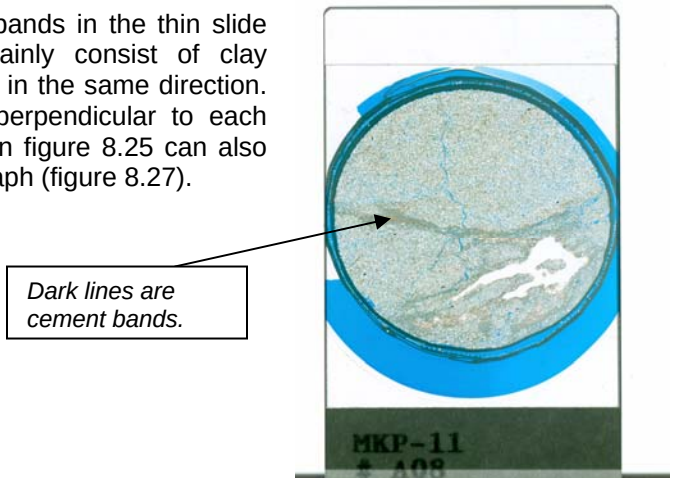

Figure 8.25: Thin slide overall photo

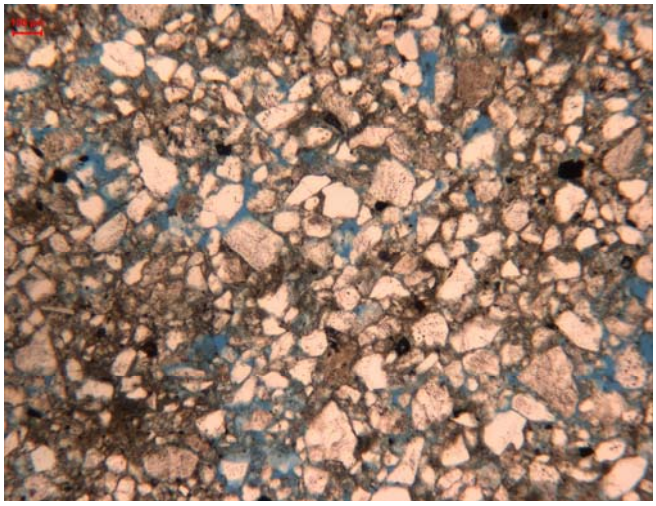

Figure 8.26: Image Analysis photo

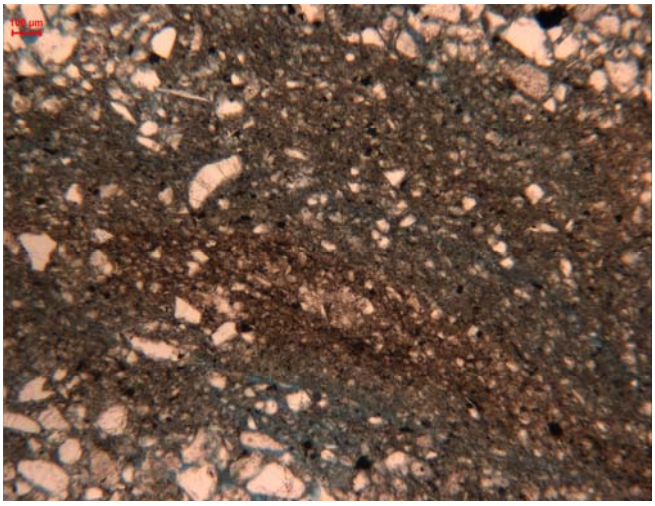

Figure 8.27: Image Analysis photo with cemented band

Porosity	24.21%
Permeability 2D	3.02 D
Permeability 3D	75.05 D
Mean length	> 53.86 µm
Grain size	Medium to coarse
Sorting	Very good

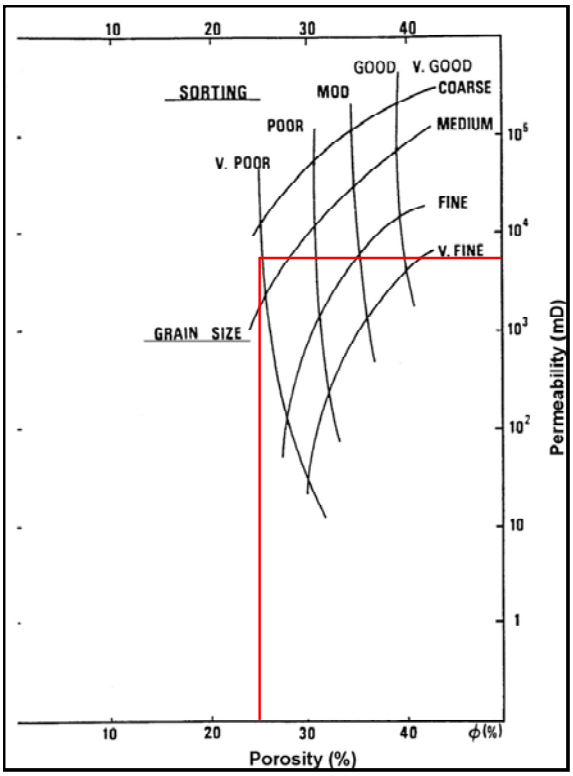

Figure 8.28: Porosity-permeability graph

The permeability according to the porosity-permeability diagram is around 75 D. This is in agreement with the calculated 2D and 3D permeabilities shown in the table above.

Sample A07

902.40 m

Figure 8.29: Photo of plug

Mineral type	Roundness	Content
Quartz	Subangular	48%
Clay cement	-	46%
Muscovite	Angular	3% (content of clay cement)
Chert	Subangular	2%
Hornblende	Subangular	2%
Accessory minerals: Quartzite, Zircon, Rutile, Titanite, Tourmaline	-	2%

Sorting	Cement type	Grain contact
Bad	Clay cement	Point contact Long contact Concavo convex contact

The sample contains much clay cement as can be seen in both thin slide photos (figure 8.30 and 8.31). The slide also consists of some bitumen.

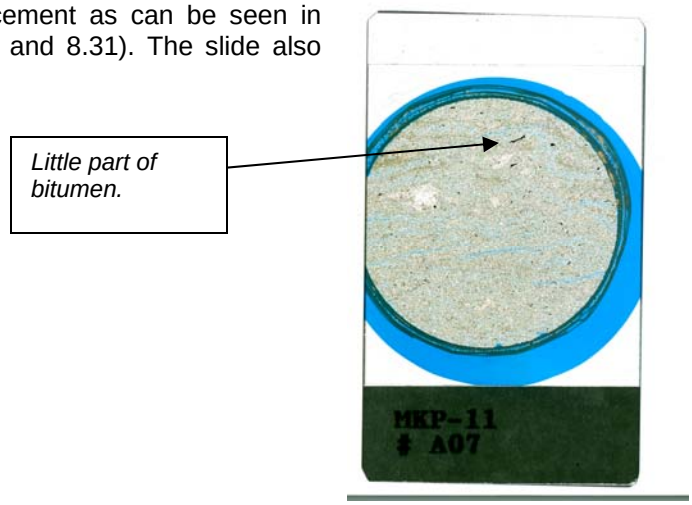

Figure 8.20: Thin slide overall photo

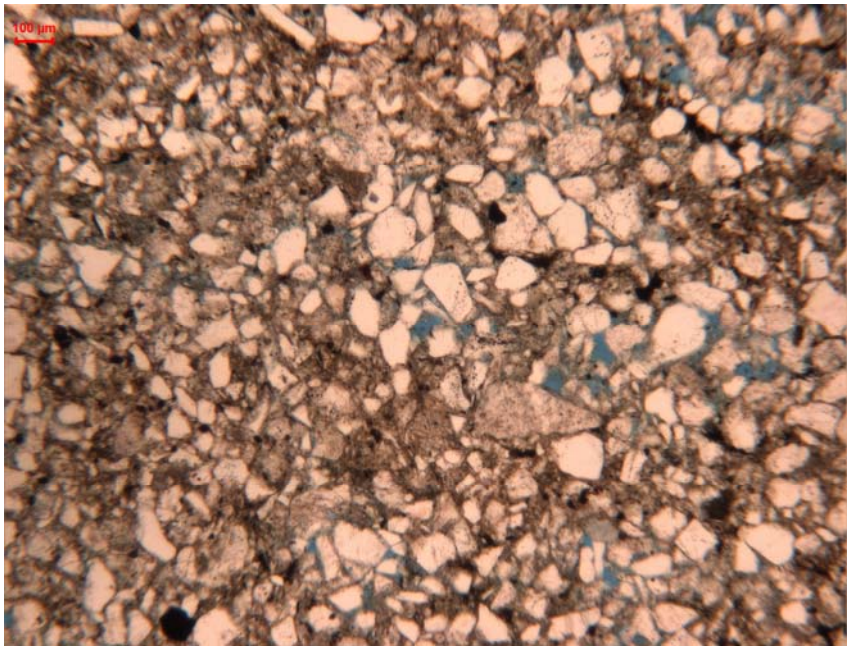

Figure 8.31: Image Analysis photo

Porosity	7.78%
Permeability 2D	1.99 D
Permeability 3D	0.55 D
Mean length	> 45.48 µm
Grain size	Fine to medium
Sorting	Very poor

The Image Analysis photograph (figure 8.31) shows that there is hardly any free space between the grains and that is in agreement with the calculated porosity and permeability as shown in the table above. It is difficult to calculate reliable values of the porosity and permeability with Image Analysis for such a thin slide with very little free space.

Sample A06

902.98 m

Figure 8.32: Photo of plug

Mineral type	Roundness	Content
Quartz	Subangular	50%
Clay cement	-	45%
Muscovite	Angular	4% (content of clay cement)
Hornblende	Subangular	3%
Accessory minerals: Quartzite, Zircon, Rutile, Titanite, Tourmaline, Chert	-	2%

Sorting	Cement type	Grain contact
Very poor	Clay cement	Point contact Long contact Concavo convex contact

The sample contains much clay cement (figure 8.33). The slide also contains some parts with bitumen (figure 8.35).

Part with bitumen. Figure 8.35 shows the detailed photo of this part.

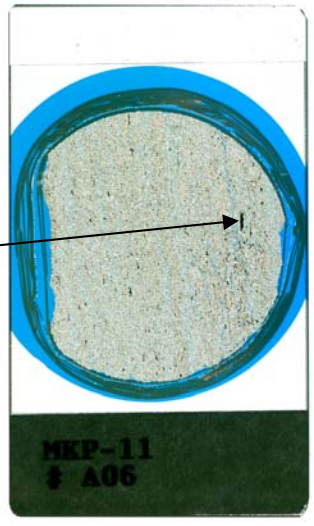

Figure 8.33: Thin slide overall photo

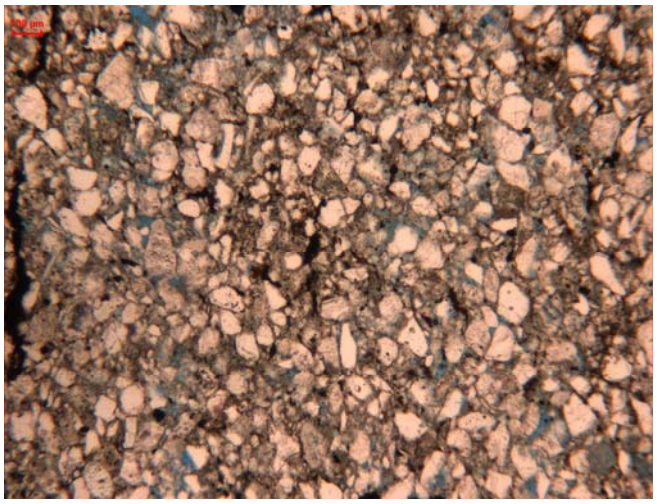

Figure 8.34: Image Analysis photo

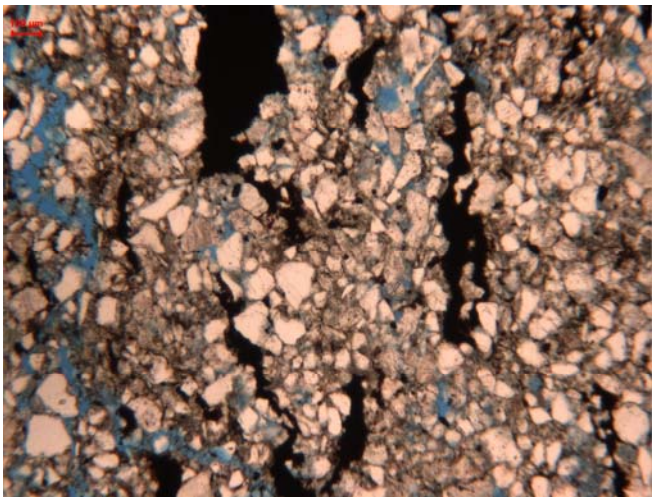

Figure 8.35: Image Analysis photo, bitumen in pore space

Porosity	10.36%
Permeability 2D	1.75 D
Permeability 3D	1.19 D
Mean length	> 48.14 µm
Grain size	Fine to medium
Sorting	Very poor

The Image Analysis photograph (figure 8.34) shows that there is very little free space between the grains and that corresponds with the calculated porosity and permeability as shown in the table above. It is difficult to calculate reliable values of the porosity and permeability with Image Analysis for such a thin slide with hardly any free space.

Sample A04.2

903.40 m

Figure 8.36: Photo of chip

Mineral type	Roundness	Content
Clay minerals	-	52%
Quartz	Subangular	42%
Muscovite	Angular	5% (content of clay cement)
Hornblende	Subangular	4%
Accessory minerals: Zircon, Rutile, Titanite, Tourmaline	-	2%

Sorting	Cement type	Grain contact
Very poor	-	Point contact Long contact Concavo convex contact

This sample contains a lot of clay cement as can be seen on the photograph of the chip (figure 8.36). On the photograph of the thin slide of the plug (figure 8.38), hardly any free space between the grains is visible. The thin slide mostly consists of clay cement with some deformed bands of cement (figure 8.39). Because it is very difficult to detect free space in this sample, it was not possible to calculate the porosity and permeability with image analysis.

Figure 8.37: Thin slide overall photo

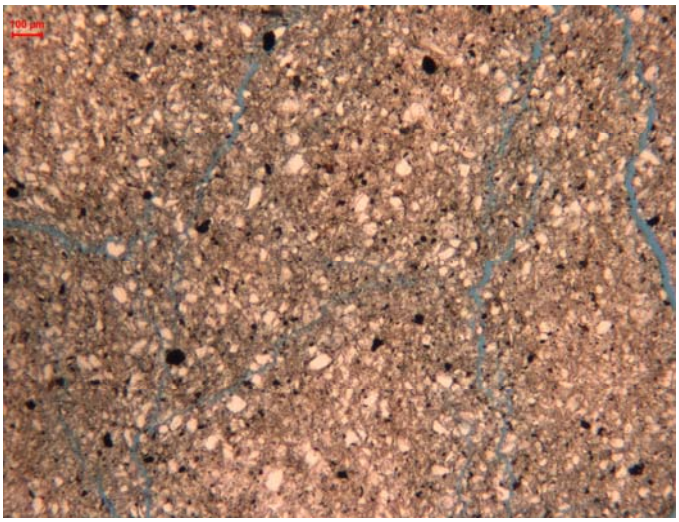

Figure 8.38: Image Analysis photo

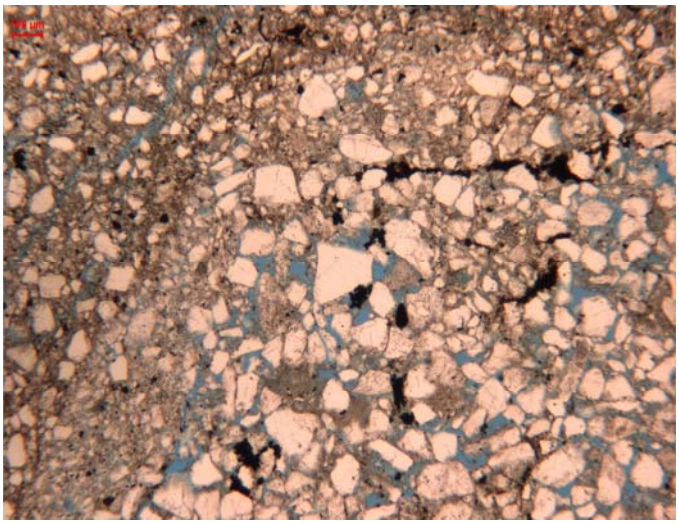

Figure 8.39: Image analysis photo with deformed cement band

Sample A04.1

903.40 m

Figure 8.40: Photo of chip

Mineral type	Roundness	Content
Quartz	Subangular	56%
Clay cement	-	36%
Hornblende	Subangular	6%
Muscovite	Subangular	3% (content of clay cement)
Accessory minerals: Rutile, Titanite, Tourmaline, Zircon	-	2%

Sorting	Cement type	Grain contact
Very Poor	Clay cement	Point contact Long contact Concavo convex contact

The thin slide of this sample contains a thick cement band in the middle and at both edges less clay cement (figure 8.41). The following pictures show the more porous edge of the slide (figure 8.42) and the cement band in the middle (figure 8.43). This sample also contains some bitumen parts.

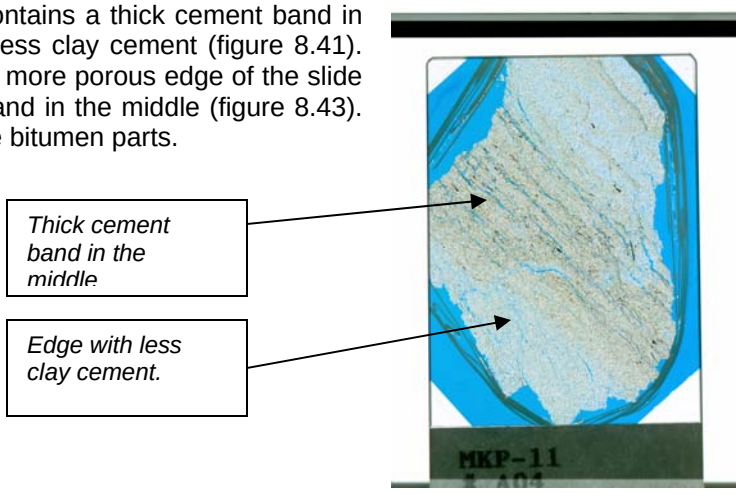

Figure 8.41: Thin slide overall photo

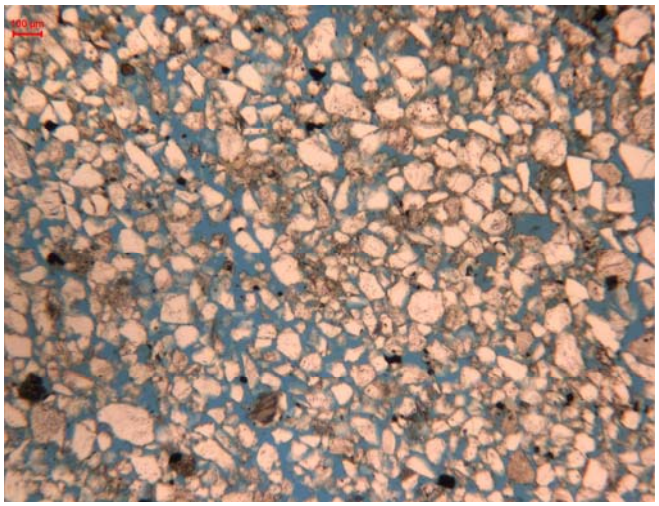

Figure 8.42: Image Analysis photo

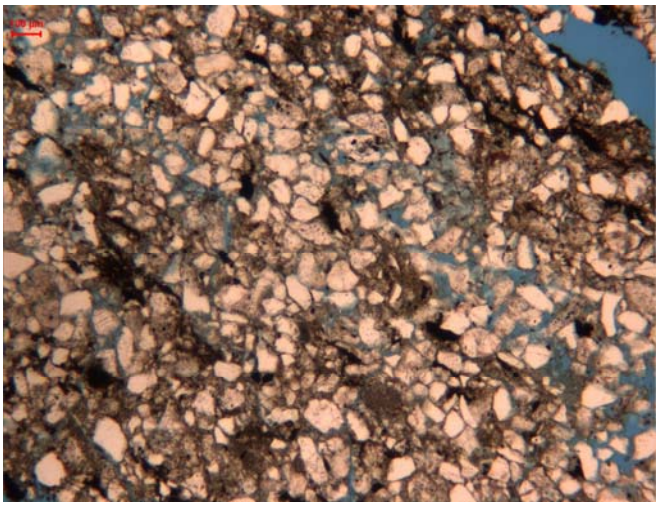

Figure 8.43: Image Analysis photo with cement band

Porosity	36.25%
Permeability 2D	2.78 D
Permeability 3D	66.19 D
Mean length	> 21.16 µm
Grain size	Fine
Sorting	Moderately to good

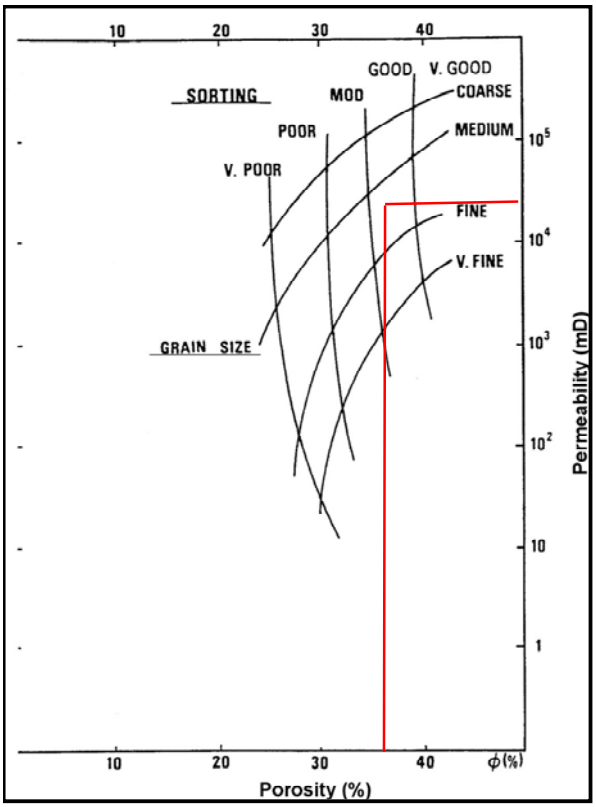

Figure 8.44: Porosity-permeability graph

The permeability according to the porosity-permeability graph is around 35 D. When the cemented parts and the less cemented parts of the slide both are taken into account, the permeability is reliable and corresponds with the calculation in the table above.

Sample A03

903.70 m

Figure 8.45: Photo of plug

Mineral type	Roundness	Content
Quartz	Subangular	50%
Clay cement	-	42%
Hornblende	Subangular	4%
Muscovite	Angular	4% (content of clay cement)
Accessory minerals: Rutile, Tourmaline, Zircon, Chert, Quartzite	-	4%

Sorting	Cement type	Grain contact
Very Poor	Clay cement	Point contact Long contact Concavo convex contact

The sample contains very thick bands with clay cement and in between some little parts with low porosity of 1.54 % (figure 8.47). Therefore it was not possible to calculate the permeability of this thin slide.

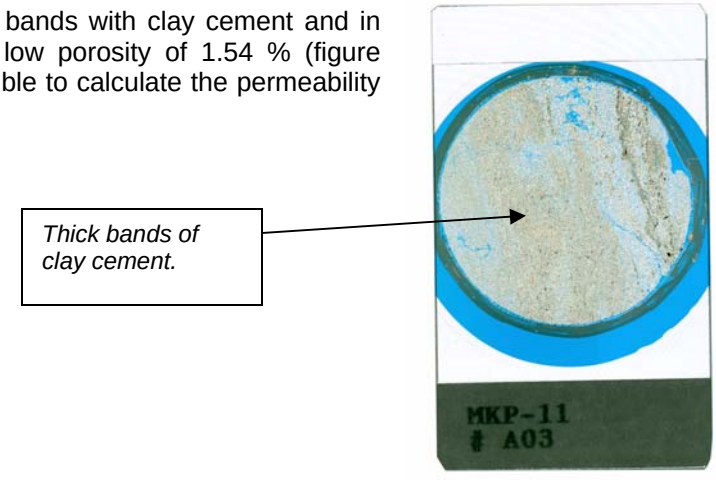

Figure 8.46: Thin slide overall photo

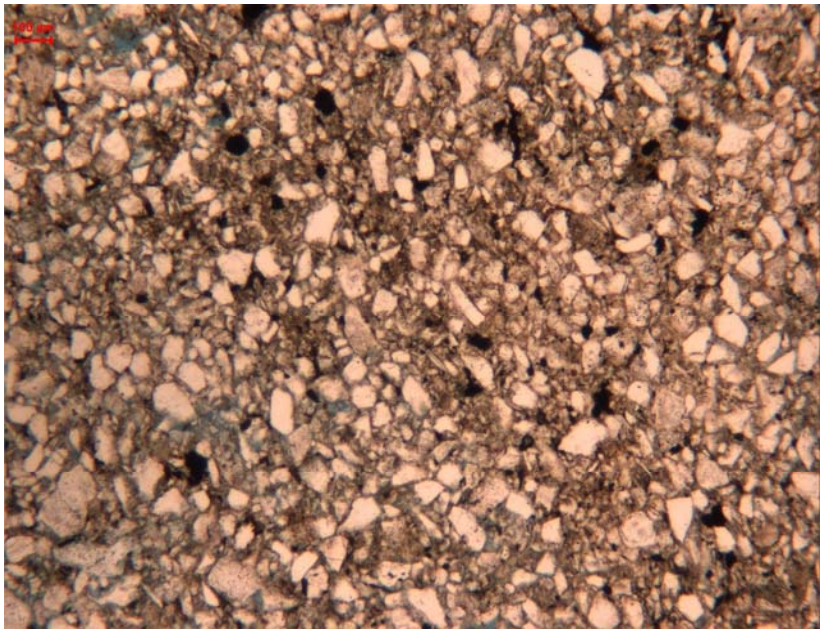

Figure 8.47: Image Analysis photo

Sample A02

903.85 m

Figure 8.48: Photo of plug

Mineral type	Roundness	Content
Quartz	Subangular	52%
Clay cement	-	40%
Hornblende	Subangular	5%
Muscovite	Angular	4% (content of clay cement)
Accessory minerals: Rutile, Tourmaline, Zircon, Chert, Quartzite	-	3%

Sorting	Cement type	Grain contact
Very Poor	Clay cement	Point contact Long contact Concavo convex contact

This sample contains some little cement bands. Because these little bands are deformed it seems that fluids flowed upwards to find a way to escape (figure 8.49).

Band of clay cement curled upwards. This could have been a way for fluids to escape. A detailed photo is shown in figure 8.51.

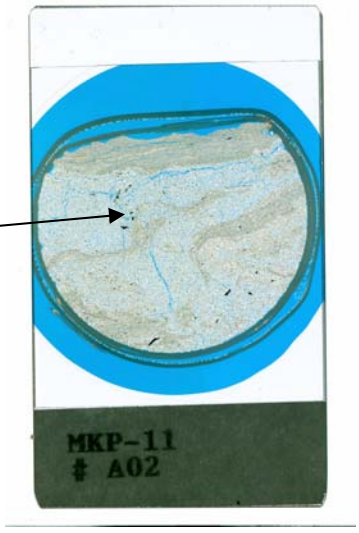

Figure 8.49: Thin slide overall photo

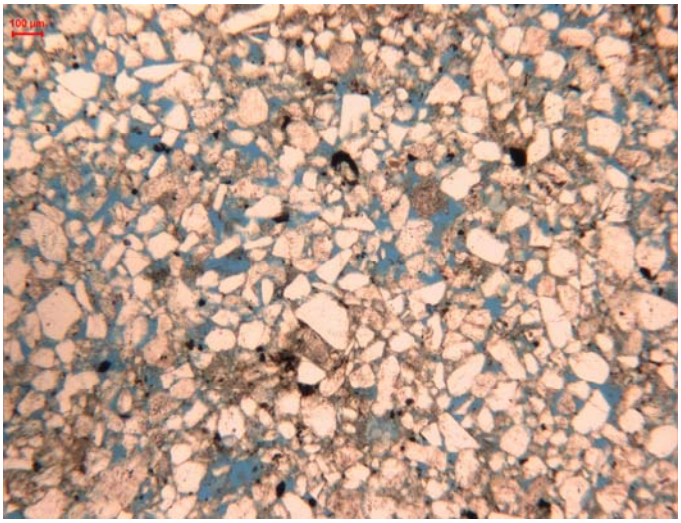

Figure 8.50: Image Analysis photo

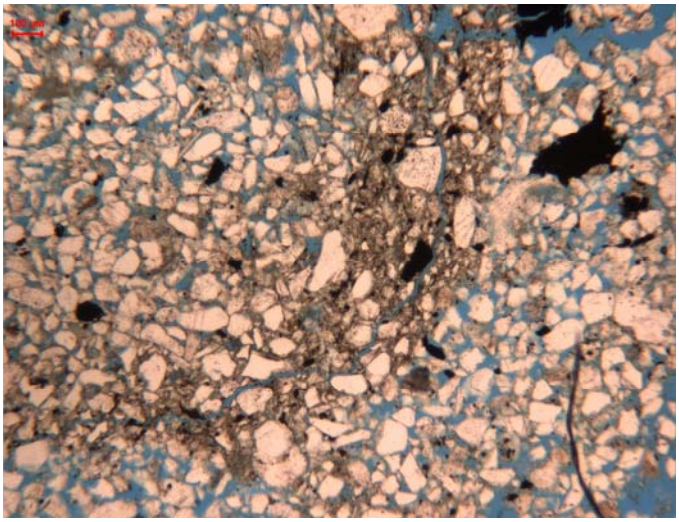

Figure 8.51: Image Analysis photo with deformed cemented band curled upward

Porosity	28.08%
Permeability 2D	3.90 D
Permeability 3D	29.89 D
Mean length	> 16.97 µm
Grain size	Medium to coarse
Sorting	Very poor to poor

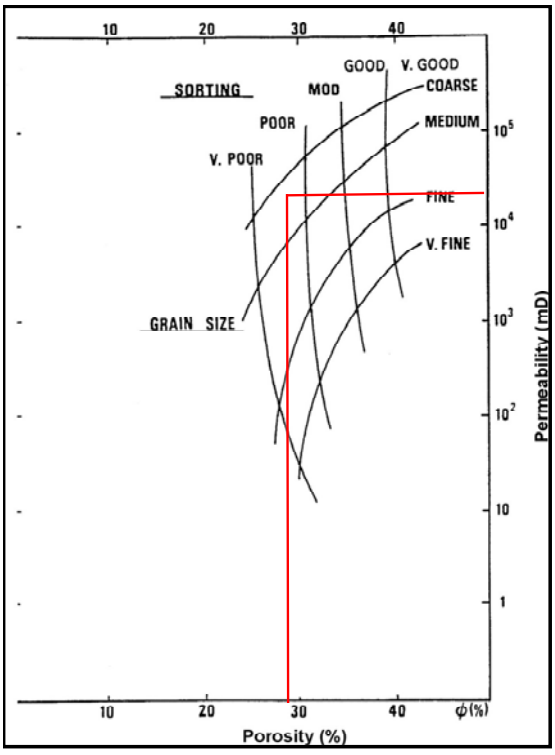

Figure 8.52: Porosity-permeability graph

The permeability according to the porosity-permeability graph is around 25 D. This corresponds with the calculated 2D and 3D permeabilities and lies in between them as shown in the table above.

Sample A01

906.55 m

Figure 8.53: Photo of plug

Mineral type	Roundness	Content
Quartz	Subangular	80%
Hornblende	Subangular	8%
Chert	Subangular	5%
Quartzite	Subangular	4%
Accessory minerals: Tourmaline, Zircon, Muscovite	-	3%

Sorting	Cement type	Grain contact
Good	-	Point contact Long contact Free floating

This sample does not contain any clay cement, only some remains of loose clay minerals.

Figure 8.54: Thin slide overall photo

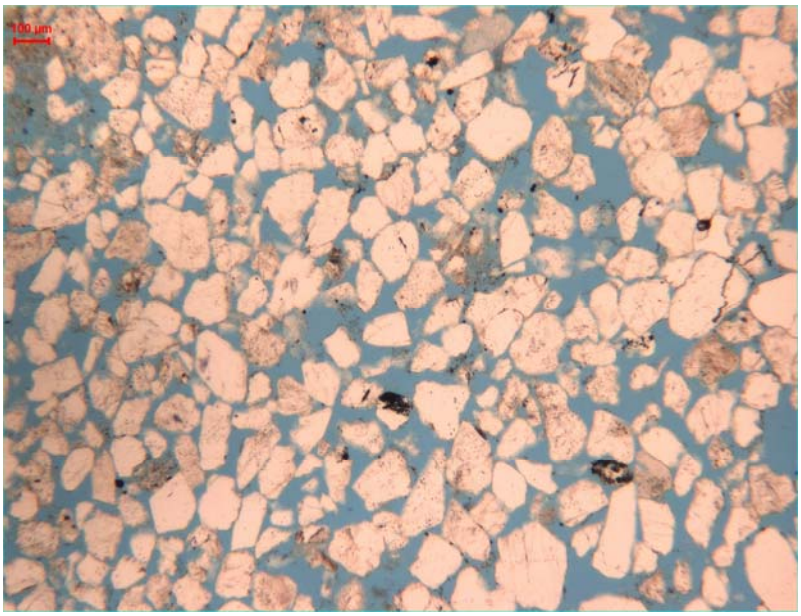

Figure 8.55: Image Analysis photo

Porosity	32.37%
Permeability 2D	23.47 D
Permeability 3D	123.07 D
Mean length	> 70.29 µm
Grain size	Medium to coarse
Sorting	Very poor to poor

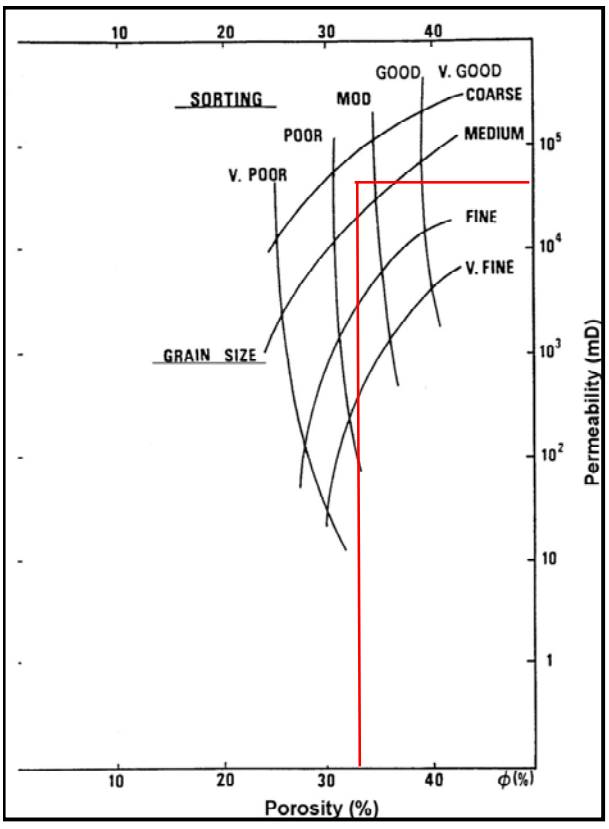

Figure 8.56: Porosity-permeability graph

The permeability according to the porosity-permeability graph is around 65 D. This is in agreement with the calculated 2D and 3D permeabilities and lies in between them as shown in the table above.

Chapter 9

Results Petrographical analysis MKP11

	Permeabilities 2D	Permeabilities 3D	Permeabilities according to graph	Porosities	Depth
	Darcy	Darcy	Darcy	-	m
C04	7.31	63.58	45	35.81	861.15
C03	17.66	173.35	50	30.35	862.00
C02	23,79	2384.86	100	32.79	868.15
C01	-	-	-	3.52	872.85
B02	2.79	0.44	0.15	7.07	881.70
B01	24.89	1520.90	115	40.83	882.63
A08	3.02	75.05	75	24.21	901.82
A07	1.99	0.55	-	7.78	902.40
A06	1.75	1.19	-	10.36	902.98
A04.2	-	-	-	3.84	903.40
A04.1	2.78	66.19	35	36.25	903.40
A03	-	-	-	1.54	903.70
A02	3.90	29.89	25	28.08	903.85
A01	23.47	123.07	65	32.37	906.55

This chapter contains an overview of all calculated porosities and permeabilities shown in the table above. The permeabilities given are the calculated permeabilities according to the 2D and 3D method and the permeabilities found in the porosity-permeability graph to check the reliability of the calculated permeabilities. The 3D permeabilities of the samples C02 and B01 are greyed out because that permeability is very unlikely.
During the preparation of the thin slides the bitumen is flushed away and as a consequence the thin slides of these samples do not contain any bitumen (Chapter 8, Introduction). Most grains in these thin slides are not in contact with each other and therefore it is very reliable that the plugs damaged during the preparation of the thin slides. This could be an indication for the unreliable high 3D permeability.

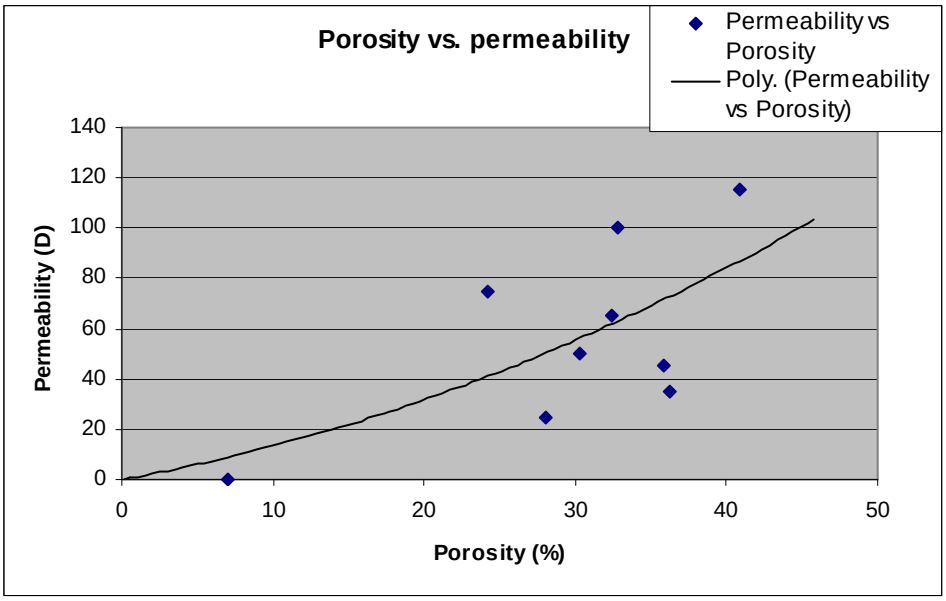

Figure 9.01: Porosity vs. permeability

The graph above describes the relation between the calculated porosity and permeability (figure 9.01). It seems that of the fourteen samples in total, five samples are not reliable because of the high clay cement content. At some of the remaining samples clay cement is still available, but not in a large amount.

The C-layer (C04, C03, C02 and C01) seems to be the best layer. It has a stable porosity of around 32 % and a good permeability between 45 and 100 D. If the photos of the thin slides of the C-layer are compared with each other, it is remarkable that the grain size of C04 to C02 becomes larger with its depth (figure 8.02, 8.06 and 8.10). Only sample C01 is very bad because of the high clay cement content and has almost no porosity.

Of all samples a cumulative distribution of the grain sizes is made. The detailed description of the cumulative distributions of the grain sizes could be a new project for further research, so only one graph is shown as an example. Remarkable is that the distribution of the grain sizes is bimodal as shown in the graph beneath (figure 9.02). Every sample seems to have a bimodal distribution of the grain sizes. The graph shows that the sample contains grains with two dominant grain sizes (for example clay, silt, sand or granules) with a mean size 1.25 µm and 3.75 µm.

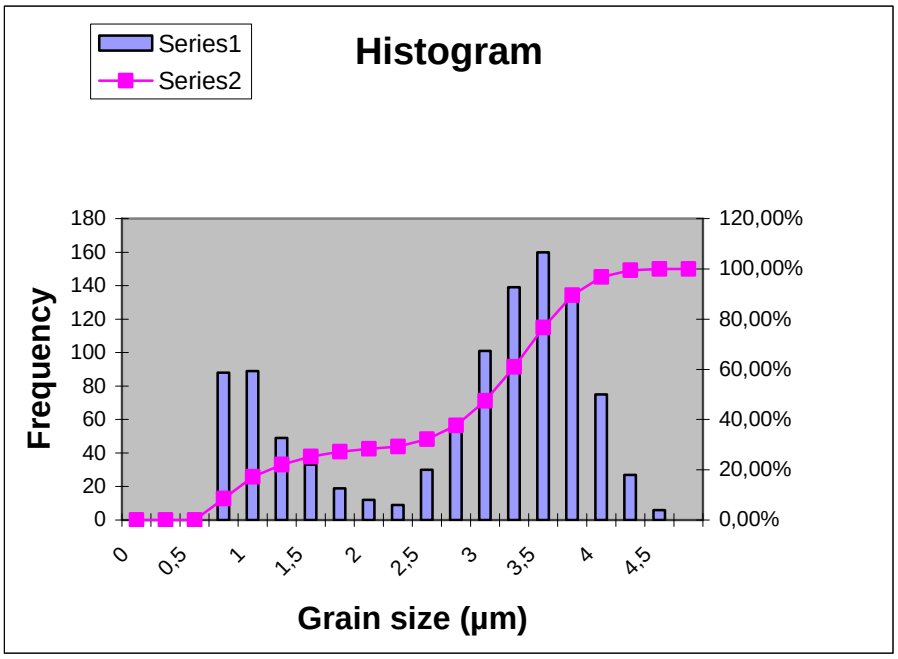

Figure 9.02: Cumulative distribution of grain sizes of sample C04

Chapter 10

Conclusions

DEL-03 conclusions

Cementation is present throughout the entire Delft Sandstone Member in three different types, namely quartz cement, clay mineral cement and siderite cement. Because the cuttings are handpicked and there is always a part of the sample which is originally from a higher part in the borehole, the cuttings cannot tell us exactly to what extent the layer at a certain depth is cemented. What is conclusive, is that siderite cement is absent in the upper part of the Delft Sandstone Member. The first observation is not until 1832 meters in depth.

The interval 1820-1860 meter is characterized by a sand content of 50 to 65 percent. The spontaneous potential log indicates a much lower content for it lies closer to the shale base line with respect to the upper part of the Delft Sandstone Member. The siderite found there can be seen as the cause. The cementation prevents the ion flow from the formation water to the drilling fluid so the SP logging tool is not able to read a good value.

With fluorescent light, residual bitumen can be spotted. All the cuttings of the whole formation are checked, but no bitumen has been found in the cuttings. Also chloroform is used to check if there was bitumen present in the cuttings. This proves that the target sandstone is clean and able to produce water only.

MKP-11 conclusions

The cores of MKP-11 at the core shed in Assen looked very friable. Some parts were so friable that one was unable to lift the core, for it would fall apart in your hands. This may be due to the age of the core, but the sandstone is definitely very friable which is good for possible production in the future.

To conclude what layer (A, B or C) in the MKP-11 section is the best probable geothermal aquifer for the DAP project, permeabilities and porosities per layer should be compared. The thickness of layer A is around 5 meters, the thickness of layer B around 1 meter and layer C around 11 meters as shown in the table below.

Layer A contains the most samples, four of eight, by which it was impossible to calculate the porosity and permeability because of its high clay content (A03, A04.2, A06 and A07). In layer B one sample has a very low porosity and permeability (B02). The high porosity and permeability of the other sample (B01) is because of high friability of the plug. The bitumen, which sticks the grains together in the plug, is missing in the thin slide. For this reason the permeability and porosity calculated from the thin slide is very high and not a really good representation of the original porosity and permeability of this sample.

The samples taken from layer C are located at the top of the Delft Sandstone in the MKP-11. The first two samples on top (C04 and C03) have a very good porosity and permeability. Sample C02 has also a very good porosity and permeability, but for this sample holds the same as for sample B01. Sample C01 contains too much clay cement to calculate the porosity and permeability.

Although layer C contains one bad sample, this layer gave the best results for a geothermal aquifer. The thin slides of C04, C03 and C02 are clean; very little clay cement is found. The interval of 861.15 to 868.15 meter covers seven meters of probable good reservoir rock.

	Permeabilities 2D	**Permeabilities 3D**	**Permeabilities according to graph**	**Porosities**	**Depth**
	Darcy	**Darcy**	**Darcy**	**-**	**m**
C04	7.31	63.58	45	35.81	861.15
C03	17.66	173.35	50	30.35	862.00
C02	23,79	2384.86	100	32.79	868.15
C01	-	-	-	3.52	872.85
B02	2.79	0.44	0.15	7.07	881.70
B01	24.89	1520.90	115	40.83	882.63
A08	3.02	75.05	75	24.21	901.82
A07	1.99	0.55	-	7.78	902.40
A06	1.75	1.19	-	10.36	902.98
A04.2	-	-	-	3.84	903.40
A04.1	2.78	66.19	35	36.25	903.40
A03	-	-	-	1.54	903.70
A02	3.90	29.89	25	28.08	903.85
A01	23.47	123.07	65	32.37	906.55

Recommendations

- ✓ There was no trace of bitumen in the Delft Sandstone Member. The Rijswijk Member does contain oil and lies on top of the Delft Sandstone Member. Therefore, it is most likely that the oil migrated through the Delft Sandstone Member. It is remarkable that no residual bitumen has been found. A study to the migration path of the oil in the Rijswijk Member may clarify.

- ✓ SEM photos may give insight in the way the siderite cements the grains. It also reveals a lot about the diagenesis as grain contacts and deformations of grains can be studied in great detail.

- ✓ The mineralogical content of DEL-03 has been studied in detail in this thesis. However, the contents may have been pulled out of its context, because the thin slides are produced of hand-picked cuttings from a fraction of the total amount of cuttings in the interval. It is an idea to do a new analysis, but this time on all grains from an interval and not just a sieved fraction.

- ✓ The image analysis is performed on photos of the thin slides from MKP-11. To get a better understanding of the porosity and permeability, some photos of DEL-03 can be looked at with image analysis. It is also a good idea to take pictures of the whole thin slide for the calculation of the porosity and permeability with image analysis and not just of a part. The apparatus of the TU Delft could not handle this, but doing it this way excludes wrong measurements on zones within the thin slides.

- ✓ Extended research on the grain size distribution within the Delft Sandstone Member can confirm or give more insight in the depositional environment. For this research both MKP-11 and DEL-03 can be looked at for they lie on a different place within the coastal delta system.

- ✓ XRD/XRF analysis of the sandstone give information on the dominance of some atoms and therefore on the mineralogical content. It will though probably confirm most of the minerals recognized by optical examination.

- ✓ Because the sandstone is very friable, sand production must be accounted for. Screens can be placed while producing to prevent sandblasting of all the equipment.

- ✓ For future cuttings analyses, one should know right from the start that data gathered from cuttings is not very accurate. You are dealing with cavings in your borehole which end up in the drilling mud and are therefore sampled at the wrong depths. The samples are taken every two meters, roughly. So the data is a blend of possibly multiple layers. And this all is only true if the mud logger does an impeccable job, which will not always be the case. So always keep in mind the degree of uncertainty.

- ✓ With all DAP projects, a lot of data and conclusions of the Delft Sandstone Member have been gathered. The upper part of the formation, the target zone, shows good results so far. Before the creation of a heterogeneous reservoir model, one must look closely to the data of DEL-03 and MKP-11 and correlate them. More data of a third borehole would be ideal, but this is not available in the near surroundings.

- ✓ With the correlation, a facies model is most important. Therefore the logs of DEL-03 have to be linked to the logs of MKP-11. This way the facies can be transferred from 12 kilometers away, where is good data, to close proximity. Once the facies are determined in the DEL-03 they can be compared with the results from the cutting analyses in this thesis. This might reveal large scale heterogeneities in the Delft Sandstone Member.

Acknowledgements

We would like to thank numerous people, but first of all Rick Donselaar for his tips and feedback on the thesis as supervisor. Karl-Heinz Wolf and Joost van Meel were very helpful with the utilization of the software Image Analysis.
There are also some companies who contributed to this thesis like the NAM who provided us with the cuttings and plugs of DEL-03 and MKP-11, but especially PanTerra for consult, the supply of work space for the first cuttings study and for the production of the thin slides. Jan de Coo en Jurriaan Nortier were very good contacts within PanTerra.
Furthermore, we would like to thank DAP for providing us with a research subject and especially Douglas Gilding for help with Petrel and useful discussion on all the topics in the world of geothermal energy. It is great to be part of a large research and hopefully we see the results of all the theory in practice in the near future.

References

Davis, J.C., 1986, *Statistics and data analysis in geology*, published by John Wiley & Sons, inc., Singapore.

De Jager, J., 2007 *Geological development* in Th.E. Wong, D.A.J. Batjes, and J. De Jager, eds., Geology of the Netherlands: Amsterdam, Royal Netherlands Academy of Arts and Sciences, p. 5-26.

De Jager, J., Doyle, M.A., Grantham, P.J., and Mabillard, J.E., 1996, *Hydrocarbon habitat of the West Netherlands Basin* in: H.E. Rondeel, D.A.J. Batjes, and W.H. Nieuwenhuijs, eds., Geology of gas and oil under the Netherlands: Dordrecht, Kluwer Academic Publishers, p. 191-209.

Den Hartog Jager, D.G., 1996, *Fluviomarine sequences in the Lower Cretaceous of the West Netherlands Basin: correlation and seismic expression* in H.E. Rondeel, D.A.J. Batjes, and W.H. Nieuwenhuijs, eds., Geology of gas and oil under the Netherlands: Dordrecht, Kluwer Academic Publishers, p. 229-241.

Geowulf, 2008, Geothermal project Den Haag Zuid-West, Geowulf Laboratories, The Netherlands.

Google maps, 2009: http://maps.google.nl/ visited on the 9th of June, 2009.

Hilchie, D.W., 1979, Old electrical log interpretation, Boulder, Colorado, p. 18-20

Nlog, 2009: www.nlog.nl visited multiple times in May and June, 2009.

Smits, P.F., 2008, *Construction of an integrated reservoir model using the Moerkapelle field for geothermal development of the Delft sandstone*, MSc Thesis, Delft University of Technology, Delft, the Netherlands.

Van Adrichem Boogaert, H.A., and W.F.P. Kouwe, comps., 1993, *Stratigraphic nomenclature of the Netherlands, revision and update by Rijks Geologische Dienst (RGD) and Netherlands Oil and Gas Exploration and Production Association (NOGEPA): Mededelingen Rijks Geologische Dienst 50.*

Van Balen, R.T., Van Bergen, F., De Leeuw, C., Pagnier, H., Simmelink, H., Van Wees, J.D., and Verweij, J.M., 2000, *Modelling the hydrocarbon generation and migration in the West Netherlands Basin, the Netherlands* Netherlands Journal of Geosciences 79, p 29-44.

Van Wijhe, D.H., 1987, *The structural evolution of the Broad Fourteens Basin*, Petroleum geology of North West Europe.

Wiggers, C.J.I., 2009, The Delft Sandstone in the West Netherlands Basin, BSc Thesis, Delft University of Technology, Delft, The Netherlands.

Wong, Th. E., 2007, *Jurassic* in Th.E. Wong, D.A.J. Batjes, and J. De Jager, eds., Geology of the Netherlands: Amsterdam, Royal Netherlands Academy of Arts and Sciences, p. 107–125.

Appendix A

Core description made by Gilding,Wiggers and Loerakker
Pluglocation made by Drost and Korenromp

D.T Gilding C.J.I Wiggers M.Loerakker GIA Drost MHA Korenromp
Core description of the Moerkapelle well 11
Average deviation of the well over cored section is 45 degrees

MKP-11
20-02-09
Pluglocations added on 15-06-2009

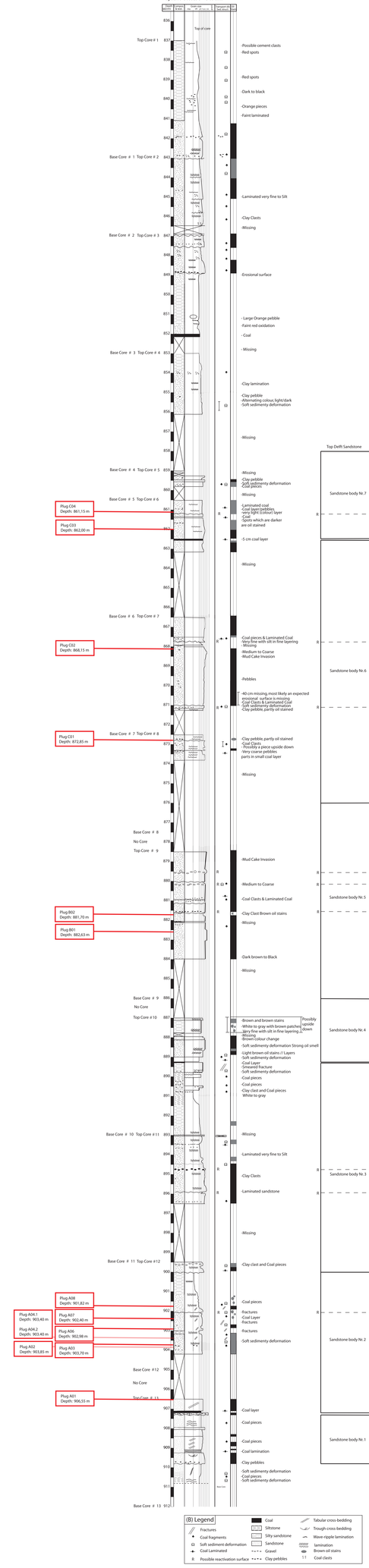

(B) Legend

- Fractures
- Coal fragments
- Soft sediment deformation
- Coal Laminated
- Possible reactivation surface
- Coal
- Siltstone
- Silty sandstone
- Sandstone
- Gravel
- Clay pebbles
- Tabular cross-bedding
- Trough cross-bedding
- Wave-ripple lamination
- lamination
- Brown oil stains
- Coal clasts

Appendix B

Depth: 903.1 - 903.25 m

Depth: 903.25 – 903.4 m

Depth: 903.3 – 903.45 m

Depth: 882.5 – 883.0 m

Depth: 906.9 – 907.4 m (Basis Delft)

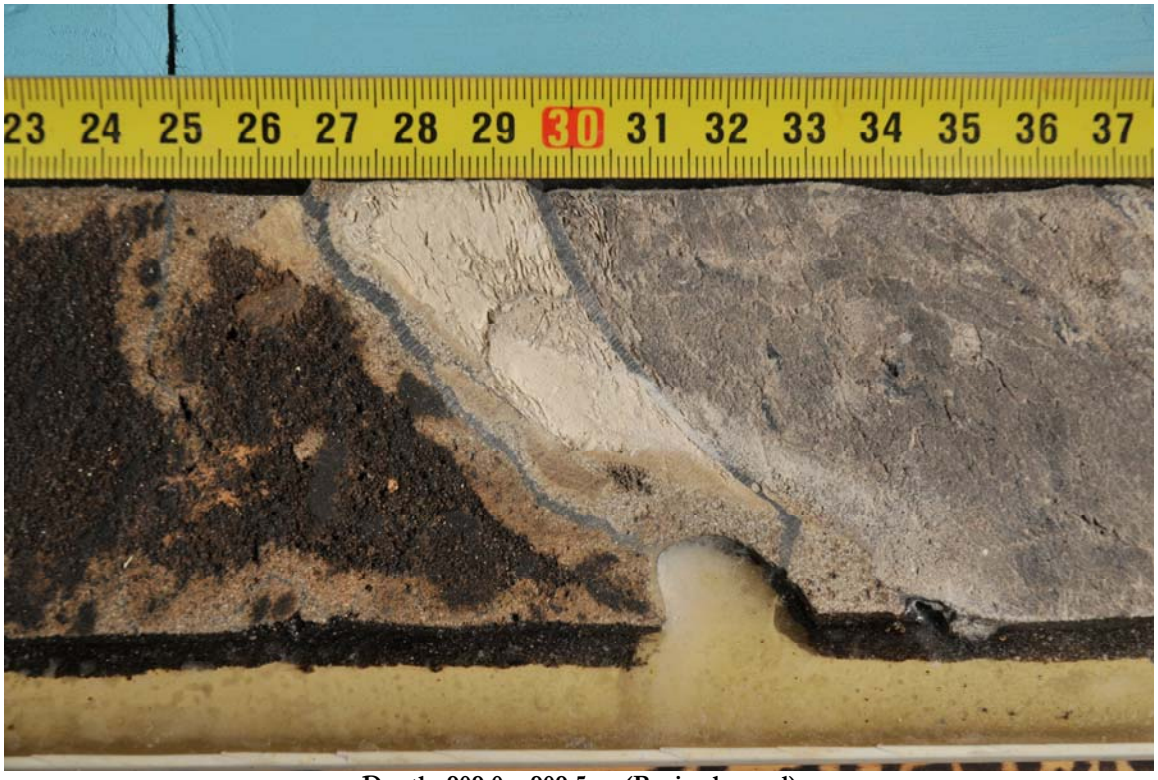

Depth: 909.0 – 909.5 m (Basis channel)

Depth: 909.8 – 910.3 m (Fractured dry)

Depth: 909.8 – 910.3 m (Fractured wet)

Depth: 902.35 – 902.45 m (Cemented)
Related plugs: A07

Depth: 902.4 – 902.55 m (Cemented)

Depth: 901.8 m (Transition zone)
Related plugs: A08

Depth: 881.7 m (Transition zone)
Related plugs: B02

Depth: 843.9 m (Pyrite)

Appendix C

This appendix contains descriptions of every plug and chip that is taken from the cores of MKP-11. These descriptions are made following the sequence of the list below. With every plug or chip comes a scaled photo. Of some chips/plugs there are photos containing the slabs at corresponding depth. Other samples lag these photos.

Every description starts with a sample number and the depth on which they are taken. Grain sizes are measured with a special ruler containing standard grain diameters.

List:

1. Sample size
2. Appearance
3. Color
4. Friable
5. Grain size

A01
906.55

1. 5 cm
2. Some small cracks and a piece came of at one end.
3. Does not look shiny. Dark-brown to black
4. Pretty friable, if you touch it some small grains stay behind on you finger.
5. Upper fine.

A02
903.85

1. 4.5 cm
2. Different permeability zones can be observed by watching at the colors. Darker brown or blackish means more residual oil so a higher perm. There are also medium grey zones, these look cementated or at least not permeable. In both zones carboniferic remains are present.
3. Brown tints to black, medium grey
4. Little friable, the plug is pretty stable.
5. Upper fine

A03
903.70

1. 3.5 cm
2. Largely fallen apart, cracks everywhere. Large coal remains spotted (rectangular).
3. Different zones from yellowish brown to black. The zones do not merge into one another but have sharp boundaries.
4. Not really friable, but the sample is weak. A possibility is that the particles are held together by the bitumen which is present in different quantities in the different zones.
5. Upper fine

A04 / 1
903.40

1. Little chunk of 3x2 cm
2. A dark brown-black sandstone intervened by a layer of light grey material of 1.3 cm thickness. Lots of cracks parallel to transition from brown to grey. Brown blurs in the grey. Light grey consists of very fine particles.
4. Sandstone is friable.
5. Lower fine.

A04 / 2
903.40

Sub angular chunk of 7x4 cm
Biggest part is light grey, no grains can be seen.
It is soft and can be rolled between the fingers. This is most definitely clay. The clay looks dried out.
Some darker, bitumen enriched, parts are adjacent to
this big boulder. The sandy parts are already described at A04/1

Depth: 903.3 – 903.45 m

A06
902.98

1. 4.7 cm, perfect cylinder
2. Broken because of lamination in sample. Lamination makes an angle of approximately 40 degrees with the axes of the plug. This means after a correction for the deviation, that these layers were deposited horizontally. Coal particles spotted
3. Light brown to dark grey
4. Not friable, very stable plug
5. Very fine upper

A07
902.40

1. 4.8 cm
2. A steep dip in an orientation can be seen if one looks carefully. It is not obvious though, may also look that way because of a crack in this direction. The angle with the plug axis is 20 degrees.
3. Light brown to medium grey colors. Also light grey (possible cemented parts) observed. Coal particles present.
4. Not friable
5. Fine lower

Depth: 902.35 – 902.45 m (Cemented)

A08
901.82

1. 5.0 cm
2. At the edges a bit broken, for the rest intact. Big very light grey part at the top/bottom with an angle of 45 degrees with respect to the axes. This part in compressible and doesn't show any structure. Looks like clay.
3. The rest of the plug has dark brown tints
4. Not friable
5. Fine lower

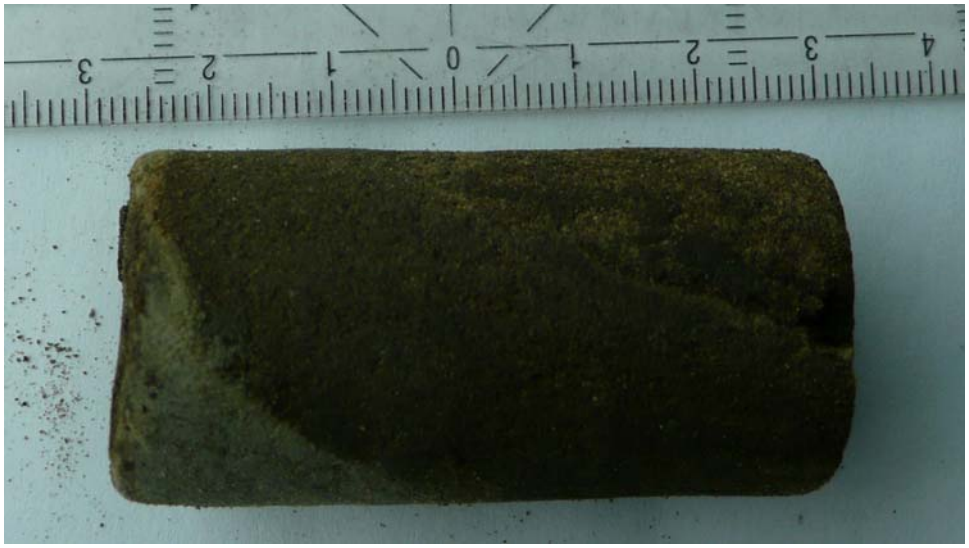

Depth: 901.8 m (Transition zone)

B01
882.63

1. Two chunks of 4x3
2. Looks like loose sand compacted by the bitumen. Deformable when pressure is applied. Sticky.
3. Dark brown with black parts.
4. Highly friable
5. Lower medium

B01 in detail

Depth: 882.5 – 883.0 m

B02
881.70

1. 4.5 cm
2. Some cracks spotted.
3. Almost uniform color, light brown-grey. Some darker brown blurs.
4. Friable, it’s got coherence. But grains stick to your fingers when you rub.
5. Medium lower

Depth: 881.7 m (Transition zone)

C01
872.85

1. Cylinder of 4 cm, broken in two parts
2. Outer part is very soft. A lot of fractures present.
3. Light grey/ broken white.
4. Falls very quick apart.
5. No particles can be identified; the best fit is a claystone.

C02
868.15

1. 2 cm
2. This sample was a try to take a plug, but it fell apart. Only a part of the cylinder is left. The surface is shiny and greasy.
3. The sample looks dark-brown to black, which means it is saturated with hydrocarbons.
4. The grains can be seen with the naked eye. This sandstone is very friable, if it will not be handled with care it will fall apart. If one grabs it, particles stay behind on the hand.
5. Medium low.

C03
862.00

1. Chunk of 6x6
2. Coal layers present, together with lots of bitumen. Light brown parts look like cement/clay.
3. Medium brown and black pieces in dark brown matrix of lower course particles.
4. Friable
5. Lower course

C04
861.15

1. Two chunks of 5x3 cm
2. It is a chunk directly next to an old plug which is taken in the past by the NAM. Dried clay parts can be observed on the outside of the sample; look like light brown flints.
3. Very dark, bitumen rich, rock lies directly next to light grey rock. This is a possible cementated part.
4. Very fine upper to fine upper.